HIGHWAY RESEARCH BOARD

Bulletin 331

Soil Behavior Associated With Freezing

National Academy of Sciences—
National Research Council

publication 1013

HIGHWAY RESEARCH BOARD

Officers and Members of the Executive Committee

1962

OFFICERS

R. R. BARTELSMEYER, *Chairman* C. D. CURTISS, *First Vice Chairman*

WILBUR S. SMITH, *Second Vice Chairman*

FRED BURGGRAF, *Director* WILLIAM N. CAREY, JR., *Assistant Director*

Executive Committee

REX M. WHITTON, *Federal Highway Administrator, Bureau of Public Roads* (ex officio)

A. E. JOHNSON, *Executive Secretary, American Association of State Highway Officials* (ex officio)

LOUIS JORDAN, *Executive Secretary, Division of Engineering and Industrial Research, National Research Council* (ex officio)

PYKE JOHNSON, *Retired* (ex officio, Past Chairman 1960)

W. A. BUGGE, *Director of Highways, Washington Department of Highways* (ex officio, Past Chairman 1961)

R. R. BARTELSMEYER, *Chief Highway Engineer, Illinois Division of Highways*

E. W. BAUMAN, *Director, National Slag Association, Washington, D. C.*

DONALD S. BERRY, *Professor of Civil Engineering, Northwestern University*

MASON A. BUTCHER, *County Manager, Montgomery County, Md.*

J. DOUGLAS CARROLL, JR., *Director, Chicago Area Transportation Study*

C. D. CURTISS, *Special Assistant to the Executive Vice President, American Road Builders' Association*

HARMER E. DAVIS, *Director, Institute of Transportation and Traffic Engineering, University of California*

DUKE W. DUNBAR, *Attorney General of Colorado*

MICHAEL FERENCE, JR., *Executive Director, Scientific Laboratory, Ford Motor Company*

D. C. GREER, *State Highway Engineer, Texas State Highway Department*

JOHN T. HOWARD, *Head, Department of City and Regional Planning, Massachusetts Institute of Technology*

BURTON W. MARSH, *Director, Traffic Engineering and Safety Department, American Automobile Association*

OSCAR T. MARZKE, *Vice President, Fundamental Research, U. S. Steel Corporation*

J. B. MCMORRAN, *Superintendent of Public Works, New York State Department of Public Works*

CLIFFORD F. RASSWEILER, *Vice President for Research and Development, Johns-Manville Corporation*

GLENN C. RICHARDS, *Commissioner, Detroit Department of Public Works*

C. H. SCHOLER, *Applied Mechanics Department, Kansas State University*

WILBUR S. SMITH, *Wilbur Smith and Associates, New Haven, Conn.*

K. B. WOODS, *Head, School of Civil Engineering, and Director, Joint Highway Research Project, Purdue University*

Editorial Staff

FRED BURGGRAF
2101 Constitution Avenue

HERBERT P. ORLAND
Washington 25, D. C.

Contents

Laboratory Evaluation of Frost Heave Characteristics of a Slag-Fly Ash-Lime Base Course Mixture

CHESTER W. KAPLAR, Head, Soils Group, U.S. Army Cold Regions Research and Engineering Laboratory, Hanover, N.H.

Sixteen specimens of a slag-fly ash-lime base course mixture were tested for frost susceptibility in the laboratory. The mixture consisted of 66 percent slag, 30 percent fly ash, and 4 percent lime, by weight. Base courses of this type are being used in certain parts of the country in competition with conventional base course materials.

The slag-fly ash-lime base course mixture used in these tests consisted of minus $\frac{3}{8}$-in. material with 30 percent finer by weight than No. 200 mesh sieve and 18 percent finer than 0.02 mm. According to criteria of the Corps of Engineers for base courses, this gradation is classified as frost-susceptible.

Different methods of cure treatment were tried and the effect of aging (up to 12 months duration) on frost susceptibility was observed on 6-in. diameter 6-in. high specimens. Cure treatment before freezing consisted of (a) curing in oven at 140 F for 7 days, (b) "moist curing" in wet sand from $1\frac{1}{2}$ to $12\frac{1}{2}$ months, (c) complete immersion in water for 2 weeks followed by "curing" in wet sand up to $12\frac{1}{2}$ months; and (d) noncuring. Some specimens were subjected to 5 or 6 cycles of freezing and others 10 cycles. Specimens were generally frozen uniaxially from top to bottom at a rate of approximately $\frac{1}{2}$ in. per day.

Test results showed that oven-cured specimens heaved insignificantly even after 10 cycles of slow freezing in an open system test, and "noncured" specimens heaved about 15 percent during a single freezing and were classified to be of low frost susceptibility. In accordance with adopted criteria, based on average rate of heave in millimeters per day, most moist-cured and soaked specimens were classified as negligibly frost-susceptible, although a few approached or were classified as very low frost-susceptible.

Specimens cured only in moist sand performed, on the whole, significantly better than those first submerged in water and then "moist-cured." On "moist-cured only" specimens, heaving decreased with increase in curing time. The maximum measured heave of any of the "cured" specimens, soaked or otherwise, during any one freezing cycle, was approximately 0.2 in. and about 3.3 percent.

•IN MANY PARTS of the country, natural sources of good, clean, base course material are becoming rapidly depleted. In metropolitan areas, it has become necessary to import materials from considerable distance or use a plant-processed product. In

any event, costs run high and are continuously climbing. Highway officials and engineers are constantly searching to achieve economies wherever possible whether in materials or design. The Division and District offices of the U.S. Army Corps of Engineers are among the foremost in searching for improved and economical approaches to all engineering problems.

This is also true of industry where constant efforts are being made to achieve economy in both production and operating costs. One of the major problems faced by big industry is the utilization of large quantities of so-called "waste" or by-products accumulated in a manufacturing or industrial process. In some modern power plants, large quantities of boiler slag and fly ash are by-products which must be either wasted or disposed of in an advantageous manner. Boiler slag is formed by the fusion of the incombustible ingredients of soft coal dust during combustion. It is collected beneath the boiler grates. Fly ash is the fine residue remaining in the smoke after combustion is completed. It is mostly silica and alumina and thus is classed as a pozzolan. The American Society for Testing Materials defines a pozzolan as "a siliceous or siliceous and aluminous material, which in itself possesses little or no cementitious value but will, in finely divided form and in the presence of moisture, chemically react with calcium hydroxide at ordinary temperatures to form compounds possessing cementitious properties."

Fly ash is a man-made pozzolan. It was originally removed by electrostatic precipitation in the flues of chimneys to avoid air polution, but later was found to be an effective pozzolan. Slag has been frequently used for fill or ballast. In recent years a number of uses have been found for the fly ash, one of them as a beneficial ingredient of portland cement concrete.

The cementing properties of volcanic ash were recognized and used by the early Romans over 2,000 years ago. The Romans found that a volcanic ash, found in beds near Naples, when mixed with lime would produce a water-tight cement which would set up under water. Use of this type of cement by the Romans dates back as early as 312 B.C. (1) and it was subsequently used in many engineering structures throughout the Roman empire. Cements thus made from natural volcanic ash are known as "pozzuolana," a name derived from the location of early beds in Italy at Pozzuoli, near Naples. Pozzuolanic cements are still being used in Italy and other countries where similar deposits of volcanic ash are available. The word "pozzolanic" is believed by some to be loosely used today to inaccurately describe a mixture of blast furnace slag, fly ash, and lime because of the similarity of the ingredients.

In the Chicago area and other large cities, such artificial or man-made pozzolanic mixtures have been used for a number of years by city, county, and local transit authorities as base courses in a number of parking areas and roadbeds because of its availability and structural advantage over conventional base course materials. Typical mixtures used consist generally of the following proportions: slag, 66 to 72 percent; fly ash, 24 to 30 percent; and lime, 4 to 5 percent. Available data indicate that the mixture may set up in a period of several months to about 2,000 psi compressive strength and 400 psi flexural strength. (2) Some available rapid freeze-thaw data show 1.9 percent loss after 12 cycles, with no brushing of the specimens. On a cost basis, this material compares very favorably with graded crushed stone, costing about $2.00 per ton at the plant, (Chicago area).

The tests reported herein were conducted by the Arctic Construction and Frost Effects Laboratory* of the U.S. Army Engineer Division, New England, Waltham, Mass. The tests were made as a result of a request for information by the North Central Division of the Corps of Engineers which furnished the necessary ingredients and the supplier's recommended mix proportions.

The Corps' interest in this material stems strictly from a utilitarian viewpoint. However, the requirements of the Corps for base course materials are stringent from the standpoint of stability and bearing capacity. The Corps' requirements specify that

---

* Now merged with the U. S. Army Snow, Ice and Permafrost Research Establishment to form the U. S. Army Cold Regions Research and Engineering Laboratory located at Hanover, N. H.

the material should be non-frost-susceptible when used in climatic areas where freezing temperatures occur. The frost susceptibility of a graded granular material is controlled by specifying that the gradation contain not more than 3 percent by weight of grains finer than 0.02-mm size. The combined gradation of slag-fly ash-lime mixture in proportion of 66, 30, 4 percent, respectively, as used in these studies contains about 30 percent passing the No. 200 sieve and 18 percent finer than the 0.02-mm size.

The laboratory tests conducted by the Arctic Construction and Frost Effects Laboratory were designed to evaluate the frost susceptibility of the mixture as a base course material, not as a cement concrete. However, because the mixture under consideration has cementitious properties, its behavior during freezing would undoubtedly be affected by the degree of cementation achieved at the time of freezing. The degree of cementation and strength that can be achieved is usually dependent on the method and duration of curing. A high degree of cementation and strength in this material has been achieved by heat curing for 7 days at 140 F. This cannot be readily accomplished on the roadbed. Whatever curing occurs must occur under natural conditions existing at the particular location. The material is likely to be exposed to extreme wetness or dryness, depending on the vagaries or vicissitudes of the weather. To evaluate frost susceptibility properly the laboratory tests were designed to take field-curing conditions into consideration. Three different methods of curing treatment were used and, in addition, two specimens were prepared and frozen within a few days of preparation after no-curing treatment except saturation under vacuum in accordance with adopted test procedures.

Other specimens were subjected to one of the three methods of curing treatment for varying periods of time. It was felt that the frost-susceptibility evaluation should consider the effect of elapsed time between placing of the material and the first freeze. If freezing behavior of the mixture should be sensitive to curing time, then a pavement base constructed in April and subjected to natural freezing in late November or December would be expected to react somewhat differently from one constructed in early November.

Another factor that needed to be considered in the evaluation was the possible effect of several freeze-thaw cycles such as might occur in a pavement in most areas of the temperate zone during a single freezing season. In many areas of the United States, the top foot of pavement would probably be subjected to several cycles of freezing and thawing during a winter.

The effectiveness of a cemented material in resisting ice lens formation also depends on its imperviousness and the quality of the cementing bonds. Any breakdown in the bonding such as might be produced by a crack or plane of separation during freezing might make the material more porous and thus provide more channels for passage and retention of water, which on further freezing expands and produces more separation and deterioration. If the bonds are sufficiently strong and the material relatively impervious, deterioration due to frost action will be resisted. Should a cemented material such as is being considered in this study deteriorate in time, irrespective of cause, to a condition approaching its original gradation before cementation, the stability of the base course would be greatly affected by the change, as well as its susceptibility to frost action under adverse conditions of moisture and temperature.

LABORATORY FREEZING TESTS FOR FROST SUSCEPTIBILITY

Sixteen specimens, 6 in. in diameter and 6 in. high were prepared by dry mixing the ingredients in the following proportions by weight: slag, 66 percent; fly ash, 30 percent; hydrated lime, 4 percent. The gradation of the ingredients and the combined gradation of the mixture are shown in Figure 1. The pertinent physical properties of the materials used are given in Table 1. Each specimen was compacted to approximately 100 percent of the maximum dry unit weight as determined by the standard Proctor method (AASHO designation T99-57, Method A) and 10.5 percent moisture content. A compaction curve relating molding water content and dry unit weight is shown in Figure 2. All specimens were compacted in a slightly tapered steel molding

cylinder having a ¼-in. larger diameter at the top, in four equal layers, using a 5.5-lb compaction hammer, 12-in. drop, and 25 blows per layer. The specimens were then removed from the molding cylinder and placed in similarly tapered lucite cylinders.

Curing Treatment

The test specimens were divided into four groups depending on the method of curing. The groups and specimens are identified in Table 2.

After curing each specimen was prepared for freezing tests according to ACFEL standard procedure.

Freezing Tests

Specimens were frozen in pairs, each pair in a separate freezing cabinet. One specimen of each pair was instrumented with thermocouples imbedded 1 in. apart

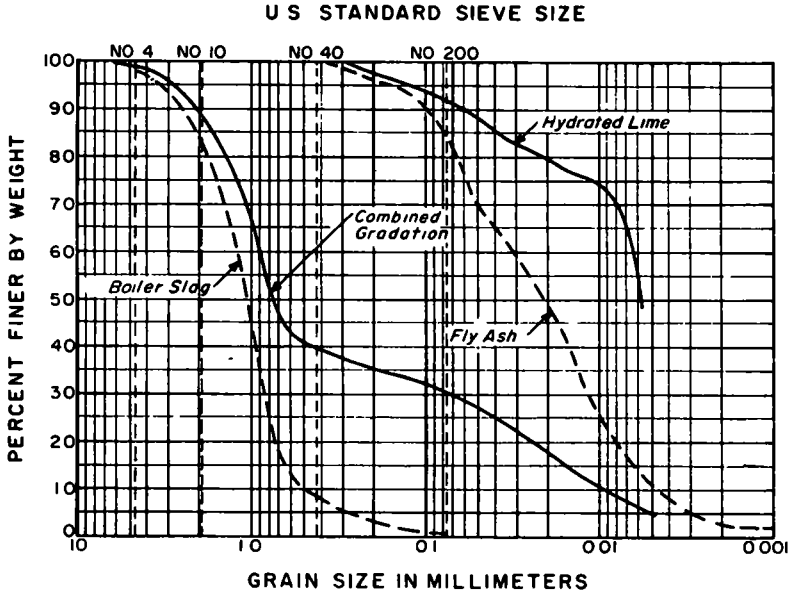

Figure 1. Grain-size distribution of combined mixture and components.

TABLE 1

PHYSICAL PROPERTIES OF SLAG-FLY ASH-LIME BASE COURSE MIXTURES

Composition		Compaction Data of Mixture[1]		Specific Gravity	
Materials Mixed	Proportion by Wt. (%)	Max. Dry Unit Wt. (pcf)	Opt. Moist. Cont. (%)	Each Ingredient	Avg. of Mixture
Slag	66			3.04	
Fly ash	30	122.5	11.0	2.55	2.88
Hydrated lime	4			2.75	

[1] By standard Proctor method (AASHO Designation T99-57, Method A).

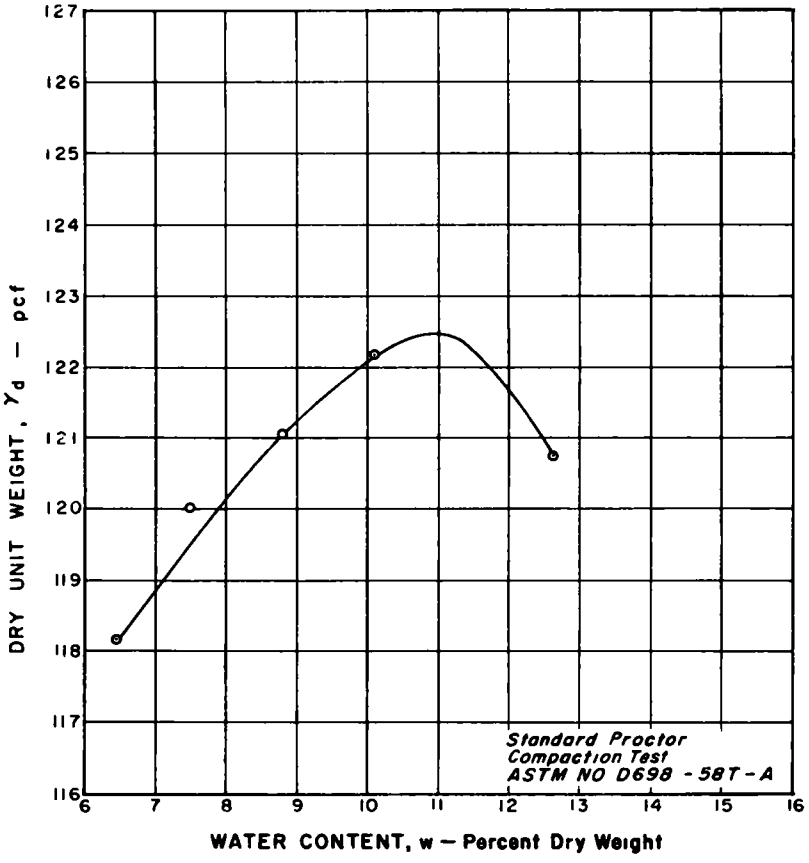

Figure 2. Relationship between dry unit weight and molding water content.

along the longitudinal centerline to measure the penetration of freezing temperature. The freezing cabinets, equipment, methods, and procedures used have been described in detail in two previous publications (3, 4).

All specimens were frozen uniaxially from top to bottom at a rate of approximately ¼ in. per day during the first freezing cycle. Subsequently all specimens subjected to additional repetitions of freezing were frozen at a rate of ½ in. per day to hasten the completion of the studies. Free water was provided at the bottom of all specimens during each freezing period. Originally it was planned to apply only 5 or 6 freeze-thaw cycles to all specimens except the noncured specimens P-21 and P-22, which were frozen only once. After the tests consisting of 5 and 6 freeze cycles were completed on each initial pair (curing period less than 6 weeks) from Groups A, B, and C, it was decided to increase the repetitive freezings to 10 cycles from one specimen of each subsequent pair (undergoing longer curing or aging periods) scheduled to be tested in Group B and C.

Frost-heave and thaw-settlement readings were recorded daily during each freezing and thawing. After final freezing, the frozen specimens were split in half longitudinally for visual observation of ice lens formation and determination of water content distribution. The specimens were thawed by simply turning off the refrigeration, opening the top cover of the freezing cabinet, and exposing both tops and bottoms of the specimens to the ambient 38 F cold room temperature around the cabinets. Thawing was generally achieved in less than 24 hr.

Some swelling was observed in all of the "cured" specimens during curing. The two

TABLE 2
METHOD OF CURING

Group Designation	Specimen No.	Method of Curing
A	P-1	Placed in metal container, sealed and placed in oven at 140 F for 7 days.
	P-2	
B	P-9	Placed in moist sand, top exposed to room temperature and humidity for 2 weeks. Top covered, specimens cured for 1 mo.
	P-10	
	P-11	Same as P-9 and P-10 except cured for 4 mo.
	P-12	
	P-13	Same as P-9 and P-10 except cured for 12 mo.
	P-14	
C	P-15	Buried in moist sand, top exposed to room temperature and humidity for 3 days, specimen placed in lucite cylinder and then submerged in water with porous stones on top and bottom for 2 weeks. Removed from water and placed in moist sand inside lucite cylinders with porous stones top and bottom for 1 mo, all within covered container.
	P-16	
	P-17	Same as P-15 and P-16 except cured for 4 mo.
	P-18	
	P-19	Same as P-15 and P-16 except cured for 12 mo.
	P-20	
D	P-21	Noncured. Specimens saturated under vacuum and freezing started within 5 days.
	P-22	

oven-cured specimens in Group A increased in length approximately 0.025 in. The increase in length of specimens in Group B ranged from 0.004 to 0.045 in. with an average increase of approximately 0.02 in. The soaked specimen in Group C increased in length by an average of 0.14 in. The two "noncured" specimens in Group D shrank 0.068 and 0.047 in., respectively, during the first day of freezing, probably as a result of the tensile stress developed in the pore water when freezing began.

Test Results

A summary of specimen preparation and freezing data is given in Tables 3 and 4. Figure 3 shows the heave and temperature penetration data of the two "noncured" specimens (P-21 and P-22) that were frozen at approximately ¼ in. per day in a standard ACFEL frost susceptibility test (one freezing only). The heave and thaw settlement data for all other specimens subjected to several cycles of freezing and thawing are shown in Figures 4, 6, and 8 showing the total heaving and amount of settlement for each cycle. The total cumulative heave (heaving less thaw-settlement) remaining after each freeze-thaw cycle has been plotted for each specimen in Figures 5, 7, and 9.

The daily heave plots for specimens in Groups A, B, and C were in most cases very similar in form to the heave plots shown in Figure 3, except for order of magnitude. Because of space limitations these plots are not presented in this paper. The greatest portion of the heaving occurred during the early part of the test. Most heave plots typically showed a fairly steep initial heave rate and a gradual flattening out, as

TABLE 3

SPECIMEN PREPARATION DATA FOR SLAG-FLY ASH-LIME BASE COURSE MIXTURE[a]

Group	Specimen No.	Molded Height (in.)	Height After Curing[b] (in.)	Increase in Height (in.)	Dry Unit Weight[c] (pcf)	Degree of Compaction[c] (%)	Void Ratio (e)
A	P-1	5 873	5 902	0 029	122 9	100	0 452
	P-2	5 875	5.897	0 022	123.0	100	0 451
B	P-9	5 99	5 994	0 004	120 8	99	0.477
	P-10	6.00	6 009	0 009	120 7	99	0 479
	P-11	5 960	5 994	0 034	121 2	99	0 472
	P-12	6 000	6 01	0 01	121 2	99	0.472
	P-13	5.99	6.004	0 01	120 3	98	0.483
	P-14	5 98	6 025	0 05	119 8	98	0 490
C	P-15	5.98	6 114	0 13	118 9	97	0 501
	P-16	5.99	6 154	0.16	118.2	97	0.510
	P-17	5 98	6 125	0 15	118.7	97	0.503
	P-18	5 98	6.118	0 14	118 8	97	0.502
	P-19	6 00	6 144	0 14	118 3	97	0 509
	P-20	5.99	6.11	0 12	118 9	97	0 501
D	P-21	5.94	-	-[d]	122 3	100	0 459
	P-22	5.93	-	-[d]	122 4	100	0 458

[a] All specimens molded at 10.5 percent water content.

[b] Curing time for each specimen given in Table 4.

[c] Before freezing.

[d] Shrank in height average of 0.058 in. during first day in freezing cabinet.

TABLE 4

SPECIMEN FREEZING TEST DATA FOR SLAG-FLY ASH-LIME BASE COURSE MIXTURE

Specimen No.	Total Curing Time (weeks)	No of Freeze Cycles	Water Content (% Dry Weight) After Curing	Water Content (% Dry Weight) After Saturation	Water Content (% Dry Weight) After Freezing Test	Percent Moisture Change[a]	Initial Height (in.)	Final Height (in.)	Total Cumulative Heave (%)
P-1	1	5	10 2	15.8	14 9	-5.7	5 90	5.93	0.5
P-2	1	5	10 0	15 7	15 3	-2 5	5 90	5.94	0 7
P-9	6	6	15.3	16.6	17 3	4 2	5 99	6 40	7 0
P-10	6	5	15.6	16 7	18.2	9 0	6 01	6.41	6 7
P-11	15	6	16.0	16 5	16 8	1 8	5 99	6 10	1 9
P-12	15	10	16 0	16 5	18 3	10 9	6 01	6 25	4 0
P-13	54	10	16 4	16 9	15 1	-10 7	6 00	6 12	2 0
P-14	54	6	16 2	17 2	16.2	-5.8	6 03	6 05	0 3
P-15	6	6	15 7	17.5	20.0	14 3	6 11	6 65	8.8
P-16	6	6	14 4	17.6	21 0	19 3	6 15	6 69	8 8
P-17	15	10	17 6	17 6	20 2	14 8	6.12	6.52	6 5
P-18	15	6	17.5	17.6	19 0	8 0	6 12	6 40	4.6
P-19	54	6	17 8	17 8	19 5	9.6	6.14	6 51	6 0
P-20	54	10	17 5	17 5	19.6	10.2	6.11	6 63	8 5
P-21	-	1	-[b]	16 1	23 1	43 4	5 94	7 06	18 9
P-22	-	1	-[b]	16 0	21 1	31 8	5 93	6.84	13.3

[a] Based on ratio of weight of moisture gained to initial weight of water in specimen before freezing.

[b] No curing.

shown in Figure 3. This is believed due to restraint caused by side friction between specimen and walls of container even though the container was tapered with larger diameter at top. Some swelling was observed in nearly all specimens during curing, as shown in Table 3. Also, generally more side friction develops, because of slight lateral expansion during freezing in specimens which exhibit negligible or very low frost heaving characteristics. In soils with more pronounced frost-susceptibility characteristics, heaving at any plane raises all the soil above that plane to a position of greater diameter in the tapered cylinder, thus minimizing frictional restraint.

The vertical water content distribution before and after completion of final freeze is shown for all specimens in Figures 10, 11, and 12.

Photographs of sections of several typical frozen specimens are shown in Figure 13. Visual observations of appearance of each specimen after final freeze are given in Table 5.

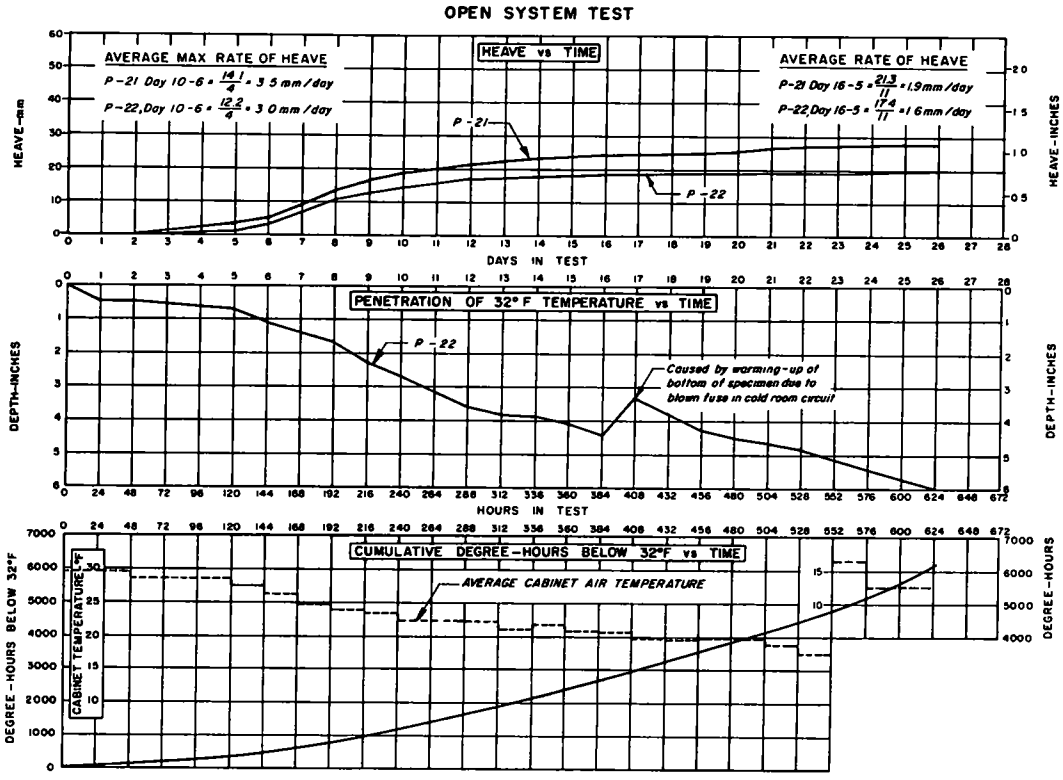

Figure 3. Temperature and heave data for specimens P-21 and P-22, not cured.

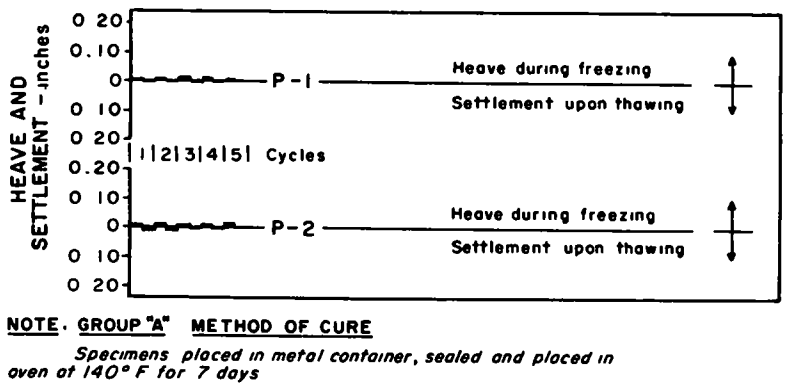

NOTE. GROUP "A" METHOD OF CURE

Specimens placed in metal container, sealed and placed in oven at 140° F for 7 days

Figure 4. Heave and settlement vs cycles of freeze-thaw for Group A.

Discussion of Results

Specimens P-1 and P-2, which were oven cured for 7 days at 140 F before freezing, were the least affected even after 5 cycles of freezing and thawing. The average cumulative heave of these two specimens was less than 0.025 in. after 5 freezings. The test results obtained for each freeze-thaw cycle for these two specimens are shown in Figure 4 in the form of a bar graph. The measured heave at the completion of each freezing is plotted above the zero reference line and the settlement occurring during

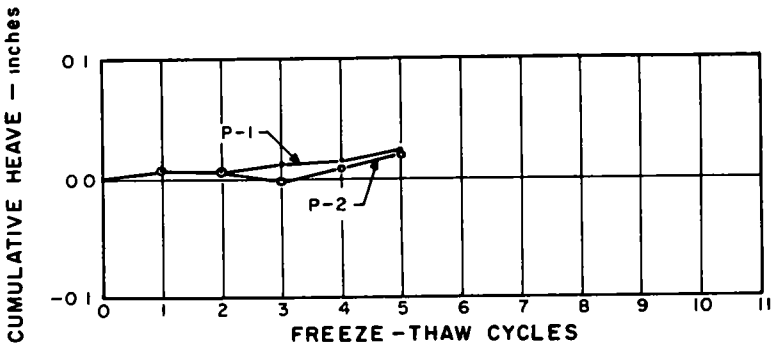

Figure 5. Cumulative heave vs time and freeze-thaw cycles.

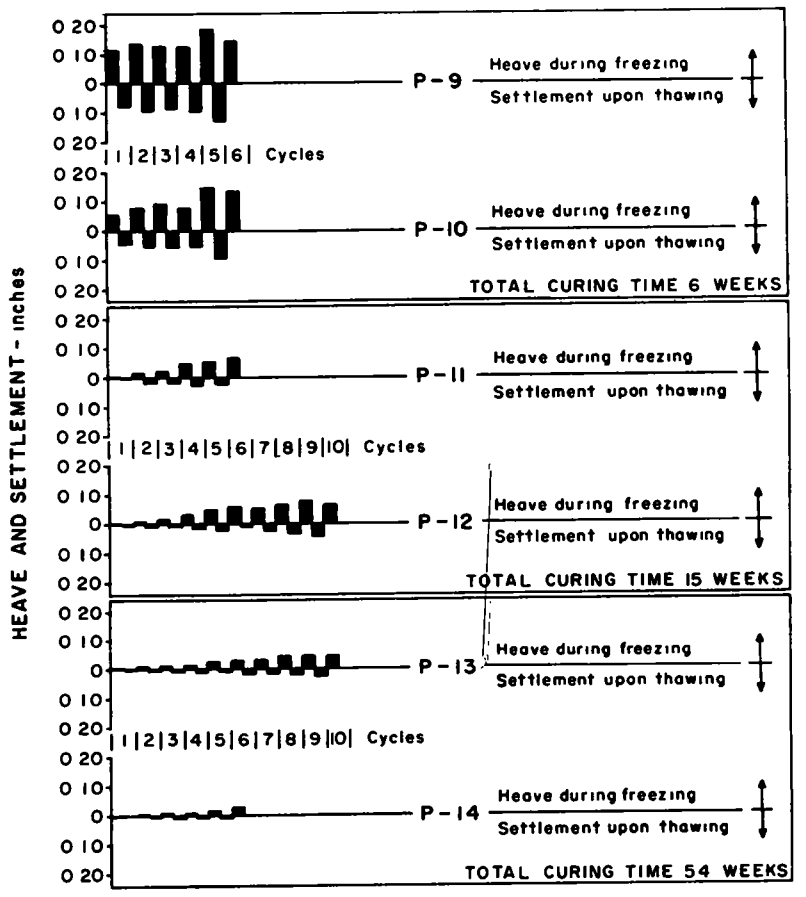

NOTE GROUP "B" METHOD OF CURE

Specimens buried in moist sand, top exposed to room temperature and humidity for two weeks, top covered and curing continued for total period as indicated above.

Figure 6. Heave and settlement vs cycles of freeze-thaw for Group B.

thaw is plotted below the reference line to permit comparison of all heave settlement data. Figure 5 shows the total cumulative heave of each specimen vs freeze-thaw cycles.

Examination of the data obtained from these tests shows that "noncured" specimens P-21 and P-22 heaved the greatest amount, approximately 1 in. The average rate of heave computed over a continuous period of 11 days when heaving and frost penetration were fairly uniform (see Fig. 3) was 1.9 and 1.6 mm per day, respectively. The average maximum rate of heave was much greater, being 3.5 and 3.0 mm per day, over a consecutive period of 4 days. According to criteria used by ACFEL the frost susceptibility of "noncured" mixture of slag-fly ash-lime is classified as low but approaching medium.

Table 6 gives the scale for classification of the degree of frost susceptibility of a soil tested during procedure described in this paper. It is based on the average rate of

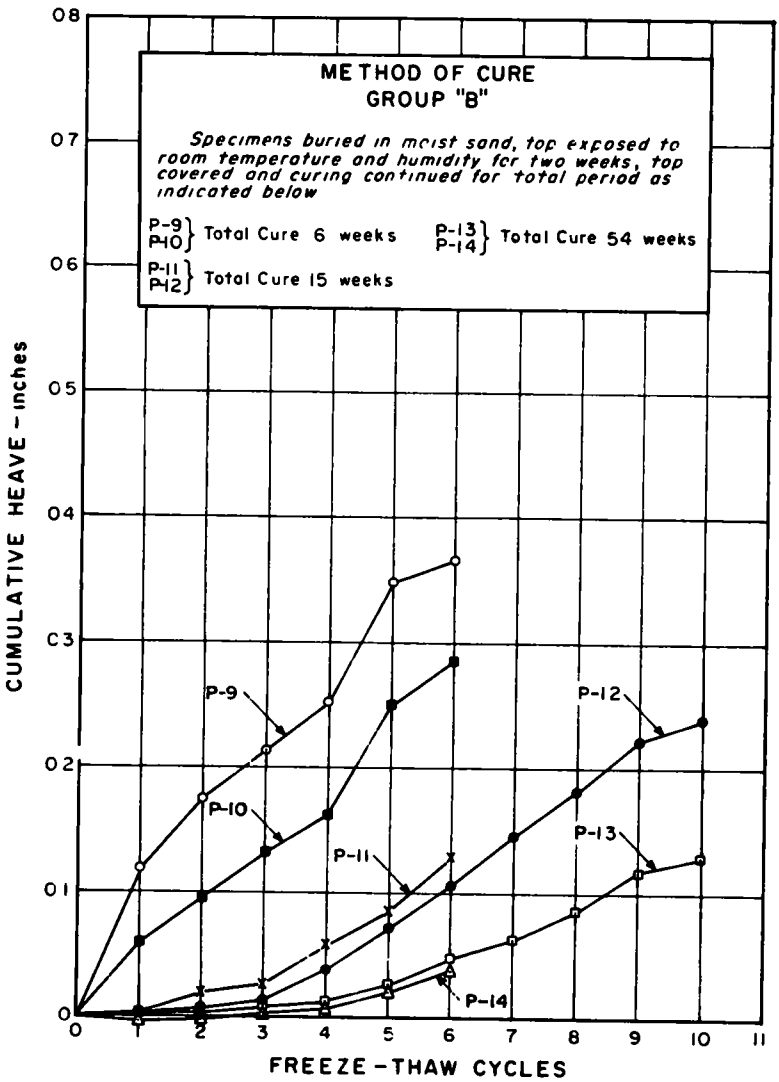

Figure 7. Cumulative heave vs time and freeze-thaw cycles.

heave over several consecutive days and has been adopted for rates of freezing between ¼ and ¾ in. per day.

Average rates of heave were computed for each freeze cycles of each specimen. Because the heave plots were not uniform, the average maximum rates of heave were also computed, generally for a 3- or 4-day period but never less than for a consecutive 2-day period. The computed heave rates are shown in Figure 14. From data presented in this figure it can readily be seen that the heaving characteristics of the soaked specimens P-15 thru P-20 were much more pronounced than those of the moist-cured specimens of Group B, with the exception of specimens P-9 and P-10, which were cured for only 6 weeks. Also in this figure there is a general tendency for both average maximum and average heave rates to increase slightly with succeeding freeze cycles. Except for two instances (P-16 and P-19) both curves remained below the critical 1.0-mm per day dividing line at which the frost susceptibility classification of a material changes from very low, to low. However, the average

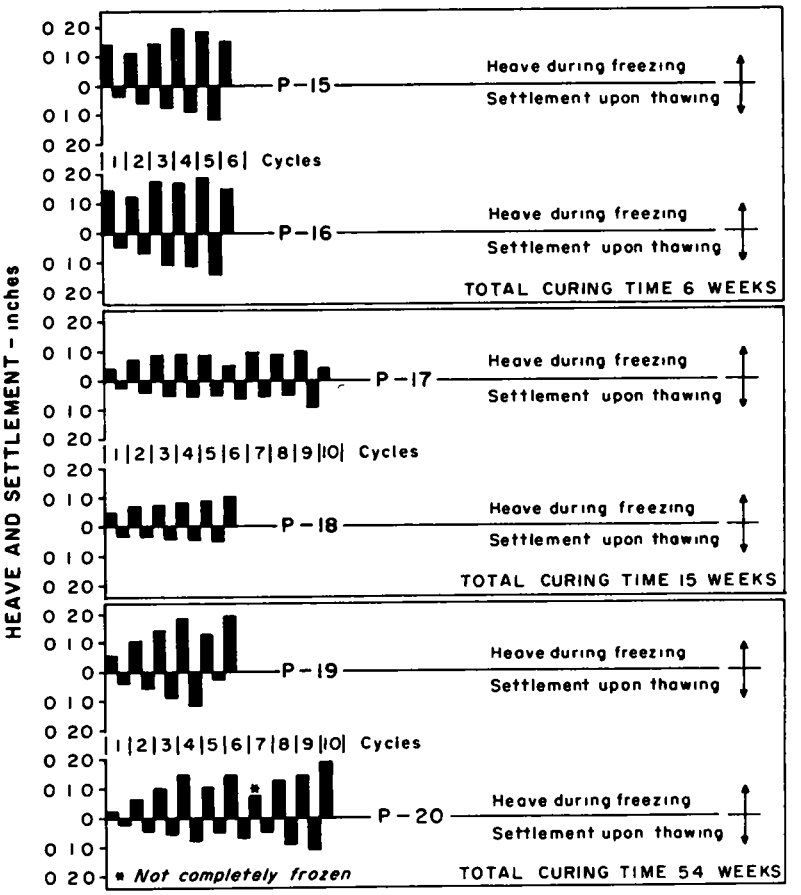

NOTE GROUP "C" METHOD OF CURE

Specimens buried in moist sand for three days, top exposed to room temperature and humidity, then submerged in water for two weeks followed by curing in moist sand for total period indicated above

Figure 8. Heave and settlement vs cycles of freeze-thaw for Group C.

maximum heave rate in specimen P-9 also came very close to this dividing line at one point. In these tests, because of the apparent frictional restraint developed in the test cylinders by the swelling of the material during curing and probable lateral expansion during freezing, the author believes the average maximum rates of heave are more truly indicative of the potential frost behavior of this material under adverse conditions of freezing than the average rates of heave.

From the data shown in Figures 6 and 8 it can be observed that there is, in general, a tendency for the magnitude of heaving to increase slightly with each succeeding cycle. Whether this would be true in a pavement where traffic would tend to densify the thawed material is not known. It appears reasonable to assume that the amount of thaw settlement in an active pavement would be greater after each thaw because of the traffic loads and that subsequent heaving might also be less because of the sustained high density of the material. In the laboratory test settlement was influenced only by the overlying weight of material and a static surface load of 0.5 psi.

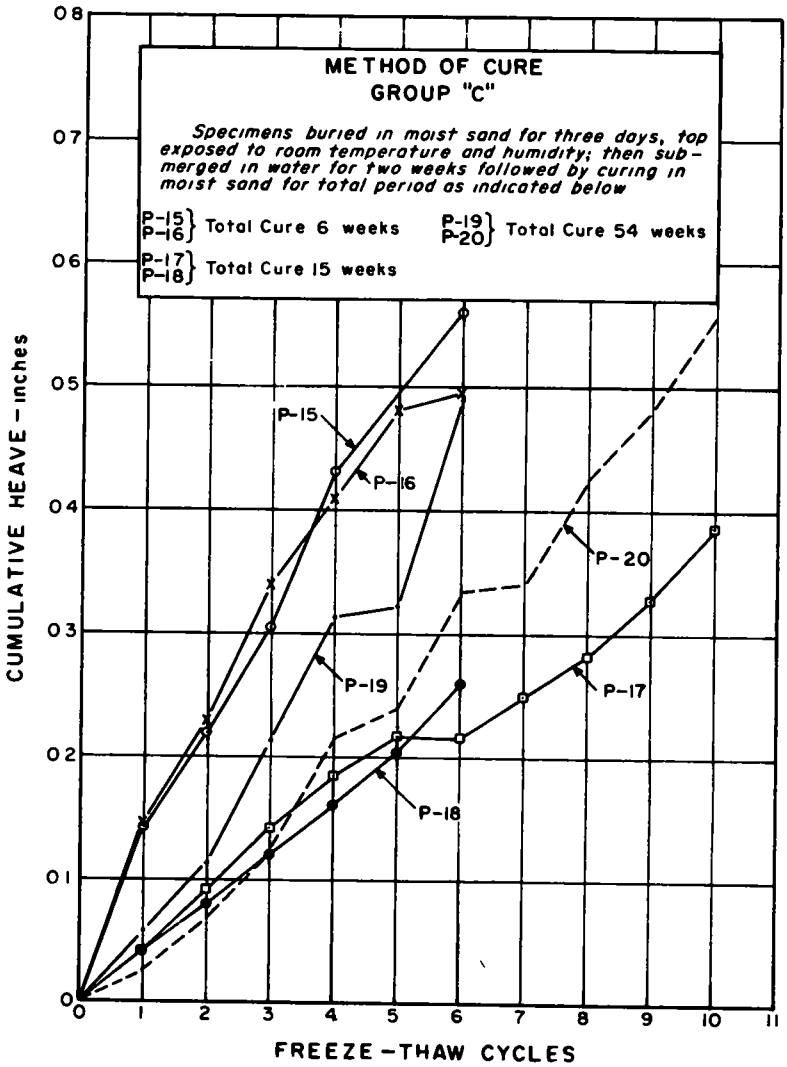

Figure 9. Cumulative heave vs time and freeze-thaw cycles.

Examination of data from specimens of Group B and C, as plotted in Figures 6 through 9, shows that specimens not previously soaked in water after preparation reacted more favorably to freezing than those soaked for 2 weeks. On these plots, for the nonsoaked specimens (P-9 through P-12) resistance to heaving was substantially improved with duration of curing time. However, specimens that were moist cured (P-9 and P-10) for only 6 weeks did not behave substantially better than those that were soaked (P-15 through P-20). Nevertheless, considerable improvement can be observed in the bar graph for the two specimen which were moist cured 4 months before freezing. Specimens moist cured for 1 yr (P-13 and P-14) show a significant reduction in frost heaving even after 10 repeated freezings. It then appears that curing conditions and duration of curing before freezing exert a considerable influence on subsequent behavior during freezing under adverse conditions of moisture availability.

Figure 15 shows a summary plot relating total cumulative heave vs freeze-thaw cycles and curing time for all specimens used in this investigation.

The water content data in Figures 10, 11 and 12 and data in Table 4 show that except for the oven-cured specimens (P-1, P-2, P-13, and P-14) all other specimens indicated some gain of moisture during the tests. The most substantial moisture gain was evident in the "noncured" specimens P-21 and P-22.

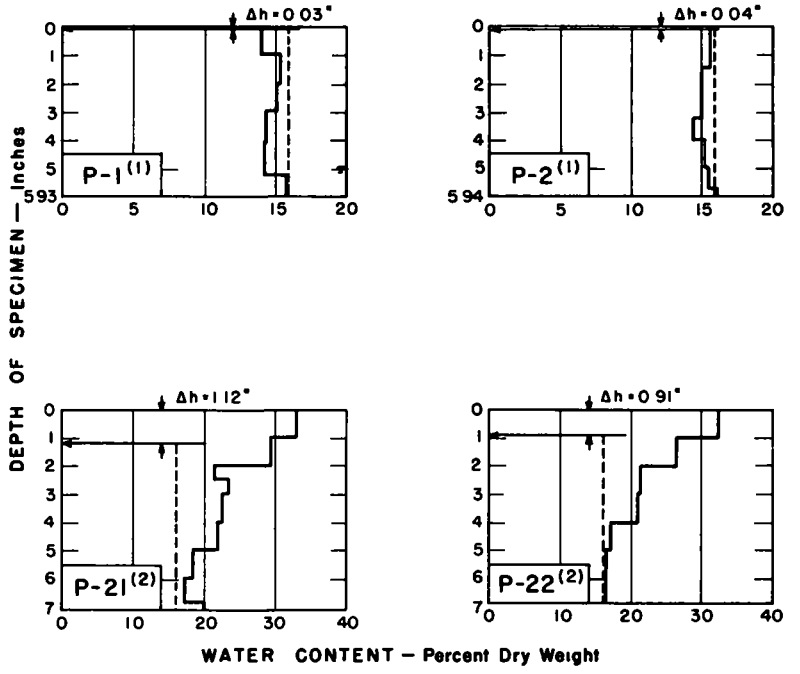

Figure 10. Water content distribution in specimens after final freezing, Groups A and D.

It can be seen in Figures 13b and 13c, that some disintegration had begun in the top portions of some of the specimens, especially those submerged in water as part of curing treatment. A description of each specimen after final freeze, based on visual observations, is given in Table 5. Based on the observations made, more disintegration and incipient disintegration was found in the soaked specimens in Group C than in those of Group B.

CONCLUSIONS AND RECOMMENDATIONS

From the data available from these tests, several conclusions are evident:

1. The mixture of slag-fly ash-lime as used in these tests is classified as low frost-susceptible but approaching medium if subjected to freezing temperatures before it has been adequately cured.

2. For moist-cured specimens (Group B) resistance to frost action was improved by increase in curing time (see Fig. 15). What the minimum time for curing should be has not been established by these studies. The available data show that, for specimens cured in moist sand, resistance to heaving improved with increase in curing time at

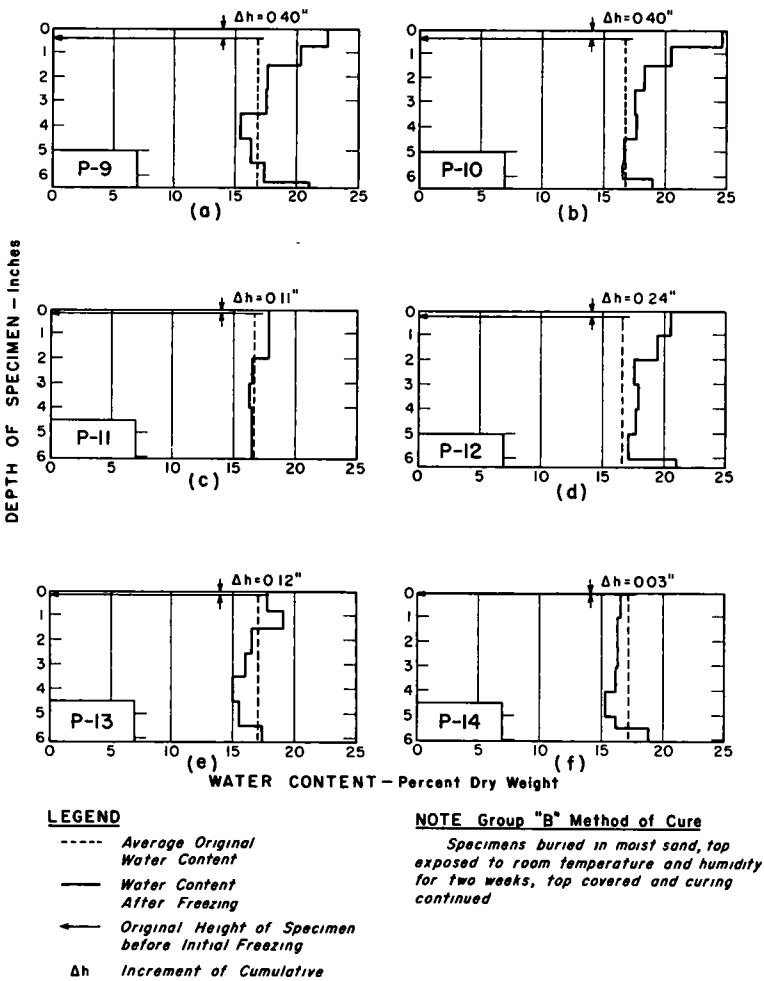

Figure 11. Water content distribution in specimens after final freezing, Group B.

least beyond 15 weeks. It is possible that optimum curing time occurs nearer the 15-week period than the 54-week period and may be adequate at less than 15 weeks.

In the use of this material as a base course in a roadway, it is important that it be placed sufficiently early in the season to permit adequate curing before onset of freezing weather.

3. Specimens that were soaked (Group C) before curing in moist sand showed less resistance to frost action than nonsoaked specimens (Group B). This is indicated by the heave data shown in Figure 6 through 9, the computed average maximum and average rates of heave shown in Figure 14, and the physical appearance of specimens after freezing as described in Table 5. Furthermore, resistance to heaving was not significantly improved with increase of curing time after soaking, as was observed for the nonsoaked specimens. In fact, the data show that heaving characteristics after 1 yr of curing were very similar to those exhibited after 6 weeks of curing.

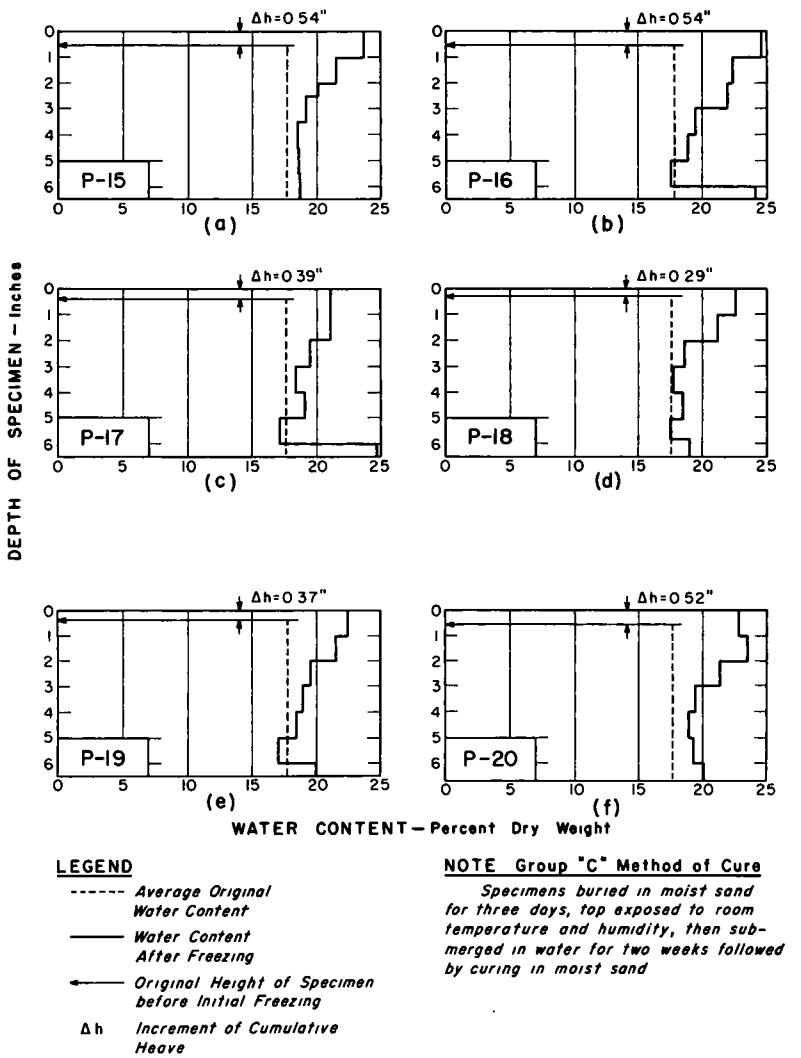

Figure 12. Water content distribution in specimens after final freezing, Group C.

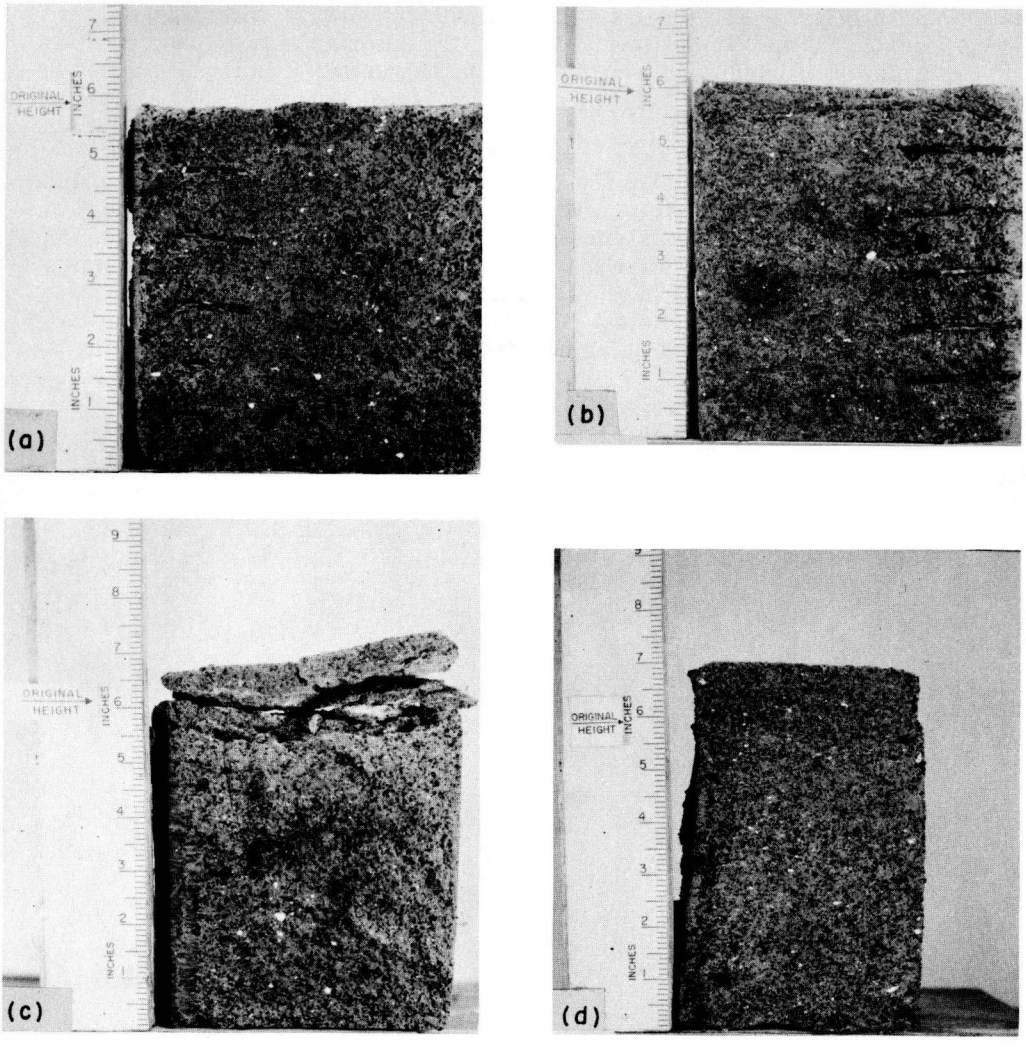

Figure 13. Photographs of vertical sections of several typical frozen specimens of a slag-fly ash-lime mixture: (a) Specimen P-1—cured 7 days at 140 F; after fifth freeze, horizontal grooves at left show locations of thermocouple wires; (b) Specimen P-13—cured 54 weeks in moist sand; after tenth freeze, horizontal grooves at right show locations of thermocouple wires; (c) Specimen P-16—cured submerged for 2 weeks and 4 weeks in moist sand; after sixth freeze; and (d) Specimen P-21—noncured; after 1 slow freeze ($\frac{1}{4}$ in. per day).

In field practice, it appears that it would be advantageous that this material be protected from being soaked or inundated soon after placing.

The computed average heave rate (over a consecutive period of 5 days or more) in these tests in no instance exceeded 1.0 mm per day except for the two noncured specimens. However, the average maximum rate of heave over a consecutive period of generally 2 to 4 days, exceeded 1.0 mm per day in two specimens during one of their respective freeze periods, namely in specimens P-16 and P-19.

Base course specimens that heave in the laboratory freezing tests at an average rate of heave exceeding 1.0 mm per day are likely to show undesirable heaving in the field, and subsequent weakening characteristics when adverse conditions of water

TABLE 5

VISUAL OBSERVATIONS OF FROZEN SPECIMEN AFTER COMPLETION OF FREEZING TESTS

Specimen No	Location, Distance from Top (in)	Ice Lenses Visible	Approx Thickness of Segregated Ice	Spacing Between Segregated Ice (in)	Other Data and Observations
P-1	0 to bottom	No	-	-	Material hard like concrete after oven-drying
P-2	0 to bottom	No	-	-	Material hard like concrete after oven-drying
P-9	0 to 1½	Yes	Hairline	1/32 to 1/16	Specimen not completely frozen
	1½ to 3½	Yes	Very fine	⅛ to ¼	
	3½ to 6¼	Yes	Very fine	Scattered	
	6¼ to bottom	-[a]	-	-	
P-10	0 to 1½	Yes	Very fine to hairline	1/32 to 1/16	
	1½ to 2½	Yes	Hairline		
	2½ to 6⅛	Yes	Very fine	Scattered	
	6⅛	Yes	Hairline	-	
	6⅛ to bottom	No			
P-11	0 to 1	Yes	Very fine to hairline	1/16 to ⅛	Some disintegration observed in top ½ in
	1 to 3	Yes	Very fine	⅛ to ¼	
	3 to bottom	No	-	-	
P-12	0 to 1	Yes	Very fine to hairline	1/32 to 1/16	Some disintegration observed in top ½ in
	1 to 2	Yes	Very fine	¼ to ½	
	2 to bottom	No	-	-	
P-13	0 to 1½	Yes	Very fine to 1/64 in	⅛ to ¼	Top ¾ in shows sharp separation of several layers due to ice lensing
	1½ to 2½	Yes	Very fine to hairline	¼ to ½	
	2½ to bottom	Yes	Very fine	Scattered	
P-14	0 to 2	Yes	Very, very fine	1/16 to ⅛	Evidence of separation of ¼-in thick layer visible at top of specimen
	2 to 5	No			
	5 to 5⅛	Yes	Very, very fine	⅛	
	5⅛ to bottom	No			
P-15	0 to 2½	Yes	Very fine to hairline	1/64 to ¼	Specimen somewhat dried around circumferential area of top portion, horizontal cracks visible in top 1 in of specimen
	2½ to bottom	Yes	Fine (short)	Scattered	
P-16	0 to 4	Yes	Very fine to hairline	⅛ to ¼	Severe layered disintegration in top 1½ in
	4 to bottom	Yes	Fine (short)	Scattered	
P-17	0 to 2	Yes	Hairline	1/32 to 1/16	Slightly dried around circumferential area of top portion, incipient and visible layered separation on top ¾ in
	2 to 3	Yes	Very fine	⅛ to ¼	
	3 to bottom	Yes	Very, very fine	Scattered	
P-18	0 to 1	Yes	Very fine to hairline	1/16 to ⅛	Incipient and visible layered separation on top ¾ in
	1 to 3	Yes	Very fine	⅛ to ¼	
	3 to bottom	Yes	Very fine	Scattered	
P-19	0 to 2	Yes	Very fine to hairline	¼	Specimen slightly dried around circumferential area of top portion, Considerable disintegration in top ¾ in and incipient disintegration in next ¾ in
	2 to 3	Yes	Very fine to hairline	⅛ to ¼	
	3 to 5	Yes	Very fine to hairline	¼	
	5 to bottom	Yes	Very fine to hairline	Scattered	
P-20	0 to 2	Yes	Very fine to hairline	1/32 to 3/32	Specimen slightly dried around circumferential area of top portion, considerable incipient spalling visible in top 1¼ in
	2 to bottom	Yes	Very fine	Scattered	
P-21	0 to 2	Yes	Very fine to hairline	1/32 to 1/16	Slightly dried around circumferential area of top portion, Specimen soft upon thawing; Crumbled easily after oven-drying
	2 to 2½	Yes	Very fine	1/16 to ¼	
	2½ to 3	Yes	Very, very fine	Scattered	
	3 to bottom	No			
P-22	0 to 1	Yes	Very, very fine	1/16	Slightly dried around circumferential area of top portion, Specimen soft upon thawing; Crumbled easily after oven-drying
	1 to bottom	No			

[a] Unfrozen

TABLE 6

CLASSIFICATION OF DEGREES OF FROST SUSCEPTIBILITY

Average Rate of Heave (mm/day)	Frost Susceptibility Classification
0 - 0.5	Negligible
0.5 - 1.0	Very low
1.0 - 2.0	Low
2.0 - 4.0	Medium
4.0 - 8.0	High
Greater than 8.0	Very high

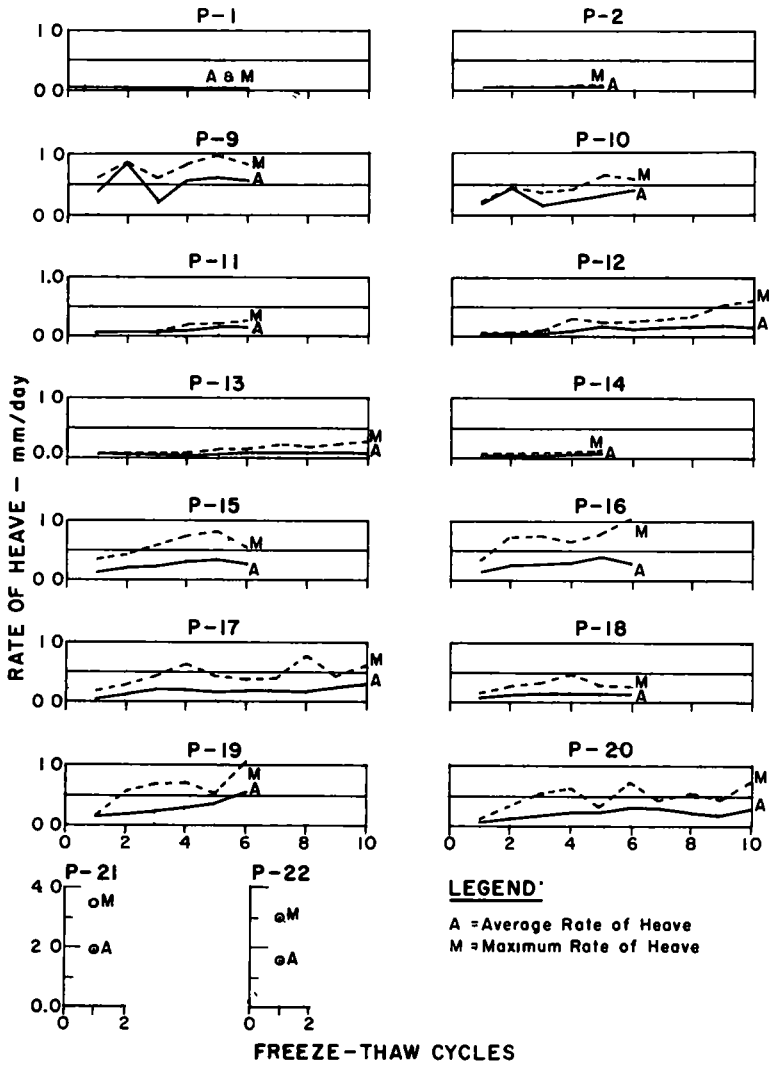

Figure 14. Rate of heave vs freeze-thaw cycles.

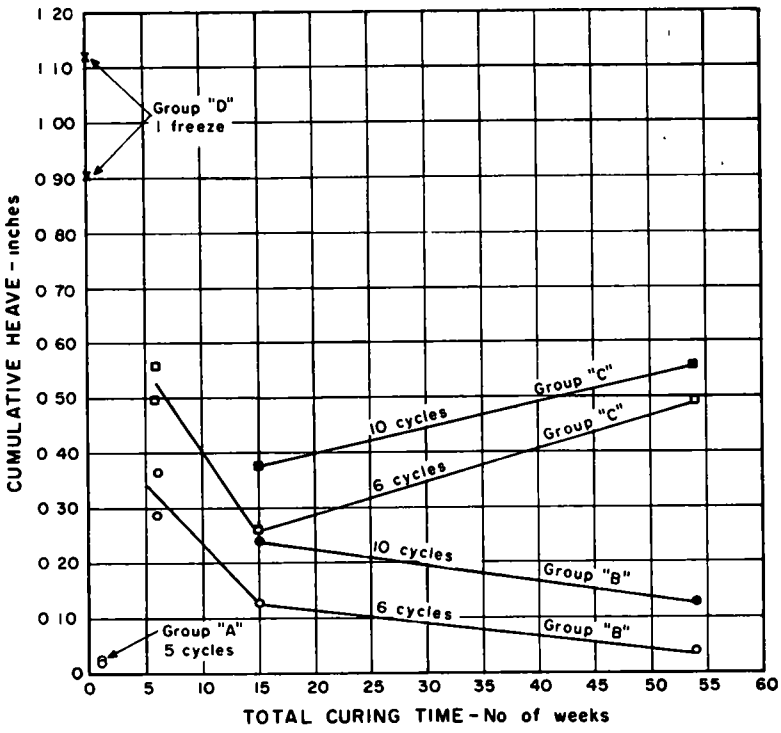

Figure 15. Summary of cumulative heave vs curing time and freeze-thaw cycles.

availability and temperature are present. The author further wishes to emphasize that the laboratory freezing tests simulate extremely severe field conditions in which an unlimited supply of water is available to the base course during the freezing process. Such a condition is seldom present in a well-designed roadway where adequate drainage has been provided. Therefore, the test results obtained in the laboratory during freezing are unlikely to be duplicated in severity under most normal field conditions.

It is recognized that the test data presented in this paper do not provide answers to all the questions that might be asked relative to the frost-heaving characteristics of slag-fly ash-lime base course mixtures. Much more study and experimentation can be done in this area, particularly to determine minimum standards of field-curing treatment and time of field placement to insure the most favorable resistance to possible effects of freezing. Freezing effects on different mix proportions, on mixes containing other types of aggregate and having different densities could be studied. No evaluation of frost susceptibility can be complete without methodical observation of field behavior of slag-fly ash-lime base courses placed in unfavorable areas under unfavorable climatic conditions Further study in all the areas indicated would provide data of considerable interest and shed more light on the frost behavior characteristics of artificial pozzolanic mixtures.

ACKNOWLEDGMENTS

The studies reported herein were carried out under the over-all direction of the Civil Engineering Branch, Engineering Division, Military Construction, Office, Chief of Engineers, Department of the Army, of which Thomas B. Pringle is Chief and Frank B. Hennion is Assistant Chief. Kenneth A. Linell was Chief of the Arctic Construction and Frost Effects Laboratory, U.S. Army Engineer Division, New England, Waltham, Mass.

REFERENCES

1. Chicago Fly Ash Company, "Chicago Fly Ash in Quality Concrete Mixes." Chicago
2. Hollon, G. W., and Marks, B. A., "A Correlation of Published Data on Lime-Pozzolan-Aggregate Mixtures for Highway Base Course Construction." Civil Engineering Studies, Highway Engineering Series No. 2, Department of Civil Engineering, Univ. of Illinois (1960).
3. Arctic Construction and Frost Effects Laboratory, "Cold Room Studies, Third Interim Report of Investigations." U.S. Army Engineer Division, New England, Waltham, Mass., Tech. Report 43, Vol. 1 (1958).
4. Linell, K. A., and Kaplar, C. W., "The Factor of Soil and Material Type in Frost Action." HRB Bull. 225, 81-126 (1959).
5. Haley, J. F., and Kaplar, C. W., "Cold-Room Studies of Frost Action in Soils." HRB Special Report 2, 246-267 (1952).

Experimental Study on Soil Moisture Transfer In the Film Phase Upon Freezing

A. R. JUMIKIS, Professor of Civil Engineering, Rutgers University

This paper reports on experimental studies on the measured magnitudes of the streaming potentials developed in open freezing soil systems in connection with film flow of soil moisture, as well as illustrates the amount of soil moisture transferred, the magnitude of the developed streaming potentials, and depth of frost penetration as a function of the porosity of the freezing soil systems. The maximum magnitude of developed streaming potential was determined to be 350 mv at about n = 41 percent porosity. The streaming potential developed is approximately proportional to the amount of soil moisture transferred. The maximum frost penetration depth occurs at the same porosity at which the maximum amount of soil moisture is transferred and at which the maximum magnitude of developed streaming potential occurs. The over-all conclusion from observations in this experimental study is that the dry side of the standard compaction test (viz., porosity) seems to be the best condition for minimum amount of soil moisture transferred and minimum frost penetration depth attained.

•THE MOTION of water forced by thermal energy through a fixed porous medium such as a column of silt or clay soil induces an electric potential difference between the two ends of the soil column. A process of soil moisture translocation from points at higher temperature to points at lower temperature in a porous medium brought about by means of a thermal potential (heat, for example) is termed "thermo-osmosis." The induced electric potential in clay-water systems where the water is moving from a higher temperature level to the lower one is also known by the term "streaming potential." The phenomenon of induced electric potential, being a component part of the electric diffuse double layer theory, offer an important basis for the theory of the mechanism for the translocation of soil moisture in the film phase, particularly upon freezing.

As described by the author (1), the phenomenon of the streaming potential, in its turn, is based on the electric diffuse double layer theory. According to this theory, the solid particle of a soil is surrounded by an electric double layer. One layer of this double layer is formed by the negative charge on the surface of the colloidal (clay) particle. The negatively charged soil particles tend to surround themselves mostly with ions of the opposite charge (cations), thus forming the second or outer layer of the electric double layer. This outer layer is formed in the soil water by orientation of the polar molecules of water at the interface between the solid colloidal particle and the dispersion medium, water. Thus in the water (film) near the solid particles an ionic aura, or atmosphere, exists. The electrokinetic effect in a porous system is induced upon the motion of one phase of the disperse colloidal system (water) relative to the other (solid particles).

On the application of a freezing thermal gradient (heat energy) across a vertical column of a soil-water system (freezing temperature at the top of the column) the soil moisture would translocate in the thermal field upward from the ground-water table toward the cold front, thus displacing upward the positive electric charges within the diffuse double layer. Hence the expression "electric diffuse double layer." This phenomenon—streaming potential—results in a potential difference between the two ends of the vertical column of the freezing soil system.

Previous studies by the author (2) on electrokinetic phenomena in open clay-water systems indicate that for each type of soil packed at different porosities different amounts of soil moisture are transferred from the ground-water table to the cold front. Depending on the intensity of the freezing temperature gradient and the position of a reference point above the ground-water table, induced electric potentials (streaming potentials) were measured in the order of magnitude from about 40 to 240 mv (1). Hence the problem in this study is to learn the relationships of the various factors involved in damage to roads by frost when the slow process of upward migration of soil moisture from the ground-water to the cold front takes place at porosities at which the film flow can be expected to be more effective than other soil moisture transfer mechanisms. Particularly, it is interesting to know what the relationship is between the developed streaming potential and the porosity, as well as the amount of soil moisture transferred.

METHODOLOGY

To learn the various relationships involved in the freezing-moisture migration-streaming potential process, Dunellen soil (-10 material), a silty glacial outwash material, classed as A-2-4 by the Highway Research Board classification system, was prepared at different porosities and subjected to a freezing thermal gradient. The particle-size accumulation curve of the soil studied is shown in Figure 1.

The porosity range studied was from n = 27.8 percent to n = 47.8 percent. The prepared soil systems were cylinders, 30 cm high and 15 cm in diameter, placed with their lower ends in "ground-water" so that during the freezing/moisture migration process the ice lenses could be connected via the soil moisture films to the ground-water supply. Thus, open soil systems were studied. The volume of these soil systems was 5,605 cu cm. To prevent lateral heat flux, the soil cylinders were insulated laterally with cork and vermiculite.

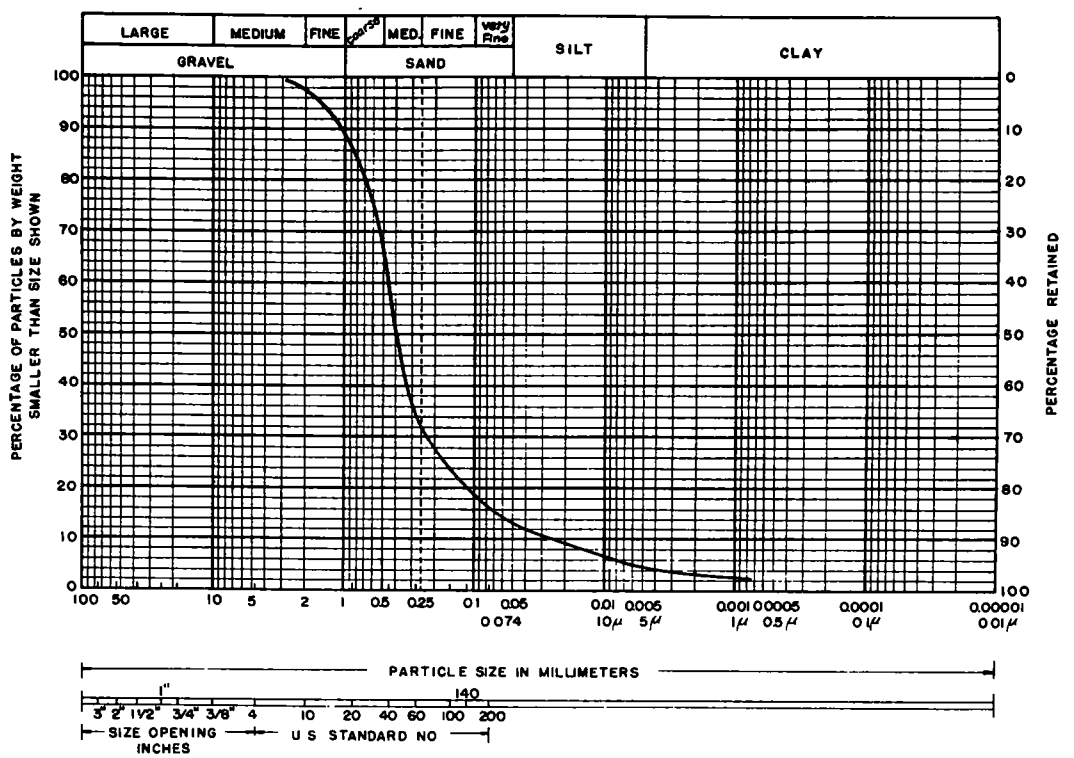

Figure 1. Dunellen soil particle-size accumulation curve.

The freezing period to which the soil systems were subjected was seven days (168 hr) duration, which being consistent with some cold spells observed during the winter months in the New Brunswick, N.J., area. The microclimate was lowered at 24-hr intervals. The lowering schedule was as follows:

Elapsed Time After Start of Test (hr)	Temperature of Microclimate in	
	°C	°F
0	-1.11	+30
14	-6.67	+20
38	-12.22	+10
62	-17.78	0
86	-23.33	-10
110-168	-28.89	-20

Except for the application of a freezing thermal gradient (from this table) across the thickness (=height) of the soil system, all processes in the systems induced by this gradient are natural ones; i.e., all consequent natural processes were triggered off by thermal energy.

INSTRUMENTATION

The freezing apparatus used in these studies was the same as used by the author in previous research on moisture migration in freezing soil systems and shown in Figure 11 (1) and Figure 4 (3).

The principal instrument used for measuring the induced electric (streaming) potentials in the freezing soil systems was a quadrant electrometer consisting of a gold-plated glass needle suspended at its center on a torsion fiber so that it could rotate between four cross-connected plates taking the place of the ordinary quadrants. The electrometer, with standardizing potentiometer and other accessories, is shown in Figure 2. The basic requirement of an electrometer for use in studies of electrokinetic phenomena in freezing soil systems is that it should not draw current from the porous system during the time of measurement of electric properties developed in such systems. The circuit diagram for measuring of streaming potentials in freezing soil systems is shown in Figure 3. The standardization circuit, which includes the potentiometer, is independent of the electrodes.

The electrodes shown in Figure 3 at five different levels in the freezing soil system for measuring the streaming potential are of platinum wire 2.54 mm in diameter. At the "ground surface" and at the bottom of the soil system (Fig. 4) the platinum electrodes are in the shape of a coil, whereas those spaced at depths of 7.5, 15.0, and 22.5 cm from the ground surface have the shape of a needle; viz., wire.

The platinum electrodes, although expensive, are inert in respect to their contamination.

At this point it is pertinent to suggest that all electrodes used in electrokinetic studies of freezing soil systems must be standardized by agreement as to material, size, and shape so that results obtained by other researchers at other institutions and in other countries may be compared with one and the same yardstick, similar to other standardized methods of tests of soils.

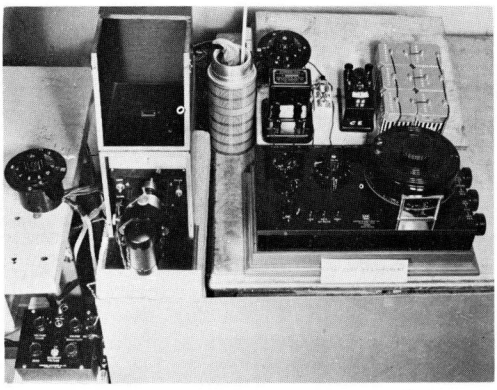

Figure 2. Electrometer with standardizing potentiometer.

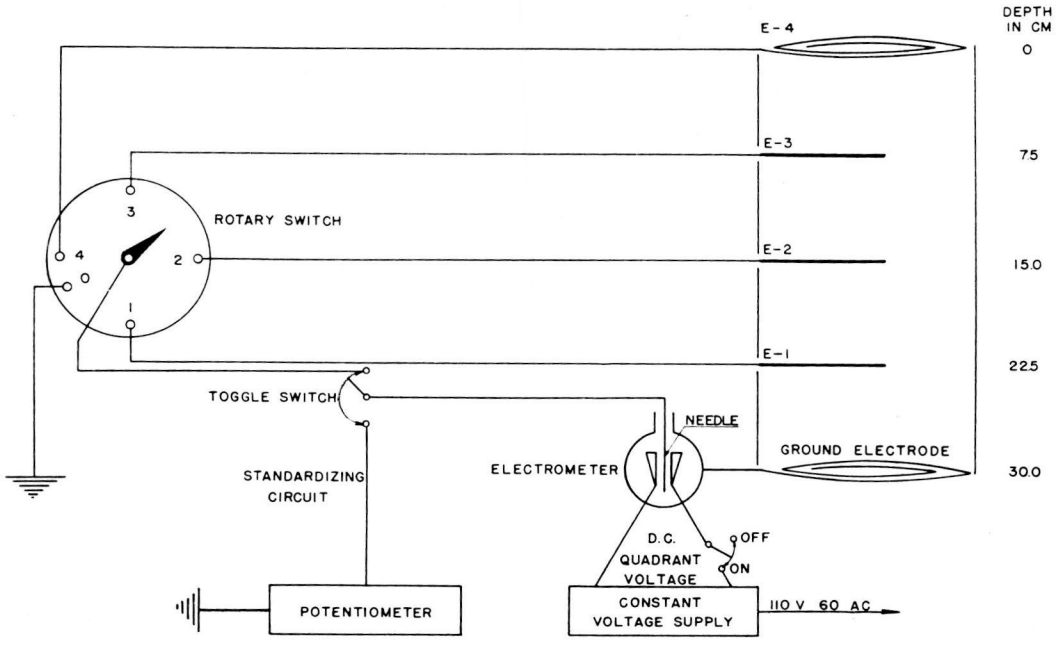

Figure 3. Circuit diagram for measuring streaming potentials.

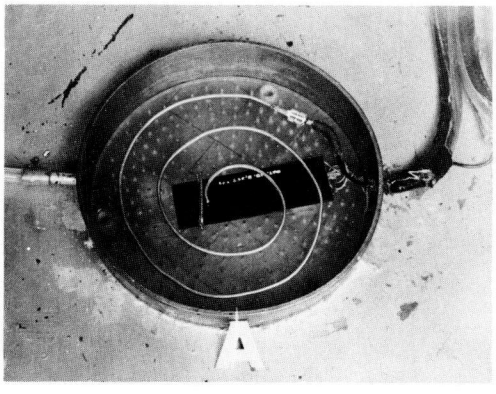

Figure 4. Ground electrode placed at bottom of soil system and located in ground-water reservoir.

Among the principal apparatus other auxiliary devices (such as ground-water supplying devices, thermistors, heat transducers and recorders) were used. The general layout of the instrumentation in these studies is given in Figure 5.

RESULTS

The results of the soil freezing experiments are shown in Figure 6. This figure summarizes the 168-hr test data and shows graphically the amount of soil moisture transferred, the developed streaming potential, and the frost penetration depth as a function of porosity of the soil systems. The nature of the moisture transfer curve has already been established by previous experiments. (2) In the streaming potential experiments described here, therefore, four points on each of the three curves describe adequately the course of these curves within the experimental range of porosities from n = 27.8 percent to n = 47.8 percent.

For the streaming potential at a given porosity, the absolute value in millivolts between the greatest deflections of the electrometer needle for the top-coiled electrode was selected as the best representative value for the 168-hr period of experiment. All other readings relative to electrodes located in the soil systems below their top surfaces are less than reported here.

Within the experimental range of porosities from n = 27.8 percent to n = 47.8 percent, the streaming potential curve may be represented satisfactorily by the general Fourier series equation,

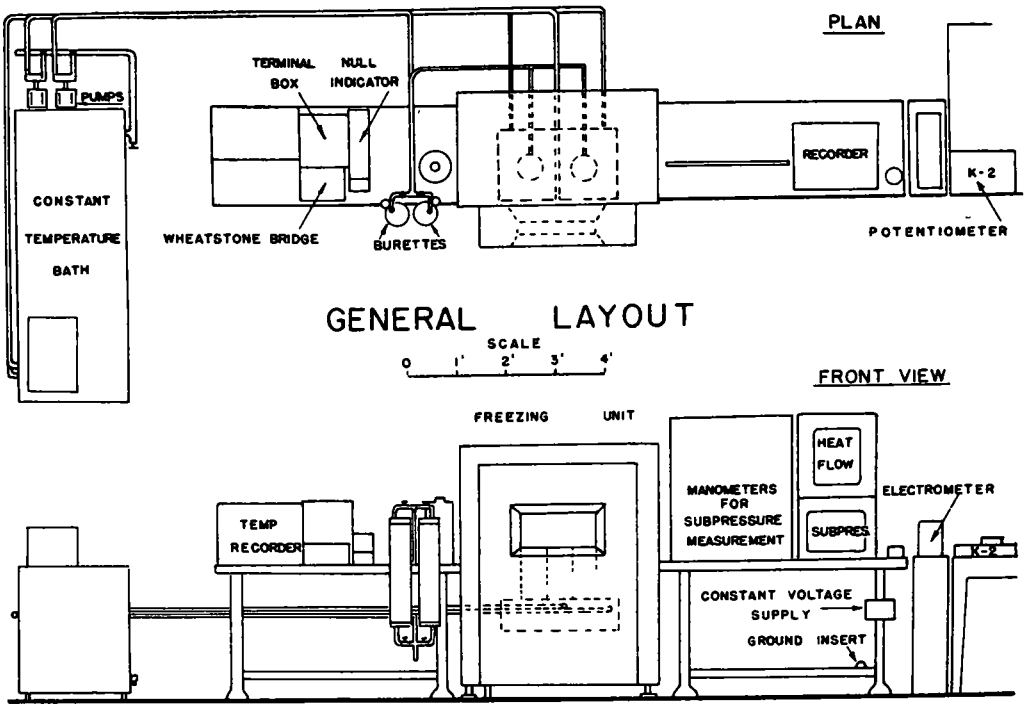

Figure 5. General layout.

$$y = f(x) = a_0 + a_1 \cos x + a_2 \cos 2x + \ldots a_m \cos mx + \ldots + b_1 \sin x + b_2 \sin 2x + \ldots b_m \sin mx + \ldots$$

in which

y = ordinate of streaming potential, EMF, in mv;
x = porosity, n, abscissa: $x = c \cdot \pi \cdot n$,
c = an experimental coefficient
$a_0, a_1, a_2, \ldots a_m, \ldots b_1, b_2, \ldots b_m \ldots$ are Fourier coefficients.

The EMF values reported here in millivolts appear to reflect the shape of the parent soil moisture transfer curve. The soil moisture transfer graph also indicates that the amounts transferred in the film phase (up to approximately n = 47.8 percent porosity) are about five times greater than by way of pure vapor diffusion (porosity range from n = 60 to 100 percent).

Thus, Figure 6 shows that the streaming potential developed in a freezing soil system is approximately proportional to the amount of soil moisture transferred in the film phase. The vapor transfer mechanism is here considered as ineffective in soil moisture translocation.

The maximum magnitude of developed streaming potential in the freezing soil system studied, as seen in Figure 6, can be scaled off as being 350 mv at about 41 percent porosity. The porosity of the Dunellen soil at its maximum dry density of 1,215 pcf = 1.95 g per cu cm by standard Proctor compaction test is n = 26.2 percent.

The frost penetration depth curve (Fig. 6) as a function of porosity n justifies the following statements:

1. The maximum frost penetration depth occurs at the same porosity as the porosity at which the maximum amount of soil moisture is transferred and the maximum magnitude of streaming potential occurs. There appears to be no time lag between these three phenomena.

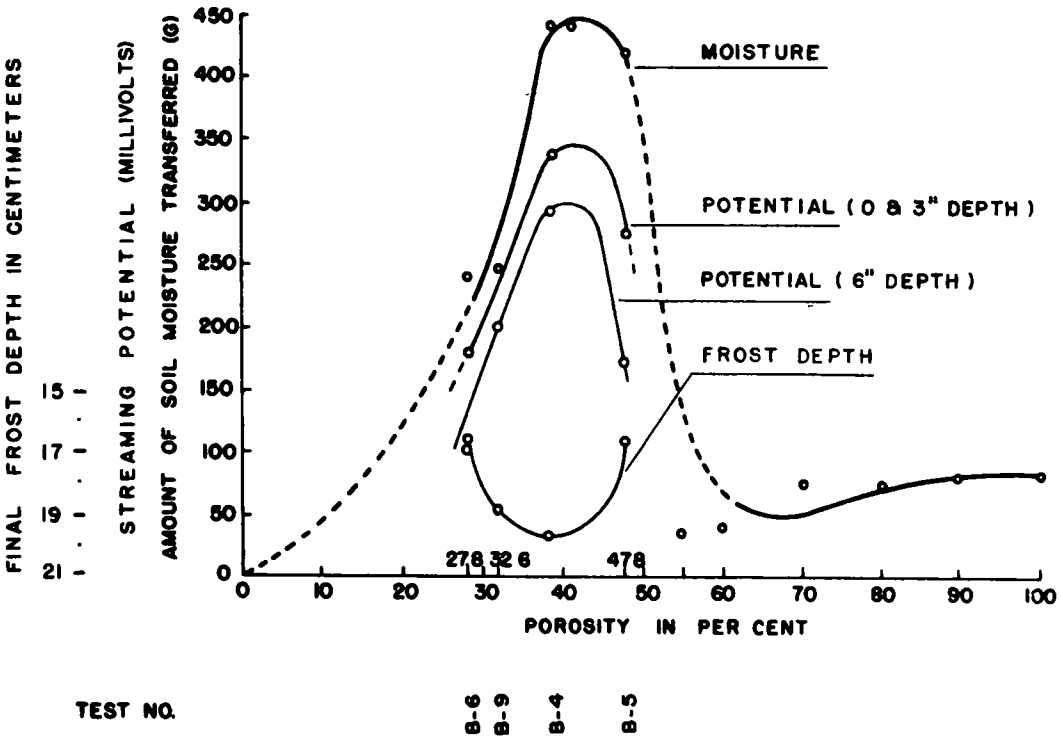

SUMMARY OF 168 HOUR TEST DATA

	POROSITY %	MOISTURE GM	POTENTIAL MV (0 & 3")	POTENTIAL MV (6")	FINAL FROST DEPTH CM
B-6	27 8	239	180	100	165
B-9	32.6	250	250	200*	188
B-4	38 5	446	340	285	196
B-5	47.8	424	275	170	165
*A-9	32 8				

Figure 6. Streaming potential, frost depth, and moisture transfer in soil upon freezing as a function of porosity.

2. At n = 27.8 percent porosity, 119.8 pcf = 1.925 g per cu cm dry density, the passages between the soil particles may be so small that they restrict to some degree the flow of heat and soil moisture and hence hinder the upward flow of the cations.

3. At n = 32.6 percent, 112 pcf = 1.795 g per cu cm dry density, the heat and soil moisture transfer is greater because the soil particles are packed less densely than in the case of statement 2.

4. At n = 38.7 percent porosity, 102 pcf = 1.635 g per cu cm dry density, to about n = 41 percent porosity the soil particles are in such a packing as to cause the most effective film moisture transfer. This brings about the maximum frost penetration depth in these experiments, and the greatest accumulation of frozen moisture in the frozen soil system.

5. At n = 47.8 percent porosity, 86.7 pcf = 1.39 g per cu cm dry density, the amount of film moisture transferred begins to decrease because of the loose packing of the soil particles. This permits the heat to rise more easily through the voids of the soil from the ground-water, retarding the downward-progressing freezing isotherm.

6. The over-all conclusion from these statements is that the standard compaction of this soil on the dry side of its optimum moisture content (~12 percent) and maximum dry density (viz., porosity) seems to be the best condition for minimum amount of soil moisture transferred and minimum depth of frost penetration attained.

ACKNOWLEDGMENTS

The experimental studies were sponsored by the National Science Foundation under NSF-G 6577 as a phase of "Upward Migration of Water in Soil Exposed to a Freezing Atmosphere." For this sponsorship the author expresses his sincere gratitude.

The author also expresses his appreciation to J. J. Slade, Jr., Director of the Bureau of Engineering Research, to M. L. Granstrom, Chairman, Department of Civil Engineering, and to E. C. Easton, Dean, College of Engineering, all at Rutgers University, for fostering these studies in many tangible ways.

C. V. Longo of the Department of Electrical Engineering at Rutgers University was consulted and checked the development of the streaming potential measuring circuit.

W. Douglas Smith, Jr., a graduate student at Rutgers University, Department of Civil Engineering, took part in the soil freezing experiments and performed conscientiously the difficult measurements of the developed streaming potentials in the freezing soil systems.

REFERENCES

1. Jumikis, A.R., "Concerning a Mechanism for Soil Moisture Translocation in the Film Phase upon Freezing." HRB Proc., 39:619-639 (1960).
2. Jumikis, A.R., "Effective Soil Moisture Transfer Mechanisms." HRB Bull. 317, 1-8 (1962).
3. Jumikis, A.R., "Some Concepts Pertaining to the Freezing Soil Systems." HRB Special Report 40, 178-190 (1958).

Vapor Diffusion in Freezing Soil Systems of Very Large Porosities

A. R. JUMIKIS, Professor of Civil Engineering, Rutgers University

The purpose of this paper is to present experimental studies on soil moisture translocation by way of vapor diffusion from ground-water to the cold front through very large voids upon freezing. The experiments brought out that (a) the amount of water diffused and the coefficient of vapor diffusion are functions of porosity of the porous medium; (b) the depth of frost penetration is a function of porosity of the porous medium, being inversely proportional to the porosity of the soil in the vapor phase range (porosity from about 60 to 100 percent); and (c) upward moisture translocation in the vapor phase through freezing soil systems is an insignificant moisture transfer mechanism as compared with other soil moisture transfer mechanisms.

These experimental studies verify the assumptions that the upward flow of soil moisture from the ground-water towards the cold front in a frost-susceptible soil takes place virtually unaccompanied by vapor diffusion, and that this finding may serve as the basis for moisture migration studies in freezing soil systems.

•THE PROCESS of freezing of natural soils is a simultaneous process with both heat flow and upward migration of soil moisture from the ground-water table towards the cold front in the direction of the drop in thermal gradient.

Whereas the heat transfer in soil as a single process is a study of relative ease, the heat transfer problems coupled with simultaneous soil moisture migration processes by way of film flow and/or vapor diffusion are of a very complex nature indeed. For example, in a freezing soil system the flow of heat as one property or potential induces a potential difference with respect to another property, such as changes in density of water (viscosity) or changes in concentration (induction of secondary or streaming potentials). Also, upon freezing, the cooling process brings about with respect to liquid water a new phase such as vapor or ice.

Although it is understood that diffusivity decreases with decreasing moisture content, decreasing temperature, increasing pressure, and increasing density of the vapor, there are not generally available mathematically formulated expressions for conditions of varying diffusivity as a function of steadily decreasing temperature and varying position of coordinates.

The study becomes even more complex if one observes that in a freezing soil system the length of the unfrozen part of the so-called porous "plug" decreases with decrease in the freezing temperature of the microclimate, that temperatures at every point of depth below the ground surface are different upon freezing, and that, therefore, the properties of the soil moisture in bulk or in the film phase are different at these points too. One usually thinks mainly of the properties such as the density of the water, viscosity, surface tension, dielectric constants of water and ice, and thermal and other properties of the soil-water-gas (air) system. Besides, the structure of liquid water itself is a matter of a very complex nature (1), and the unsaturated flow processes

in a porous medium such as freezing soils are even more complex. Also, the soil moisture transfer problem is usually further complicated by changes in the moisture transfer mechanisms (such as the film mechanism or vapor diffusion, or both) or in bulk, as the porosities of the soil vary.

The simultaneously coupled complex processes in a moist porous medium (such as the freezing soil system) induced by a thermal gradient are unexcelled by any other system of heat transfer. The interrelationships between the multitude of factors affecting the translocation of soil moisture under freezing conditions are too complex to be studied analytically. It is for these reasons that the studies on vapor diffusion in freezing soil systems of very large porosities were undertaken experimentally and described here. Particularly, it was the purpose of these studies (a) to elucidate the vapor diffusion phenomenon in freezing soil systems, (b) to study vapor diffusion in freezing soil systems as a function of porosity of the soil packing, and (c) to verify that the upward flow of soil moisture takes place virtually unaccompanied by vapor diffusion; i.e., that vapor diffusion is an ineffective soil moisture transfer mechanism as compared with film flow.

DEFINITIONS

1. Diffusion. — Diffusion is the distribution of the molecules within a single phase brought about by molecular motion of translation and mutual bombardment (water vapor is still air). Thus, diffusion is the process by which matter is transported from one part of a system to another as a result of random molecular motion towards an environment of lower concentration.

The concept "diffusion" is used when there takes place a movement of molecules of one kind between molecules of another kind; for example, water vapor molecules in the air. The driving forces of the diffusing molecules of the vapor then are temperature gradients, or partial pressure differences, or density differences or gradients. Density gradients may be destroyed by diffusion.

The resistance to motion of the water vapor molecules comprises then the collision of the molecules in question with the other type of molecules, as well as the collision of the molecules with the soil particles, and the change in direction because of the irregular paths of travel through the porous medium.

For unidirectional diffusion through an isotropic medium through an area A (cm^2) in the direction of x (cm), and for C = constant (= concentration of diffusing matter) over the area A, Fick's first (linear) law of gaseous diffusion may be approximately applied (2):

$$dW = - D \cdot A \cdot \frac{dC}{dx} \cdot dt, \qquad (1)$$

in which

dW = mass of substance (in grams), vapor; for example, diffusing in time dt (seconds) through an area A in the direction of x, when the concentration gradient is dC/dx (in $g \cdot cm^{-3} \cdot cm^{-1}$),
D = coefficient of proportionality, or coefficient of diffusion, in $cm^2 \cdot sec^{-1}$.

The negative sign in Eq. 1 expresses the fact that diffusion occurs in the direction opposite to that of increasing concentration.

2. Soil System. —A system, in general, is a separated region of space or a finite part of matter set apart from its surroundings. In the system, changes of state of matter and transfer of energy and/or mass can be studied. As to the soil, a soil system as used in this paper is a vertically supported cylindrical soil sample with a simulated ground-water table at its lower end, or else pebbles arranged in a cardboard cylinder so that the pebbles may or may not be in contact with each other. In these experiments, the solid phase of the soil is fixed. Such particular systems subjected to freezing studies and dealt with here are termed in this paper "soil-moisture-temperature."

3. Open System. —An open system is one that can exchange matter as well as energy (heat) with its surroundings—water can enter the soil system from below from the ground-water freely, and heat energy can cross the lower and upper boundaries of the vertical, cylindrical soil system.

4. Freezing Soil System. —The freezing of an open soil system is brought about by removing heat from the system and results in a full or partial transformation of the soil moisture into ice at the cold front.

5. Porous Medium. —A porous medium is a solid body that contains pores. Pores, in their turn, are void spaces contained in a porous body; for example, soil. The voids may be fully or partially filled with air and/or gas and/or water, or both air and water.

6. Soil System of Very Large Porosity. —This study deals with soil systems having large voids; i.e., voids that are interconnected. The particles forming the porous medium are not in contact with each other. Hence the term "very large porosity." More precisely, by very large porosity is to be understood here as porosity the magnitude of which ranges from about n = 60 to 100 percent (no soil particles in the cardboard cylinder).

The very porous soil systems were simulated by packing pebbles screened out from Dunellen soil, a glacial outwash material. The particle sizes of this material are shown in the particle-size accumulation curves (Fig. 1). The porosities studied range from n = 40 to 100 percent. The arrangement of the pebbles (soil particles) for n = 90 percent porosity is shown in Figure 2. Thus, the porous system of soil is an artificial one.

If in this artificial porous medium the soil particles are not in contact, then no upward flow of soil moisture by way of film or water in bulk takes place along the solid particles from ground-water towards the cold front. Hence only vapor diffusion is possible.

It is also assumed that in this system the pebbles themselves are not porous. Otherwise vapor transfer through pebbles would encounter a much greater resistance than through the voids of the packing of the pebbles, and would complicate the studies considerably.

The "soil particles" were supported on chairs made of brass wire and coated with paraffin. The chairs, at various elevations in the soil system, are independent of each other, thus eliminating film flow along the supports from one chair to the other.

The chairs, in their turn, were placed in 30-cm high waterproofed cardboard cylinders, 15 cm in diameter. The wires of the chairs had no contact with the cylinder.

Figure 2 also shows the helical arrangement of the thermistors in the soil system.

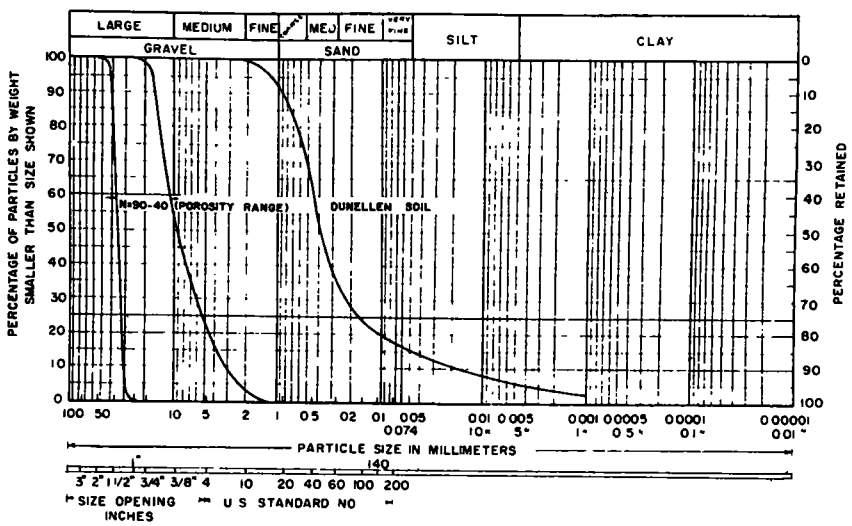

Figure 1. Soil particle-size accumulation curves.

PROCEDURES

Geometry of Pores

The geometry of the pores of the porous medium so prepared is very indeterminate. The shapes and sizes of the solid particles differ among themselves, thus influencing considerably the process of flow of heat and water vapor. Because of the irregular shape of the voids, the flow paths of the upward vapor diffusion are tortuous. The tortuosity-forming voids, in these experiments, connect into one another.

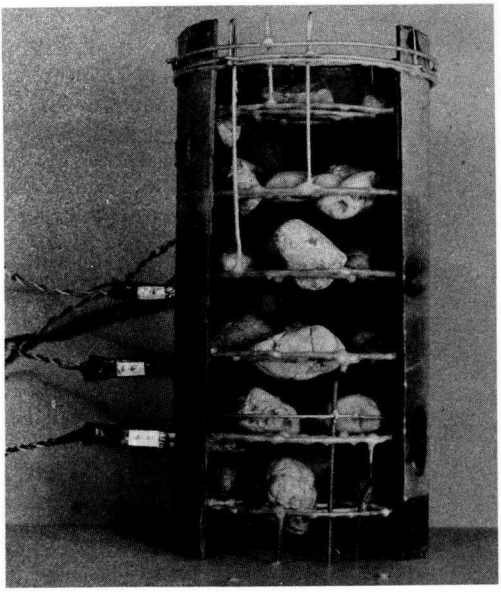

Figure 2. Arrangement of pebbles for n = 90 percent porosity.

Instrumentation

The cylindrically shaped system of large porosity soil was placed in a freezing chamber and immersed with its lower end 1 cm deep into "ground-water," with a watertight connection. It was equipped with thermistors for temperature measurements. The thermistors were placed at various elevations and helically spaced (Fig. 2), and taped for air-tightness. The thermistors were connected to temperature-recording devices. A round plexiglas plate 3.0 mm thick was placed on top of the soil sample, simulating an impervious pavement.

The soil systems of artifically packed pebbles so prepared, two in each test, were laterally insulated with cork and vermiculite to minimize heat flux laterally to provide for unidirectional, upward heat flow from the ground-water table to the cold front. Relative to lateral insulation, it must be said that in nature there are no absolute boundaries; thus, all systems "diffuse" more or less with their surroundings. Because no boundary is absolute, a system cannot be isolated and insulated completely. Hence, open systems transferring some heat energy laterally are more or less, so to say, incomplete, and so are the freezing soil systems as here described.

The ground-water container was connected with ground-water burettes (Figs. 3 and 4). These burettes were zeroed so as to maintain a constant ground-water table at the lower part of the vertical soil systems and permit observing the absolute amount of water evaporated from the ground-water up into the soil system or empty cylinder (at n = 100 percent porosity). Figure 4 shows the layout of instrumentation used in these studies.

The soil system so prepared was ready for freezing. The soil samples were frozen in a specially designed freezer from their top downwards. Hence the freezing soil system simulates in these experiments natural conditions as closely as possible, and the processes involved, triggered off by the heat energy (freezing) are natural ones too.

The ground-water in the freezer was kept at an average temperature of +8 C.

Freezing Schedule

After some experimentation and studies of weather report data, a seven-day period of freezing was established as being consistent with some of the cold spells during the winter months, and short enough not to consume an undue amount of time during these freezing experiments. The surface temperature (micro-climate) was lowered as follows:

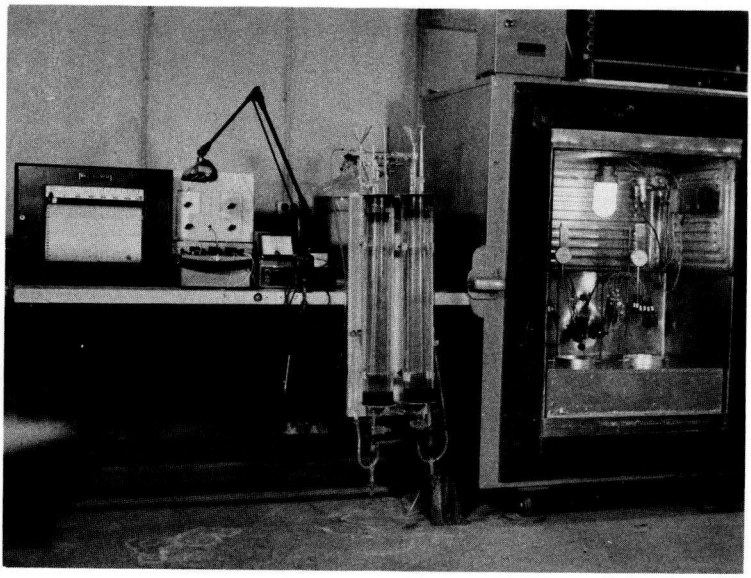

Figure 3. Instrumentation used in vapor diffusion studies.

Elapsed Time After Start of Tests (hr)	Temperature of Microclimate	
	°F	°C
0	+30	-1.11
14	+20	-6.67
38	+10	-12.22
62	0	-17.78
86	-10	-23.33
110-168	-20	-28.89

(This freezing stepdown schedule is also shown in Figure 7.)

As the microclimate is lowered the rate of removal of heat from the ground-water through the soil packing is increased, and, in its turn, the more rapid is the 0 C-isotherm.

In these experiments the following relationships were studied:

1. Amount of moisture diffused from the ground-water table upwards to the cold front as a function of porosity of soil packing.
2. Temperature profiles in the very porous soil.
3. Vapor pressure profiles in the freezing porous soil systems.
4. Depth of frost penetration into the artificial soil packings as a function of porosity.
5. Coefficients of vapor diffusivity as a function of porosity.

The porosities used in these experiments were n = 40, 55, 60, 70, 80, 90 and 100 percent.

NATURE OF VAPOR DIFFUSION PROBLEM

To elucidate some of the processes that take place in the slowly evaporating soil system upon freezing the nature of the vapor diffusion problem is examined.

The rate of soil moisture diffused in the vapor phase depends mainly on the thermal gradient imposed on the soil. The thermal gradient induces a vapor pressure gradient, causing the vapor to translocate from points of warmer temperature (or from points of higher vapor pressure) to points of lower temperature (to points of lower vapor pressure) in the freezing soil system. Upon freezing from the top of the system the 0 C-isotherm is a downward-moving boundary.

Besides these factors, there exists an obscurity of a number of influencing factors in a freezing system of large-sized voids; for example, porosity and the granulometry

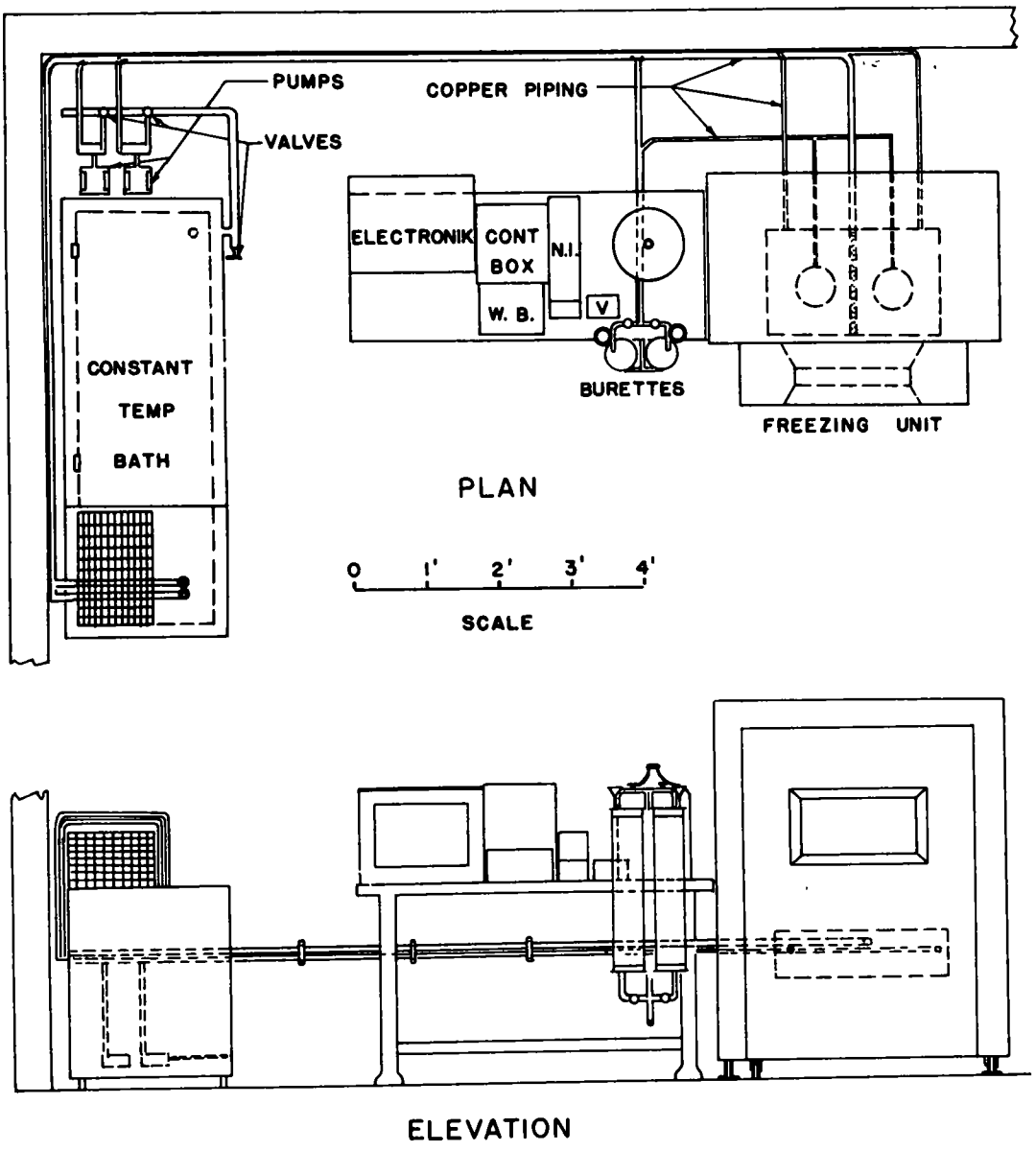

Figure 4. Arrangement of equipment.

of the soil packing material forming the voids. The amount of soil moisture transferred upward by vapor diffusion also depends on the distance vapor translocates from the ground-water table to the elevation of condensation; viz., freezing. In the freezing process, this distance decreases as the 0 C-isotherm moves downward. Besides, the amount of soil moisture transferred in the vapor phase depends also on the intensity of the freezing temperature gradient. Freezing, in its turn, as has been pointed out already, brings about changes in the physical properties of water; viz., water vapor.

Physical Process of Vapor Diffusion

Physically, the vapor diffusion problem in very porous soil upon freezing as studied and reported in this paper is a thermal problem associated with simultaneous heat and moisture transfer in the vapor phase. Upon lowering the surface temperature at the top of the very porous soil system, and keeping the ground-water at a constant temperature of +8 C, the porous system is, so to speak, placed in an upward directed thermal field. In the laterally insulated porous soil systems the heat flows unidirectionally upward from points of higher temperature at the ground-water table to points of lower temperature at the cold front (for example, freezing microclimate), and so does the aqueous vapor evaporating slowly from the ground-water table (Fig. 5), moisture that thus tends to translocate in the direction of the flow of heat.

A flat surface of water (such as the ground-water table) has a definite vapor pressure at a given temperature. The physical state of the fluid is gas; viz., water vapor. Thus water evaporates at the ground-water table because of the thermal gradient and because the partial vapor pressure on the warmer side is larger than at the cooler one. The thermal energy upon freezing triggers the natural processes in the soil system, among them the vapor diffusion process, a process that is in full accordance with those that occur in nature.

In the freezing systems studied, the unidirective diffusion of water vapor from the ground-water takes place into gas such as air (evaporation). The air above the ground-water table cannot translocate downwards through the surface of the ground-water table. Thus, according to Stefan (3), it may simply be assumed that in the system the air does not move, hence the velocity of the air is everywhere zero.

Voids of Packing

Obviously, the upward vapor movement in a freezing soil system is affected by the porosity of the soil system. It is the voids of the packing that determine the amounts

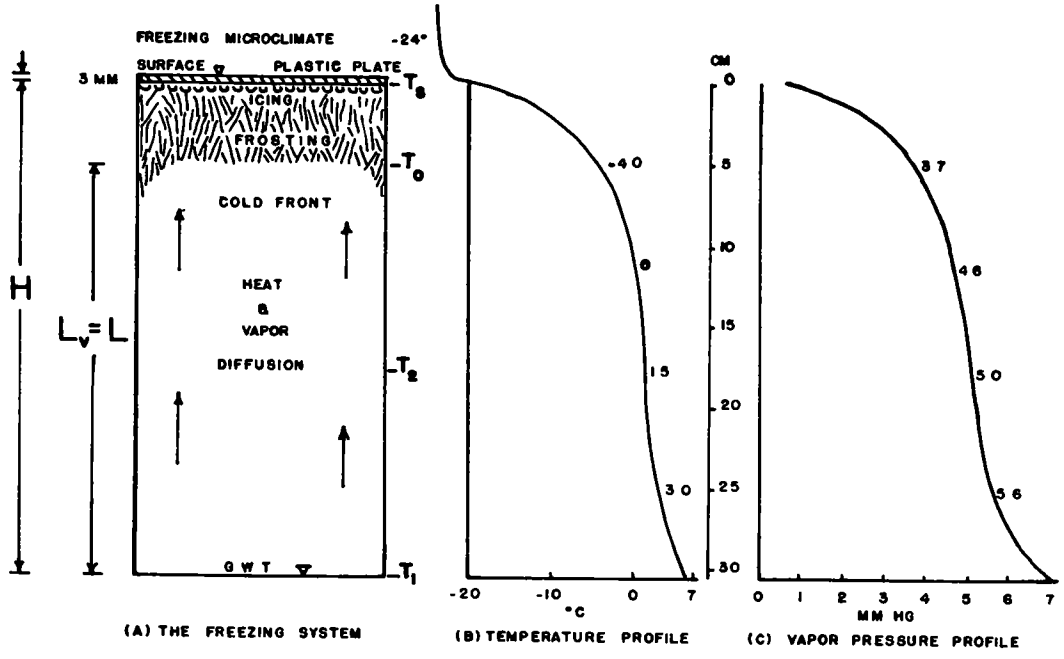

Figure 5. Physical elements of vapor diffusion system of 100 percent porosity after 168 hr of freezing.

of soil moisture transferred; viz., vapor diffused. If the voids are small and the soil particles are in contact, vapor diffusion may be reduced to a minimum, and other soil moisture transfer mechanisms (such as the film flow) become more effective. The coarse-sized soil particles in the large-porosity systems studied are inert in film moisture transfer, and provide only an inactive bulk to the soil.

It is very difficult to specify the geometry of the voids in natural or artificially packed soils, because the porous medium soil cannot be represented by an ordered system consisting of a bundle of vertical, parallel, circular capillary tubes. On the contrary, the model of the experimental soil system under consideration is a disordered one, consisting of twists and constrictions in the water and/or vapor moving channels. Thus the nature of the shape of the voids is irregular; the diameters of the voids vary along the path of moisture travel, and the tortuosity-forming voids join into one another. Hence cross-sectional areas through which vapor translocates cannot be described by a capillary diameter. Hence the large-porosity flow paths of the upward-diffusing water vapor must be characterized as tortuous. Therefore, vapor diffusion through a porous material is not a characteristic of the material of the porous packing but rather a function of the porosity of the packing.

Main Factors Affecting Vapor Diffusion

The foregoing discussion on the nature of the vapor diffusion problem indicates that the vapor diffusion through a large-voided porous medium should be characterized by three quantities: porosity, tortuosity, and the system's over-all transmissibility to water vapor. Because of the complex nature of the singular factors involved, the vapor diffusion studies were made experimentally on a basis of over-all performance of the system as a whole. This is because the zigzag paths of vapor diffusion in the freezing soil system cannot be simplified by way of the concept of an equivalent diameter of the voids and/or granulometry. Such simplications afford approximative qualitative and rough quantitative vapor diffusion calculations only, and never render a universal substitute for the real porous medium.

RESULTS

Amount of Soil Moisture Diffused as a Function of Porosity of Soil Packing

The experiments brought out that the porosity of the packing affects the amount of vapor diffused (Fig. 6). The porosity range for pure vapor diffusion may be set from a porosity of about n = 60 percent to one of n = 100 percent. The more porous the packing, the more vapor diffused. The absolute amount of water diffused at n = 60 percent was 41 g, whereas at n = 100 percent the amount of water transferred by diffusion was observed to be 83 g during a 168-hr period of freezing. If the amount of water vapor diffused at n = 100 percent is designated by a relative figure of 1.00, then the relative amount transferred at n = 60 percent is $41_{60}/83_{100} = 0.494$, or about 49 percent of the amount diffused at 100 percent. The maximum amount, 83 g, of vapor diffused at n = 100 percent, however, compared with the amount of 445.6 g of soil moisture transferred in the film phase at about n = 40 percent makes only $83.0_{100}/445.6_{40} = 0.186$ of the maximum film flow, or about 18.6 percent (Fig. 7). This indicates that soil moisture transfer in the vapor phase is a relatively ineffective soil moisture transfer mechanism upon freezing.

Temperature Profiles

The temperature regimen within the soil systems depends greatly on the freezing surface temperature, the ground-water temperature (Fig. 7, freezing curves), and the porosity of the packing, as reflected in such freezing curve plots. Figure 7 shows curves for (a) room temperature, (b) ground-water temperature, (c) temperatures at various depths of the freezing systems, (d) temperature of the microclimate (surface temperature), a graph that also reflects the freezing stepdown schedule, and (e) the cumulative amount of water consumed by vapor diffusion. This figure shows that the temperature regimen in the freezing systems at a given surface temperature is affected greatly by the temperature of the ground-water—every fluctuation in the

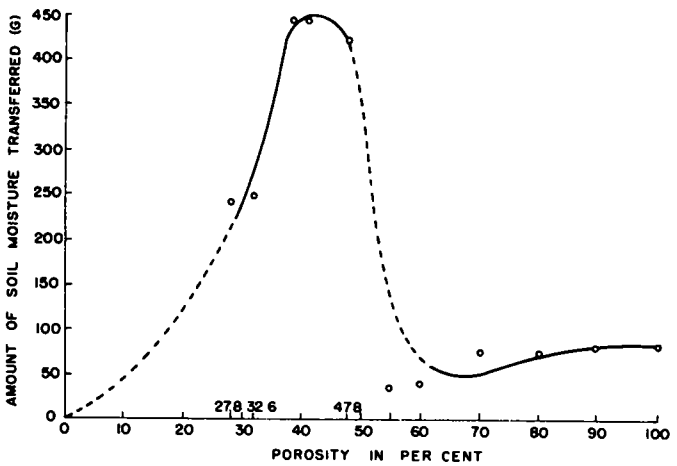

TEST NO		B-6	B-9	B-4	B-7	B-5	A-8	A-6	A-5	A-3	A-4	A-7
EFFECTIVE MOISTURE TRANSFER MECHANISMS		LOWER POROSITIES THAN N = 27.8 % DIFFICULT TO ATTAIN IN PRACTICE		EFFECTIVE FILM FLOW			FILM AND VAPOR FLOW		PURE VAPOR TRANSFER			
OPTIMUM M C IN %		12.6	15.3	13.8	12.8	12.4	-	-	-	-	-	-
MAXIMUM DRY DENSITY IN LB/FT^3		119.8	119.7	102.1	97.7	86.7	71.2	63.0	46.5	29.9	13.4	0
VOID RATIO (e)		0.385	0.484	0.626	0.695	0.916	1.22	1.50	2.33	4.00	9.01	∞
AMOUNT OF MOISTURE TRANSFERRED	ABSOLUTE AMOUNT IN GRAMS	239.0	250.0	445.6	445.0	424.0	36.0	41.0	77.0	75.0	82.0	83.0
	RELATIVE TO MOISTURE TRANSFERRED AT 100 % POROSITY	2.88	3.01	5.47	5.46	5.11	0.43	0.49	0.93	0.90	0.99	1.00

Figure 6. Moisture transfer in soil upon freezing as a function of porosity.

ground-water temperature is reflected by corresponding temperature waves at various depths of the freezing soil systems.

The room temperature indicates its minor effect on the other variables. It does affect somewhat, however, the temperature of the circulating water in the cooling bath by about ±2 C. In all experiments the room temperature was kept at a range from T = 20 C to T = 25 C. Figure 8 shows that at about a 23-cm depth all the temperature profiles seem to merge, indicating that the effect of the freezing microclimate is balanced by the upward-flowing heat from the warmer ground-water.

Also, the greater the porosity the shallower the depth at which the 0 C-isotherm is halted (Fig. 8).

Vapor Pressure Profiles

The vapor pressure profiles are shown in Figure 9. The greater the porosity, the less the vapor pressure difference in the lower two thirds of the system; therefore, the smaller the driving force for vapor movement. The vapor pressure profiles were plotted from temperature measurements.

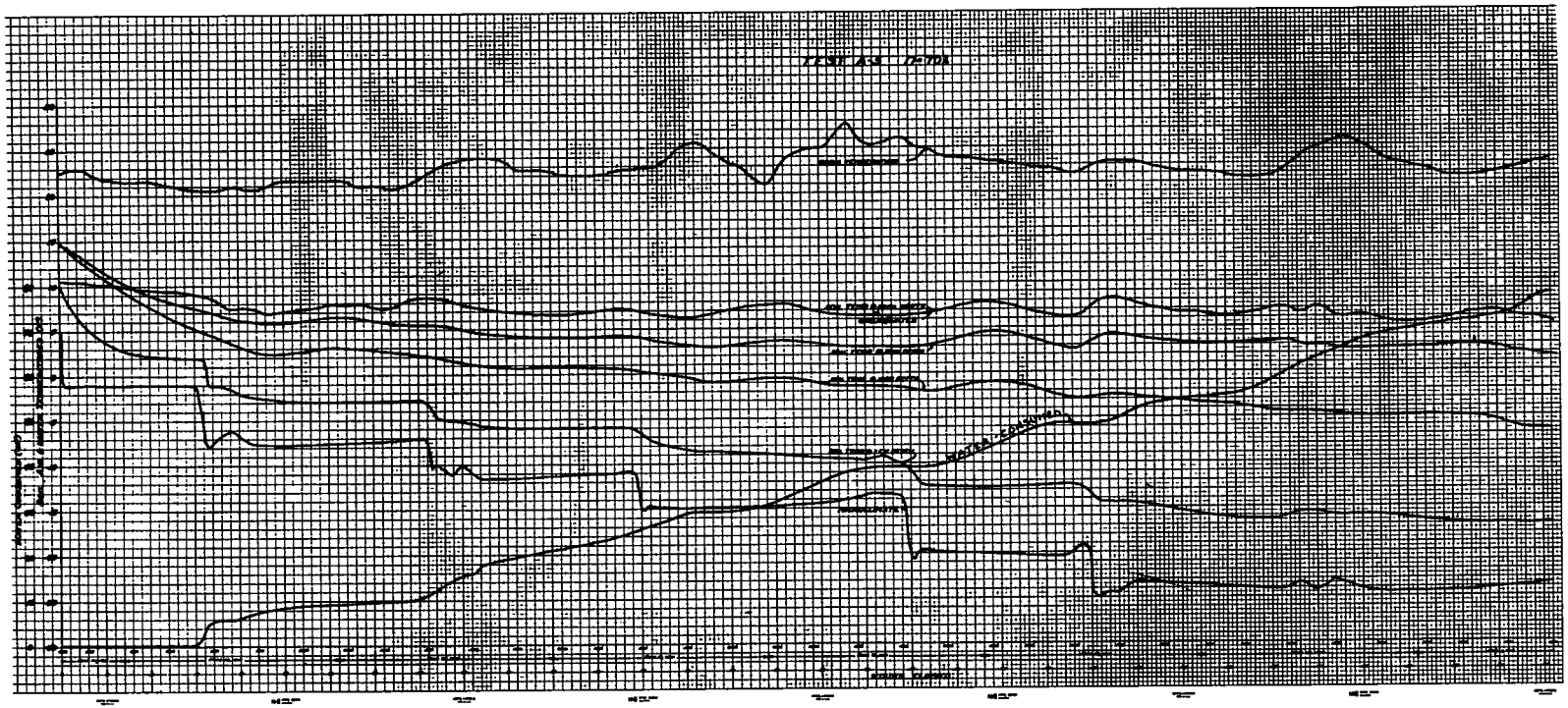

Figure 7. Temperature regimen.

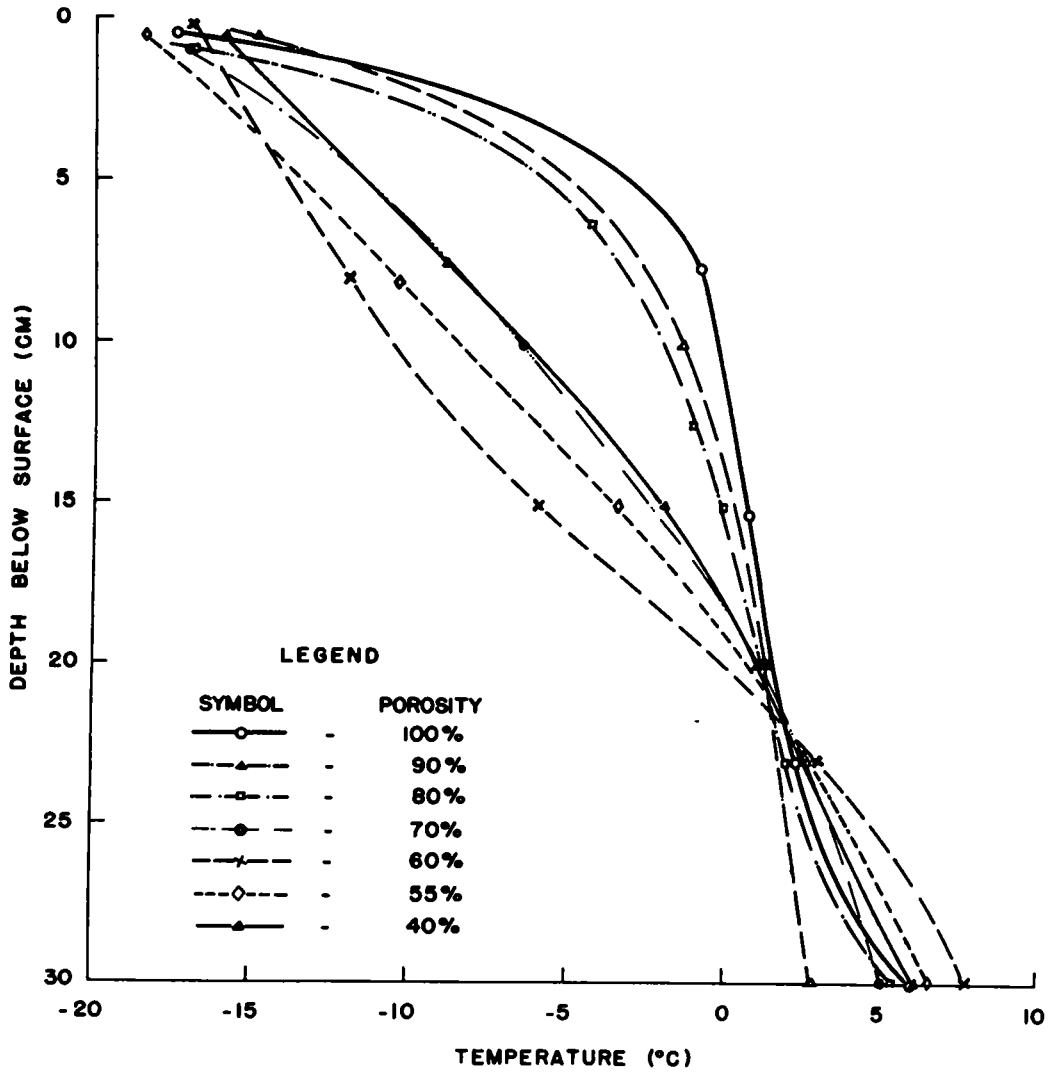

Figure 8. Temperature profiles after 168 hr of freezing.

Depth of Frost Penetration into Artificial Packings as a Function of Time and Porosity

Time.—The main purpose of studying this topic was to provide data for ascertaining the diffusion lengths, L_v, necessary for the calculation of the vapor diffusion coefficients—in other words, to establish the location of the 0 C-isotherm at any time. The change in the 0 C-isotherm (frost penetration) as a function of time for the various porosities is shown in Figure 10. The increase of the slopes of the zero-isotherm curves shows a general trend of decrease in porosity. Also, this figure shows that to attain equal frost penetration depth (say, 8 cm) the small porosities (except n = 40 percent) take less time than the large porosities. The lower parts of the 0 C-isotherm curves illustrate particularly well the effect of the porosity of the packing on the increasing rate of frost penetration. All in all, in the upward soil moisture transfer by way of vapor diffusion, the smaller voids bring about greater frost penetration in a shorter time than the larger ones. However, at a porosity of about n = 55 percent

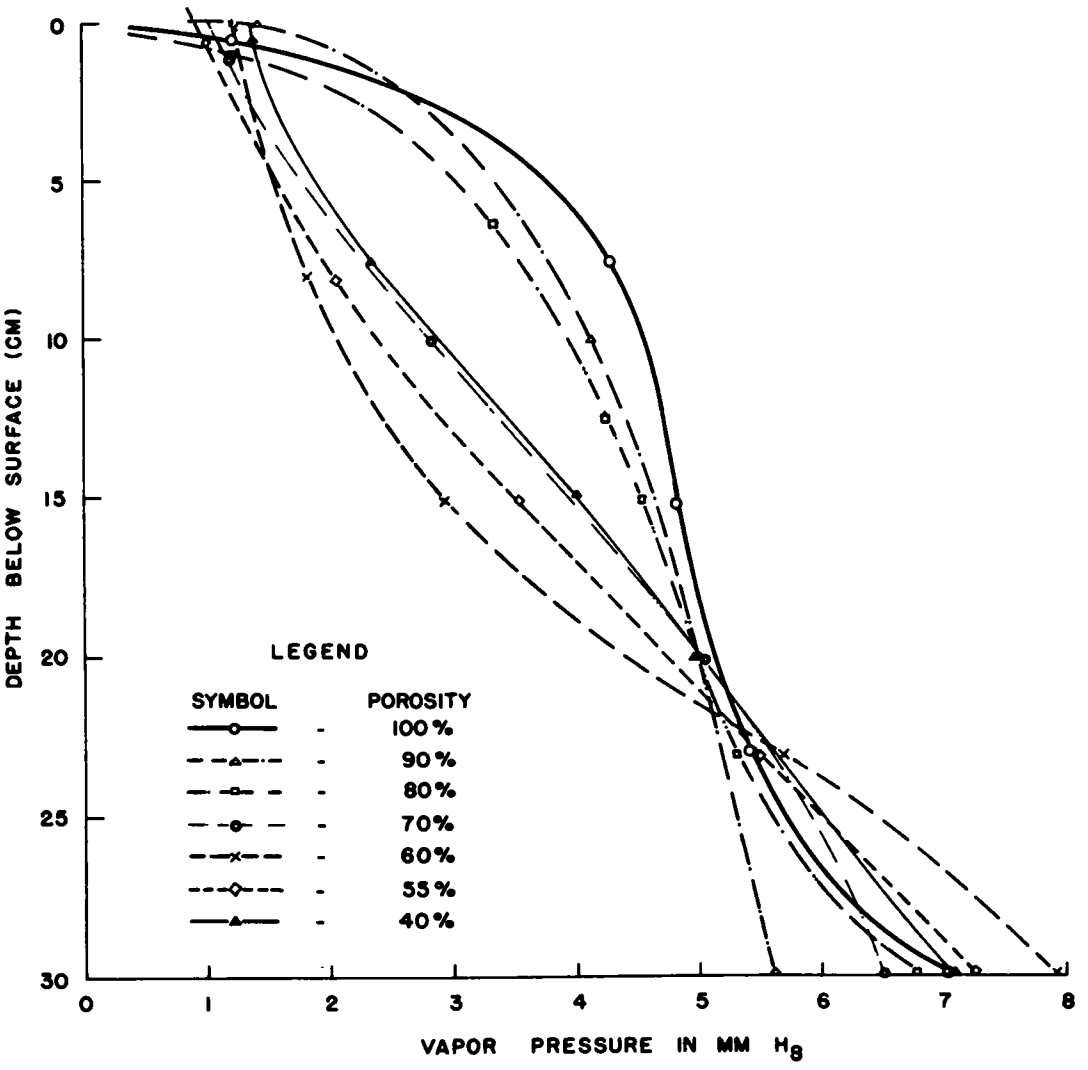

Figure 9. Vapor pressure profiles after 168 hr of freezing.

and less, this trend ceases. Thereafter, the time required again increases because the moisture film transfer mechanism sets in.

Because of the physical nature of the system and the freezing and diffusion processes, the frost penetration curves should not convey the impression that the rate of frost penetration increases with time. In these experiments, below a depth of approximately 14 cm the frost penetration rates decrease with time until they cease entirely. This decrease is due to the warming effect of proximate ground-water. Thus, in the porosity range of n = 60 to 100 percent it is the latent heat of fusion (80 cal per g) that controls the rate of frost penetration.

When the frost penetration depth curves, as shown in Figure 10, are plotted as a function of the square root of elapsed time; i.e.,

$$\xi = f(\sqrt{t}) \tag{2}$$

in which

ξ = frost penetration depth in centimeters, and
t = time in hours,

then they plot out as straight lines of

$$\xi = m \cdot \left(t^{1/2}\right) + b \text{ [cm]} \quad (3)$$

in which m = slope of lines, in centimeters per half hour

$t^{1/2}$ = square root of time ordinates, and
b = cut-off on the ξ-axis, in centimeters.

The values of the m and b parameters in Eq. 3 for porosities between n = 60 and 100 percent are given in Table 1. Intermediate values of m and b may be sufficiently accurately obtained by interpolation from the best fit curves m = f(n), and b = F(n), respectively.

Porosity.—The variation of the frost penetration depth, ξ, as a function of porosity in the vapor phase for 168 hr of freezing is shown in Figure 11. The function turned out to be linear:

$$\xi = -(34.0)n + 41.6 \text{ [cm]} \quad (4)$$

in which

n = porosity in decimal fractions,
-34.0 = slope of the ξ-line, and
+41.6 = intercept on the ξ-axis.

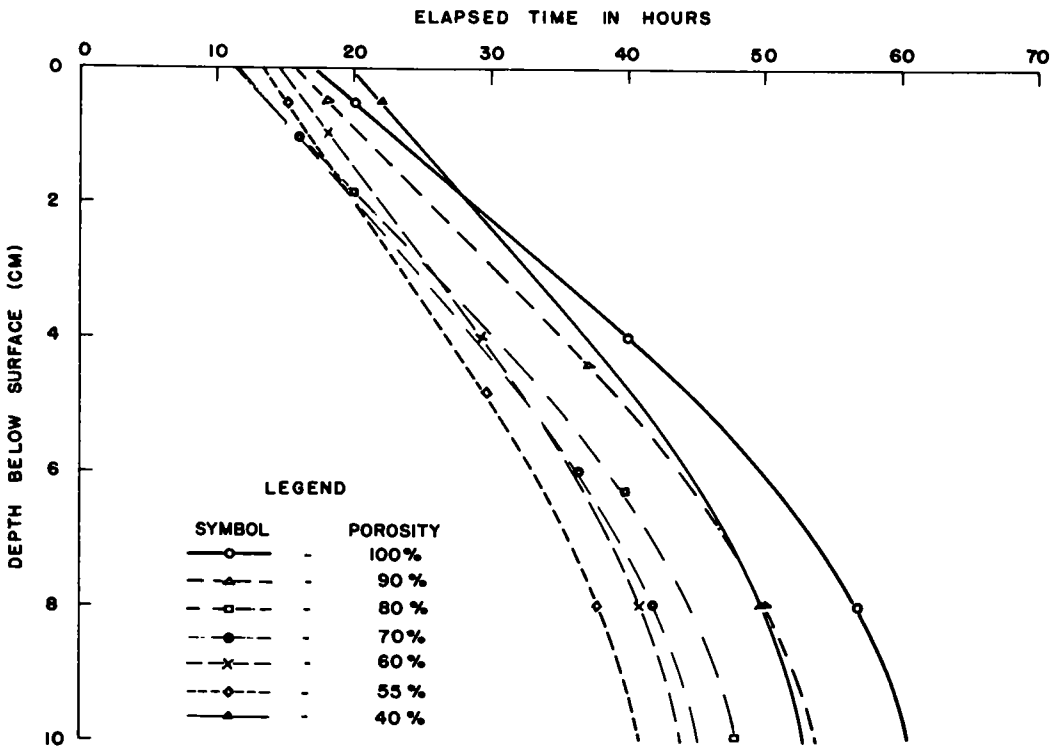

Figure 10. Penetration of 0 C-isotherm.

This equation is good for the porosity range of $1.00 \leq n \leq 0.6$.

Also, the frost penetration depth depends on the proximity (viz., position or elevation) of the ground-water table. The deeper the ground-water table, the deeper the frost penetration below the ground surface.

When the upward-diffusing water vapor strikes a chilled surface (there is a plastic plate at the top of the vertical cylindrical system), the vapor normally condenses in a sheet of water, and part of the condensate, upon freezing, may transform into ice. The phenomenon occurring when liquid water transforms into ice on solid surfaces is termed here icing. Massive icing formed only on the under side of the plastic plate.

TABLE 1

THE m AND b PARAMETERS

Porosity n (%)	m	b	Test No.
60	3.05	-11.75	A-6
70	2.80	-10.20	A-5
80	3.28	-12.94	A-3
90	2.65	-10.72	A-4
100	2.58	-11.23	A-7

Under certain conditions, however, vapor may condense into drops, and part of it may roll off the chilled surface by gravity. Such condensation is termed dropwise condensation. The phenomenon occurring when the condensate of water vapor transforms into a solid, like snow, is termed here frosting.

Because the frosting does not fall down, it grows as long as there is evaporation from the ground-water table, and the freezing gradient continues to prevail across the soil system. Upon continuous evaporation the vapor comes into contact with the ice needles of the frosting, and the vapor condenses on the moisture films of these needles and eventually solidifies to give new needles of ice, thus increasing the thickness of the frosting. The increase in the thickness of the frosting brings about resistance to the upward flow of the heat from the surface of the ground-water table in the direction of the cold front. Thus the continued increase in frosting, in its turn, decreases the coefficient of the heat transmission.

Figure 12 shows massive ice drops in the matrix of solid icing on the lower side of the plastic plate formed at large porosities. The massive icing is underlain by frosting—a very porous needle-like ice (Fig. 13).

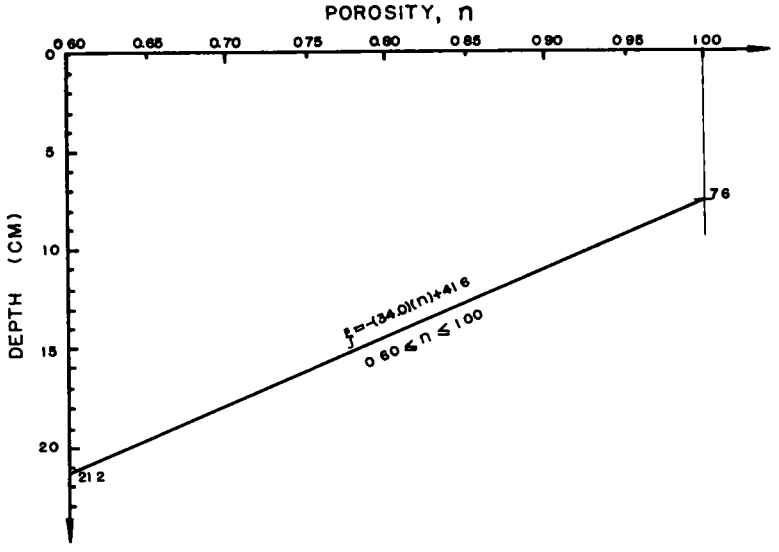

Figure 11. Variation of frost penetration depth with porosity (vapor phase).

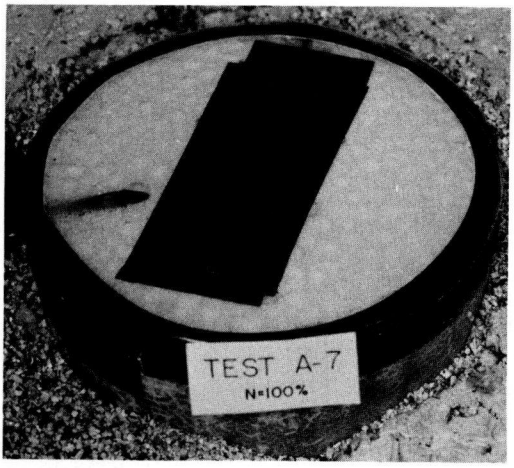

Figure 12. Massive ice drops in matrix of solid icing on lower side of plastic plate formed at large porosities.

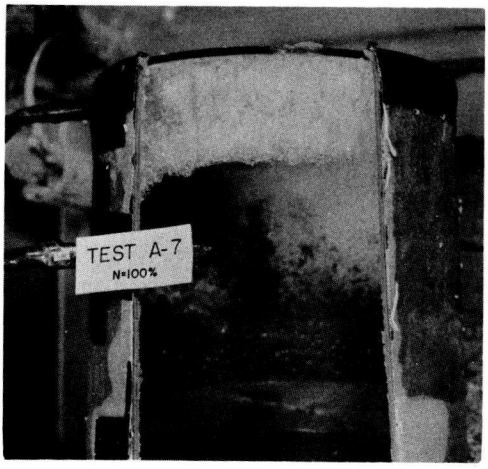

Figure 13. Frosting underneath a 2-mm thick icing.

Coefficients of Diffusivity

The values of the coefficients of diffusivity, D, shown in Figure 14 were calculated as follows:

1. The amount of soil moisture transferred for each porosity reported and up to a certain elapsed time (e.g., t = 64 hr) was established from the amount of water consumed from the "ground-water" burettes during that freezing process.
2. The diffusion height, L_V, was computed by subtracting the corresponding frost penetration depth, ξ, from the total effective height, H = 29.0 cm, of the cylindrical system of packing.
3. For each porosity the net horizontal cross-sectional area of the cylindrical system of packing was determined.
4. The vapor pressure difference between those at the ground-water table and at the corresponding 0 C-isotherm were calculated based on temperature measurements at these elevations.
5. The appropriate values were then substituted in Fick's first diffusion equation and solved for the coefficient of diffusivity.

Based on the coefficients of diffusivity thus experimentally obtained, the empirical equation of coefficient of diffusivity, D, for the packings studied is established as a function of porosity n as

$$D = (0.6)n - 0.174 \left[cm^2/sec \right] \tag{5}$$

and the equation for a dimensionless ration of D/D_0 is established as a function of porosity n as

$$D/D_0 = (1.425)n - 0.425, \tag{6}$$

in which $D_0 = 0.426$ = coefficient of diffusivity at a porosity of n = 100 percent. In these equations, however, for the sake of consistent units, n is in decimal fractions. Graphs of these equations are shown in Figure 14.

These equations are good for the experimental porosity interval from n = 60 percent (n = 0.60) to n = 100 percent (n = 1.00). Thus Eqs. 5 and 6 permit calculation of coefficients of diffusivities D for any porosity between n = 60 and 100 percent. Below porosities of n = 60 percent the equations are not good because other soil moisture

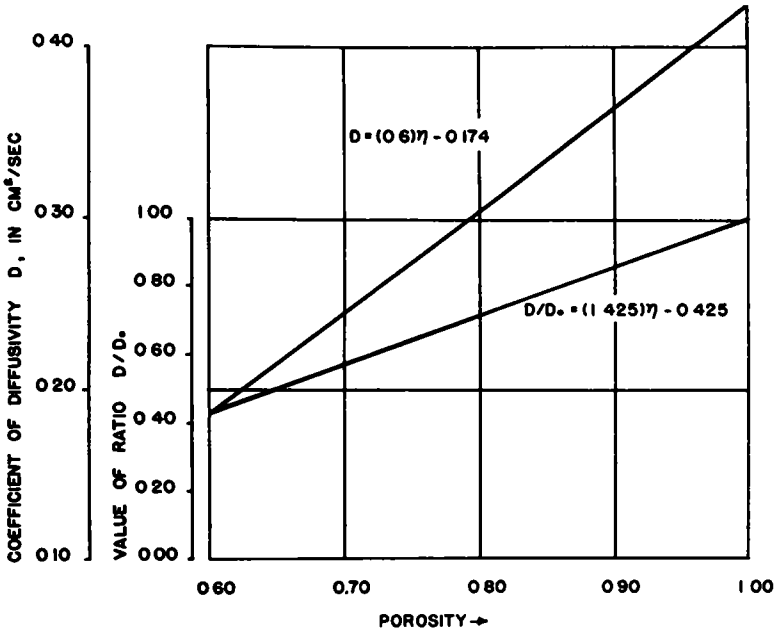

POROSITY - η IN DECIMAL FRACTIONS	COEFFICIENT OF DIFFUSIVITY - D IN CM²/ SEC	RATIO D/D₀ AT 100 % POROSITY D₀ = 0 426	TIME ELAPSED IN HOURS
1	2	3	4
0 60	0 186	0 43	64
0 70	0 246	0 58	62
0 80	0 304	0 71	72
0 90	0 366	0 86	64
1 00	0 426	1 00	50

Figure 14. Coefficients of diffusivity as a function of porosity.

transfer mechanisms beside vapor diffusion begin to show their effect, and the plot is no longer linear. Eqs. 5 and 6 show clearly that the denser the packing of the soil system the less vapor is transferred to the chilled zone; i.e., the more difficult it is for the vapor to move through the packing.

These experimentally obtained coefficients of water vapor diffusion into air at temperatures below freezing agree satisfactorily from n = 60 to 70 percent. From n = 70 to 100 percent, the experimentally obtained diffusion coefficients are somewhat higher than those (about D = 0.200) found in the literature; for example, D = 0.203 by Houdaille (4) and D = 0.198 as determined by Winkelmann (5). This may be brought about partly because of the coupled heat potential, and possibly for other reasons. Of course, the values of the D-coefficients also depend on the elapsed time of the experiment and the temperature gradient used. The temperatures at which these diffusion coefficients were calculated were from T_S = -16 C to T_S = -20 C at the top surface of the cylindrical system of packings, assumed T_O = 0 C at the 0° (freezing temperature) isotherm, and T_1 = 8 C of the ground-water.

CONCLUSIONS

1. Very porous real soils, as defined in this paper, are uncommon in nature. Artificially prepared highway and airfield base courses and railroad ballast, however, have relatively large porosities. In such packings, the vapor transfer mechanism is the most effective one.
2. Although the aqueous vapor diffusion process through a porous medium is in itself a very complex process, these experiments, however, elucidate under what conditions the vapor transfer mechanism in a freezing soil system prevails.
3. The pure vapor diffusion mechanism is active within the porosity range of a soil packing from about n = 60 percent to n = 100 percent.
4. The rate of moisture transfer in the vapor phase depends mainly on the intensity of the freezing thermal gradient imposed on the soil system. This gradient gives rise to a vapor pressure gradient that is the driving force for the movement of vapor.
5. The total amount of soil moisture transferred by the vapor diffusion mechanism depends on the porosity of the soil.
6. At porosities from about n = 40 percent to n = 55 percent, the coefficients of vapor diffusivity turn out to be relatively large. This fact indicates that next to the vapor diffusion mechanism other soil moisture transfer mechanisms start to set in. The particles of the packing are in contact with each other. This porosity interval therefore indicates the coexistence of the vapor diffusion mechanism and the film flow mechanism, or it indicates a transition from film flow to vapor diffusion of soil moisture.
7. The experimentally obtained coefficients of vapor diffusivity range from D = 0.183 at n = 60 percent porosity to D_o = 0.426 at n = 100 percent porosity of the packings. Generally, the diffusion coefficients increase with increase in porosity of the soil packing.

In general, these experimental studies clearly brought out that the degree of packing of soil is very important to know and to report, as this gives a clue as to what kind of mechanism would be most likely to take place in the upward soil moisture transfer in the soil system—vapor diffusion, film flow, or both.

Further, these experimental studies justify the assumption made to serve as a basis for soil freezing experiments on soil moisture transfer by way of the film mechanism, namely, that the upward flow of soil moisture through frost-susceptible packings of soil of ordinary porosities (between about n = 28 percent to n = 40 percent porosity), as encountered in soil engineering practice, takes place virtually unaccompanied by vapor diffusion.

ACKNOWLEDGMENTS

The author is grateful to the National Science Foundation for financially sponsoring a research project at Rutgers University on "Upward Migration of Water in Soil Exposed to a Freezing Atmosphere," Grant NSF-G6577. This article constitutes a small phase of this project.

Joseph M. Casero diligently performed the freezing experiments.

The author's appreciation goes to J. J. Slade, Jr., Director of the Bureau of Engineering Research at Rutgers University, for discussing certain aspects in this study, and to M. L. Granstrom, Chairman, Department of Civil Engineering, and E. C. Easton, Dean, College of Engineering, both of Rutgers University, for their efforts in improving working conditions in the Soil Mechanics and Foundation Engineering Laboratory to facilitate the prosecution of this project.

REFERENCES

1. Jumikis, A.R., "Concerning a Mechanism for Soil Moisture Translocation in the Film Phase upon Freezing." HRB Proc., 39:619-639 (1960).
2. Partington, J.R., "An Advanced Treatise on Physical Chemistry. Vol. I: Fundamental Principles; The Properties of Gases." Longmans Green (1949).
3. Stefan, J., "Versuche über die Verdampfung." Sitzungsbericht der Math.-Naturwissenschaftlichen Klasse der K. Academie der Wissensch., Vienna, 68: Pt. 2 (1874).

4. Kaye, G.W.C., and Lahy, T.H., "Tables of Physical and Chemical Constants." Longmans Green (1948).
5. "Smithsonian Physical Tables." Smithsonian Institution, 7th ed.
6. Jumikis, A.R., "Soil Moisture Transfer in the Vapor Phase upon Freezing." HRB Bull. 168, 96-115 (1957).
7. Winterkorn, H.F., "Earth Environment, ERDL Project Contract No. DA-44-009 Eng. 1773." Pennsylvania College, Dept. of Engineering Research, App. C (Nov. 28, 1953).

The Frost Behavior of Soils
II. Horizontal Sorting

ARTURO E. CORTE, U. S. Army, Cold Regions Research and Engineering Laboratory

Laboratory experiments have been performed with a special "closed-system" side freezing cabinet in which completely saturated soil samples were subjected to alternate freeze-thaw cycles without surcharge. A vertical or nearly vertical freeze-thaw plane was obtained in the side freezing cabinet. The soil used was a straight-graded noncohesive material with 14 percent finer than the No. 200 (0.074 mm) mesh sieve. According to existing criteria, the soil would be classified as nonfrost susceptible.

All experiments were run for 22 cycles. Freezing was at rates of 30, 33, and 42 mm per hr. The initial dry density was approximately constant for each test at 1.8 gr per cc or 112.4 pcf.

The tests under saturated conditions showed an over-all increase in volume during the cycles, but the movement of particles away from the freezing front caused a noticeable loss of volume close to the cooling plate. The rate of movement of the fraction finer than 0.074 mm for the closed-system condition was in the order of 0.05 percent per cycle. Differences in fines (finer than the 0.074 mm fraction) concentration between cold and warm faces after 22 cycles show 3.4 percent for the unwashed and 0.9 percent for the washed sample. Lines connecting equal amounts of like particle sizes have a tendency to be vertical at low rates of freeze and become inclined at higher rates of freezing.

The phenomenon of vertical and horizontal sorting is considered a problem of volume change. Volume changes produced by a sieving action without freezing and thawing show that the volume change produced by the sorting of a straight-graded sample is a function of the uniformity coefficient.

The active layer in the permafrost shows vertical sorting whenever horizontal sorting is encountered and sorting occurs in soils with and without particles finer than 0.02 mm. Because vertical sorting is produced by freezing and thawing from the top and horizontal sorting by freezing from the sides, it is expected that vertical and horizontal sorting should be found in seasonally frozen soils besides the permafrost regions where the soil freezes from the top and sides.

A general principle of sorting is presented: When freezing from the top, fine particles migrate downward away from the cooling front and this movement is facilitated by gravity and pore space left by the freezing action. When freezing from the bottom up, the vertical sorting is increased by (a) fines migrating upward in front of the freezing plane, and (b) fines coming down in the unfrozen part. For the side freezing, gravitational forces cause a parabolic path of the migrating particles. A heterogeneous soil with or without particles finer than 0.02 mm has a natural tendency to become vertically and horizontally sorted if it is frozen from the top, the bottom, or the sides. As in the case of vertical sorting, this principle implies that a well-graded gravelly soil, with or without fines, will be sorted whenever subjected to a sufficient number of

freeze-thaw cycles. Although such a soil may not form ice lenses during the first freeze-thaw cycle, the chance for such a formation will increase during the subsequent cycles as more fines segregate.

It is recommended that particle migration caused by side freeze-thaw cycles be studied for engineering application in certain types of construction.

•LABORATORY experiments and field data reported in Part I (1) show that "vertical sorting" of particles of different sizes is produced by a horizontal freeze-thaw plane moving from the bottom up or from the top down in the soil layer. Vertical sorting is defined as a segregation of coarse particles at the top and fine particles at the bottom of the freeze-thaw layer. Results of the study on horizontal sorting produced by a vertical freezing plane are presented here.

The freeze-thaw plane may vary from the horizontal to the vertical depending on two conditions: (a) the change of the uniformity coefficient over short horizontal distances and (b) the arrival of large particles at the soil surface by vertical sorting. If the uniformity coefficient (C_u D_{60}/D_{10}) increases from the two ends of a certain vertical plane to a maximum at the center, volume changes directly related to C_u will occur. The mound created by the greater volume change will produce a freezing direction normal to the slope of the mound. Large particles rising to the surface of the mound by vertical sorting will gravitate down the slope, leaving a center of fine material surrounded by coarse particles. In the case of large particles brought to the surface by vertical sorting, the freeze-thaw plane will follow the contour of the stone. As stones have a higher thermal conductivity than the surrounding material, the particles adjacent to the stones are subjected to a side freezing component.

This report deals with the effects of a vertical freeze-thaw plane moving laterally in heterogeneous and skip-graded mixtures. The results of laboratory data are used to explain one type of sorting in nature. In the cold regions of the earth, the soil surface is characterized by the formation of areas of fine particles surrounded by coarser ones, called "horizontal sorting." Since the beginning of the Twentieth Century, the problem has attracted the attention of scientists, and, by 1927, 21 theories had been proposed to explain the origin of ground sorting (2, p. 182). Hundreds of papers have been published in different countries expanding on various theories and findings on the subject.

The problem of sorting is complex. A necessary step is to isolate the main factors responsible for the segregation of particles. Because this is a complicated matter, an appropriate approach to the solution is through experimental work in the field and laboratory where controlled conditions can show the effect of the different variables of frost behavior. USA SIPRE (CRREL) has been experimenting with the problem of soil sorting since 1955.

One type of sorting is purely mechanical and is produced by gravitation of particles into depressions. The type of sorted feature depends on the geometric pattern of the soil depressions, according to field and laboratory studies at CRREL. Sorting is produced by wind and rain in desiccation cracks (3) and by differential melting of ice under various thicknesses of gravel (4). However, the melting of glacier ice under a layer of heterogeneous material or the collapse of permafrost due to melting of ice masses cause a more or less rounded irregular pattern (4).

A second type of sorting is produced by cyclic freeze-thaw. The sorting effects of a horizontal freeze-thaw plane has been already reported (1). The present report on the effects of a vertical freeze-thaw plane should be considered as an extension of the previous one on vertical sorting. In the conclusions the results of both papers are brought together.

LABORATORY EXPERIMENTAL DATA

Experimental Procedure

In Part I of this report (1) it was demonstrated that, when a soil is subjected to a cyclic freeze-thaw action in a horizontal plane, coarse particles will move up and fines

will move down. When a large particle reaches the surface and remains partially embedded, it will create a change in the freeze-thaw condition because its thermal conductivity is greater than the surrounding material. The soil adjacent to the larger particle will freeze more quickly and the freeze-thaw plane will be parallel to any point on the stone. Therefore, the freeze-thaw plane will vary from a horizontal to a vertical position depending on the point in question. For that reason, it is necessary to understand the effects of a vertical freeze-thaw plane in heterogeneous and nonheterogeneous materials.

Materials Used for Experiments.—The two types of material used in the experiments had straight and discontinuous gradation (Fig. 1). Three samples were prepared in the laboratory: Sample a-5-2 had a straight gradation with 14 percent crushed quartz particles (Silicrete) finer than No. 200 sieve. Samples X-1 and X-2 were mixtures of two ranges of particle sizes. Sample X-1 contained 66 percent (between 7.93 and 10.0 mm) and 34 percent (between 0.71 and 1.00 mm). Sample X-2 contained 71 percent (between 7.93 and 10.0 mm) and 29 percent (between 0.037 and 0.074 mm) (Silicrete). Samples a-5-2 and X-1 are located in the so-called never-frost heaving moraine soils of Beskow (5, p. 125).

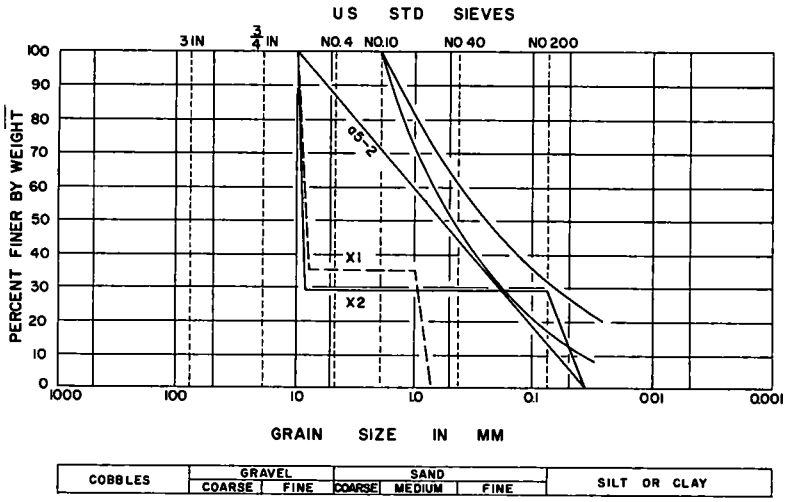

Figure 1. Samples a-5-2, X_1, and X_2, compared with the frost susceptibility limiting curves of Beskow (solid heavy lines).

Before the cyclic tests were performed, the samples were compacted to a dry density of approximately 1.8 g per cu cm (112.4 pcf). A small rubber piston was used for compaction so as not to crush the grains. A lucite plate was placed at the top of the soil sample as a bearing surface for a dial gage installed to measure soil heave. The tests were carried out under saturated conditions; water was added every five cycles to maintain saturation. In this closed system, no overburden pressure was applied.

Apparatus and Experimental Control.—The apparatus for this side-freezing experiment was a square box with a cross-section 15 by 15 cm constructed from 2-in. plywood (Fig. 2). The bottom and sides of the freezing cabinet were treated with shellac to make them watertight. A vertical freeze-thaw plane was obtained by placing two aluminum plates connected by five 1-in. diameter aluminum cylinders against the side of the cabinet. A heating tape was placed in the side of the cabinet opposite the cooling surface to control the freezing rate. By regulating the voltage drop across the heating tape, freezing rates varying from 2 to 42 mm per hr could be obtained. Most of the

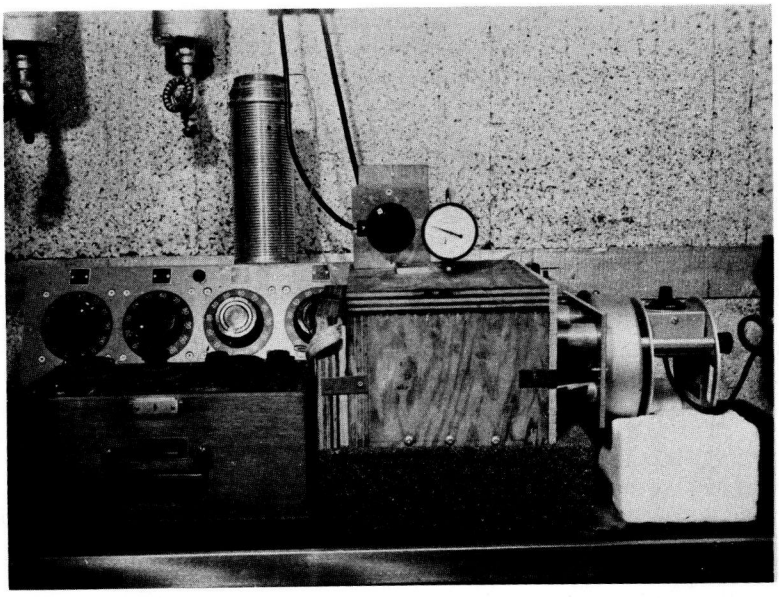

Figure 2. Closed-system side-freezing cabinet.

tests were conducted at rates ranging from 30 to 42 mm per hr. For the problem of vertical sorting, Part I of this report showed that the amount of segregation or particle movement increases with a decrease in rate of freezing. Therefore, it is expected that low rates would produce a greater particle movement. Tests conducted by the Arctic Construction and Frost Effects Laboratory on so-called "frost-susceptible" soils with freezing rates of 0.2 to 0.7 mm per hr show that low freezing rates are more likely to produce ice segregation than the higher rates (6, p. 114).

Experimental Results

Sample a-5-2.—Side freezing tests were performed with the following rates of freezing: 30, 33, and 42 mm per hr. The rate of thawing was approximately the same, 25 mm per hr. The initial dry density of 1.8 g per cu cm (112.4 pcf) was determined before cyclic action and was approximately constant for all the tests. The horizontal surface of the soil near the cooling surface became deeply inclined toward the cooling plate while the average height of the sample continuously increased. Volume changes computed for 1- and 30-mm per hr rates of freezing (Fig. 3) show that the difference in the volume changes for different rates are not as great as in the bottom-up freezing and thawing tests (1, p. 13). This is because of water supply. In the side-freezing test there is not an outside water supply; it is a closed system. It is expected that with an open-system side-freezing cabinet the differences in volume change should be greater under such rates of freezing.

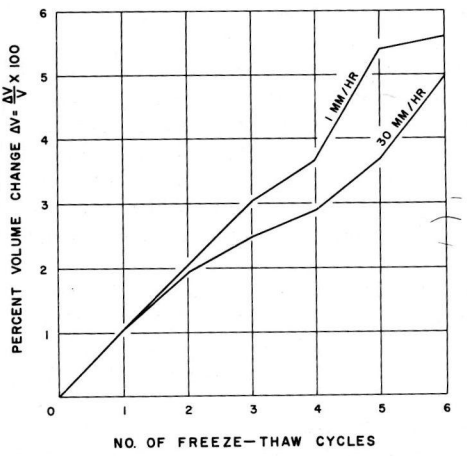

Figure 3. Volume change through six freeze-thaw cycles at two different freezing rates; initial density 1.8 g per cu cm or 112.4 pcf.

After 22 freeze-thaw cycles at 30 mm per hr the sample was divided into nine rectangles 15 by 5 by 2.7 cm. Three layers were taken and each layer included three samples. A grain-size analysis was made on these nine samples and the percentage by weight of particles finer than 0.074 mm was plotted in diagrams (Fig. 4a, b, and c). It was observed that after 22 cycles the percentage of particles finer than 0.074 mm moved steadily away from the cooling plate (Fig. 4a). Also, there is a tendency for the fines to increase from the surface downward. Points having equal percentage of fines were connected. These isograms have a tendency to be parabolic with the axis pointing away from the cooling front. If the samples were smaller, the differences in the amount of fines between extreme planes would become greater. The initial percentage of particles finer than 0.074 mm was 14 percent by weight. This was mixed with other particle sizes in the sample container before conducting the cyclic test. The difference in the percentage of the fraction finer than 0.074 mm before and after the test is a consequence of dry sieving, which gives a smaller amount of fines than the initial percentage mixed (14 percent 0.074 mm). In dry sieving, finer particles cling to larger ones. For the size of samples used, and dry sieving, the difference in fines concentration between the warm and the cold face after cycling is 3.5 percent (Fig. 4a). Fines migrated at a rate of 0.15 percent per cycle.

A second test was performed with sample a-5-2 at the rate of 33.0 mm per hr. The same cabinet was used and the moisture was maintained at saturation. The initial dry density was 1.8 g per cu cm (112.4 pcf). During the freeze-thaw test, it was observed again that soil level close to the plate dropped while at the far side increased slightly in height. After 20 cycles, the sample was divided into 9 rectangular slabs to determine the distribution of particles finer than the 0.074-mm fraction. Again, fines migrating from the cooling plate and from the top down increased. The isograms are inclined toward the cooling plate, but are less inclined than in the preceding experiment with a lower freezing rate of 30 mm per hr (Fig. 4b). Inasmuch as the rate of freezing in this second test was increased to 33.0 mm per hr, it is possible that the inclination of the isograms is a consequence of the freezing rate. More experiments are needed on this matter. The difference in the percentage of the fraction finer than 0.074 mm before and after the test is quite the same. Because this data was obtained with wet sieving this indicates that such sieving is more reliable than the dry sieving performed in previous experiment. The difference in fines concentration between cold and warm faces after cycling (Fig. 4b) is 0.9 percent indicating that fines moved at a rate of 0.04 percent per cycle. The difference in migration between this experiment at 33.0 mm per hr and the previous at 30.0 mm per hr is only a consequence of the sieving method. Wet sieving for this kind of sample is a more reliable test.

A third experiment was made at 42 mm to determine segregation at greater rates of freezing. The initial density 1.8 g per cu cm (112.4 pcf) was approximately the same as in the preceding case. After cycle 20 was completed, although the soil adjacent to the plate dropped 1.7 cm, the over-all height of the sample increased. The sample was cut into nine 15- by 15- by 2.7-cm parallelograms and the percentage by weight of the 0.074-mm fraction was determined. The isograms were more horizontal than in the preceding case, indicating the presence of vertical sorting. With the exception of 17.4 percent close to the freezing plate, there was clear vertical sorting across the sample with a maximum concentration of 18.2 percent opposite the cooling plate (Fig. 4c).

With freezing rates of 30.0, 33.0, and 42.0 mm per hr, the isograms of the finer than 0.074-mm fraction tend to become horizontal as the rate of freezing is increased. It seems that, with higher speed, the particles are knocked down rather than being pushed ahead of the freezing line. More experiments are needed on effect of the rate of freezing.

Samples X1 and X2. —To show the actual migration of particles, a new experiment was set up with two size ranges. At the bottom of the freezing cabinet, a layer was placed with particles ranging between 7.93 and 10 mm in diameter. The coarse particles were placed at the bottom of the container and one-half of this layer was surrounded by uniform sand of size range between 0.71 and 1.00 (X-1, Fig. 5), the other half were surrounded by particles of size range between 0.03 and 0.07 (X-2, Fig. 5). The thickness of the layer was smaller than the size of the coarser particles (7.93 mm).

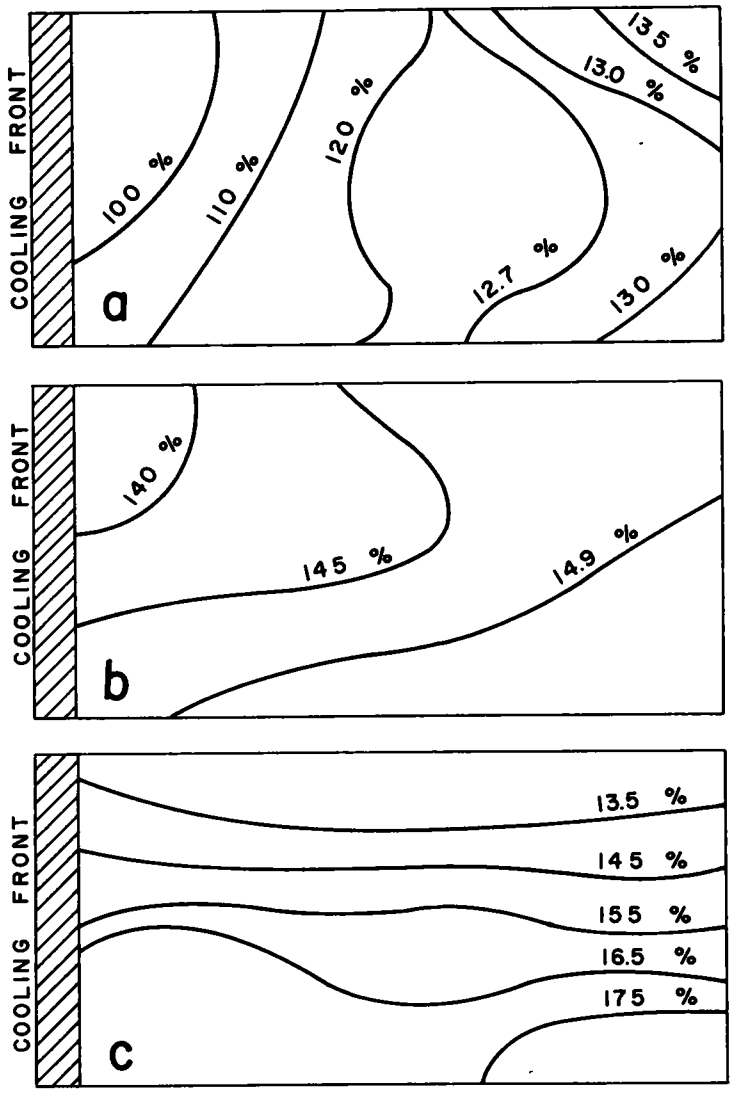

Figure 4. Effect of vertical freeze-thaw plane on distribution of fraction finer than 0.074 mm; closed-system side-freezing cabinet. Rates of freezing at 30.0 (a), 33.0 (b), and 42.0 mm per hr (c) for 22, 20 and 20 cycles, respectively, Sample a-5-2.

Accidentally some of the fines fraction were moved into the coarser material before subjecting the sample to the cyclic freeze-thaw test, as shown in Figure 5. However, the accident proved to be an asset to the experiment. The soil was subjected to 30 freeze-thaw cycles at a freezing rate of 30 mm per hr and pictures were taken at cycles 0, 7, 17, and 30 (Figs. 5 through 8). The cooling side is located at the right side of the picture and the freezing plane moves to the left. By comparing Figures 5 through 8 it can be seen that after 7 cycles the coarse sand which was accidentally moved into the fines has been pushed away from the cooling plate by the freezing front. Also, the white silicrete has moved away from the cooling plate. At cycle 0, only 7 stones were visible; after 30 cycles, 20 more stones can be counted closed to the plate. Fine particles moving from the cooling side cover the exposed stones at the lower half of the box. Of four stones, a, b, c, and d, visible before cycling, only the first (a) remains partly visible after 17 cycles (Fig. 7). The upper part of the coarse-grain sample shows

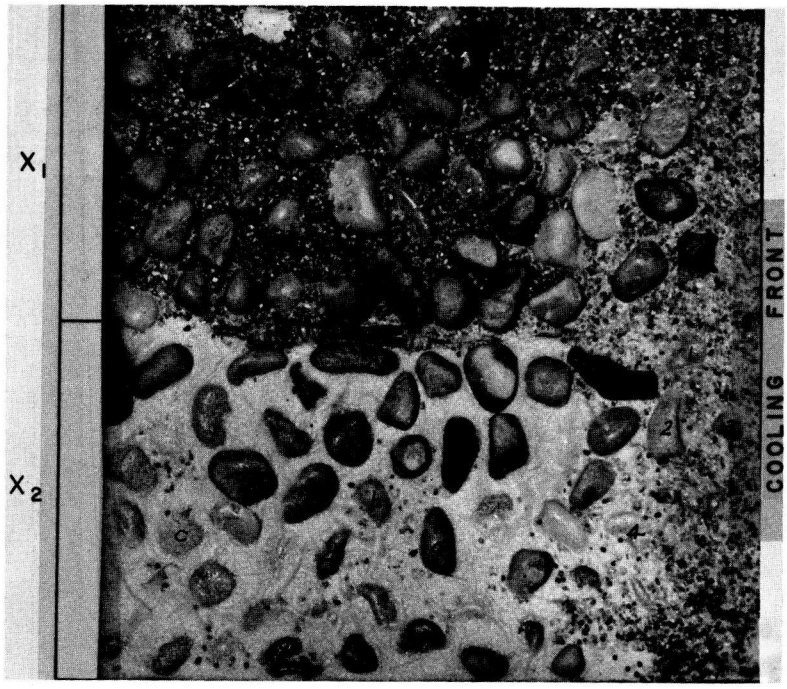

Figure 5. Top view of samples X_1 and X_2 before freeze-thaw cycles.

Figure 6. Samples X_1 and X_2 after cycle No. 7.

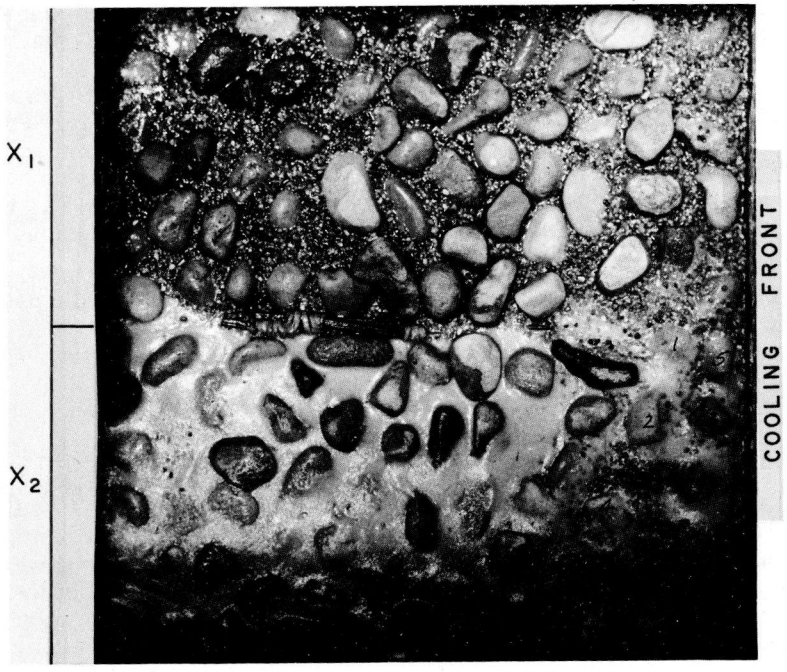

Figure 7. Samples X_1 and X_2 after cycle No. 17.

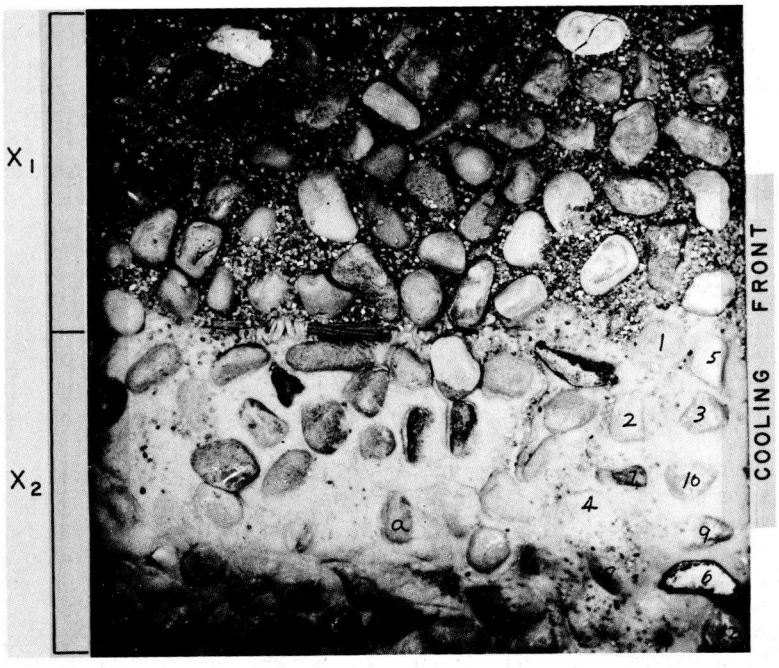

Figure 8. Samples X_1 and X_2 after cycle No. 30.

that the coarser particles are more visible near the cooling plate and that the large particles have moved away from the cold front (Figs. 5 through 8). It may be possible that the coarser particles are heaved at the same time.

The results of this experiment support previous findings that particles move away from the cooling front when the freezing rate is about 30.0-mm per hr. For this experiment the fraction finer than 7.93 mm did move a little at the 30.0-mm per hr rate compared to the finer material. It is likely that lower freezing rates and wider channel openings between particles will aid the movement of the medium size particles.

Mechanics of Sorting.—From the experiments the following conclusions can be derived:

1. Fine particles migrate away from the cooling front in a parabolic path. The downward motion is produced by gravitational forces.
2. Coarse particles between 7.9 and 10 mm also migrated away from the cooling front.
3. The rate of volume change by freeze-thaw cycles for the closed system condition is greater at lower freezing rates than at higher rates.

The mechanics of the sorting phenomenon are not yet fully understood. A few preliminary remarks are given here before a report on the subject. By freezing from the bottom in a laboratory experiment, it is observed that particles tend to migrate or "ride" in front of the ice interface. Particles 3 to 4 mm in diameter have been carried from the top of a saturated soil specimen when the rate of movement of the interface plane was approximately 0.6 mm per hr. For higher rates, the migration of such sizes was not observed. It is expected that each particle size requires a certain rate of movement of the interface in order to be moved. While this report was being revised, the movement of different sizes and shapes of particles at different rates of freezing has been investigated in the laboratory (7).

The following is a summary of the experimental information on the mechanics of sorting obtained from this report and from the previous one (1).

In top-down freezing, coarse particles heave because of either ice lens or expansion by the change of state of water; fines migrating in front of the freezing plane will gravitate (Fig. 9) into the void left by the coarse particles. For the top-down freezing and thawing, coarse particles move up and fines move down (1).

For side freezing, laboratory experiments show that coarse and fines migrate away from the cooling front (Fig. 10). Fines migrate more than coarse particles.

For a better understanding of the movement of particles in the bottom-up freezing, it is necessary to observe the unfrozen soil away from the freezing plane as well as the frozen part. Experiments with freezing from the bottom show that, although the lower part of the soil sample is being frozen, coarse particles are extruded from the unfrozen part of the sample at the surface. There is a concentration of fines at the interface where fines coming down from the unfrozen part are coalescing with fines going up in front of the freezing plane. This sorting is produced mechanically and is observed in the unfrozen soil when the freezing line is in the lower part of soil specimen. For the present experimental setup and by freezing from the bottom up, it is possible to say that mechanical sorting prevails over sorting by migration in front of the freezing plane. Therefore, two kinds of sorting by freezing are differentiated: (a) sorting by migration of particles in front of a moving freezing plane (this kind of sorting is observed when freezing proceeds from the top and the sides), and (b) mechanical sorting produced when freezing from the bottom up.

It can be concluded that soil particles tend to become sorted because of a tendency for the ice to exlude the particles that are in front of the growing ice. The size most likely to be excluded is the one that can migrate in the openings of the pores. It is envisaged that the migration rate of a certain particle size depends on the movement rate of the interface plane where the particle is riding. Experiments in progress are proving the validity of this concept (7).

Volume Change.—In Part I (1) it was demonstrated that sorting by sieving heterogeneous mixtures produces volume changes; for the case of straight-graded samples, there is a clear relationship between the volume changes and the uniformity coefficient of the sample (Fig. 11). If the gradation of the sample is linear, then (1, p. 15)

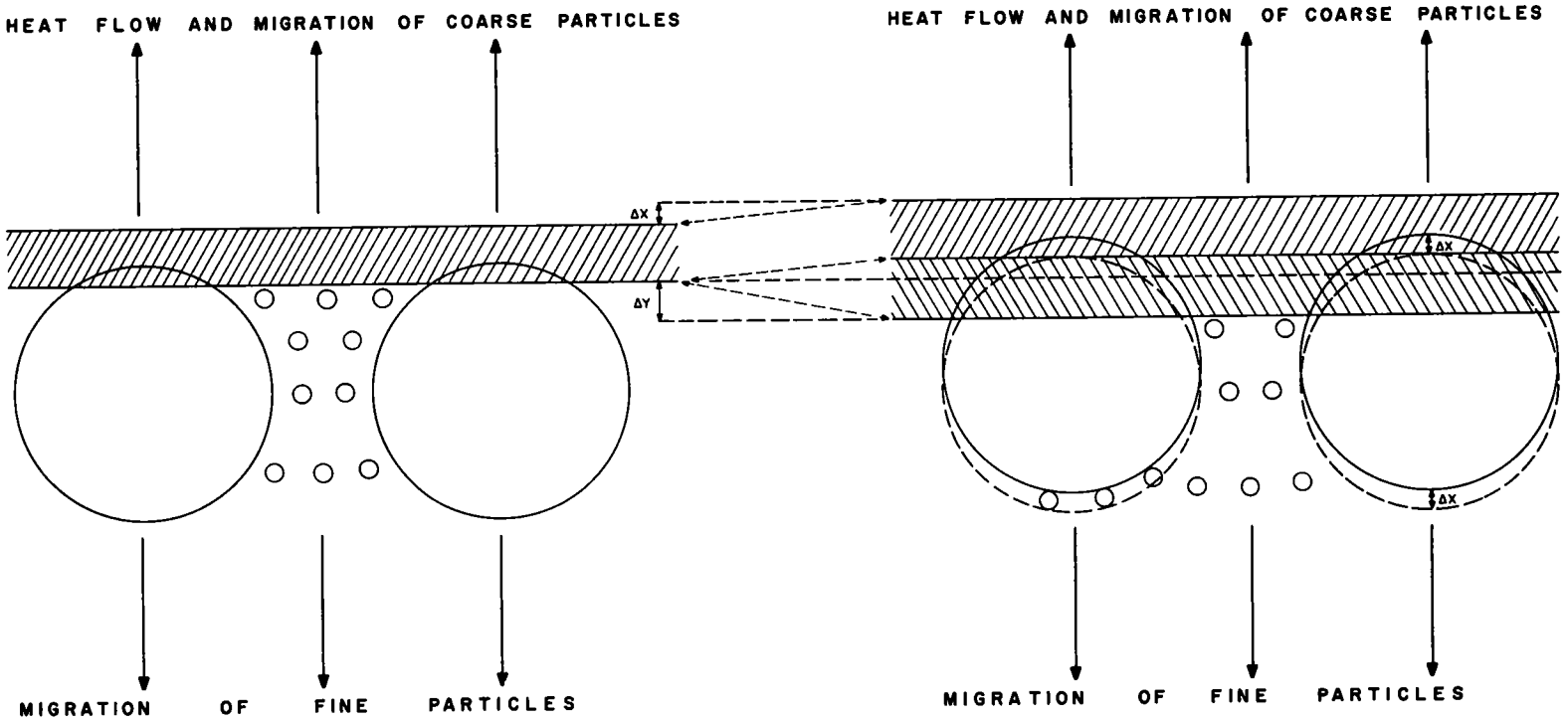

Figure 9. Sorting produced by horizontal freezing plane moving from the top down. As coarse particles are pulled up by freezing, fines migrate downward to voids left by coarse particles.

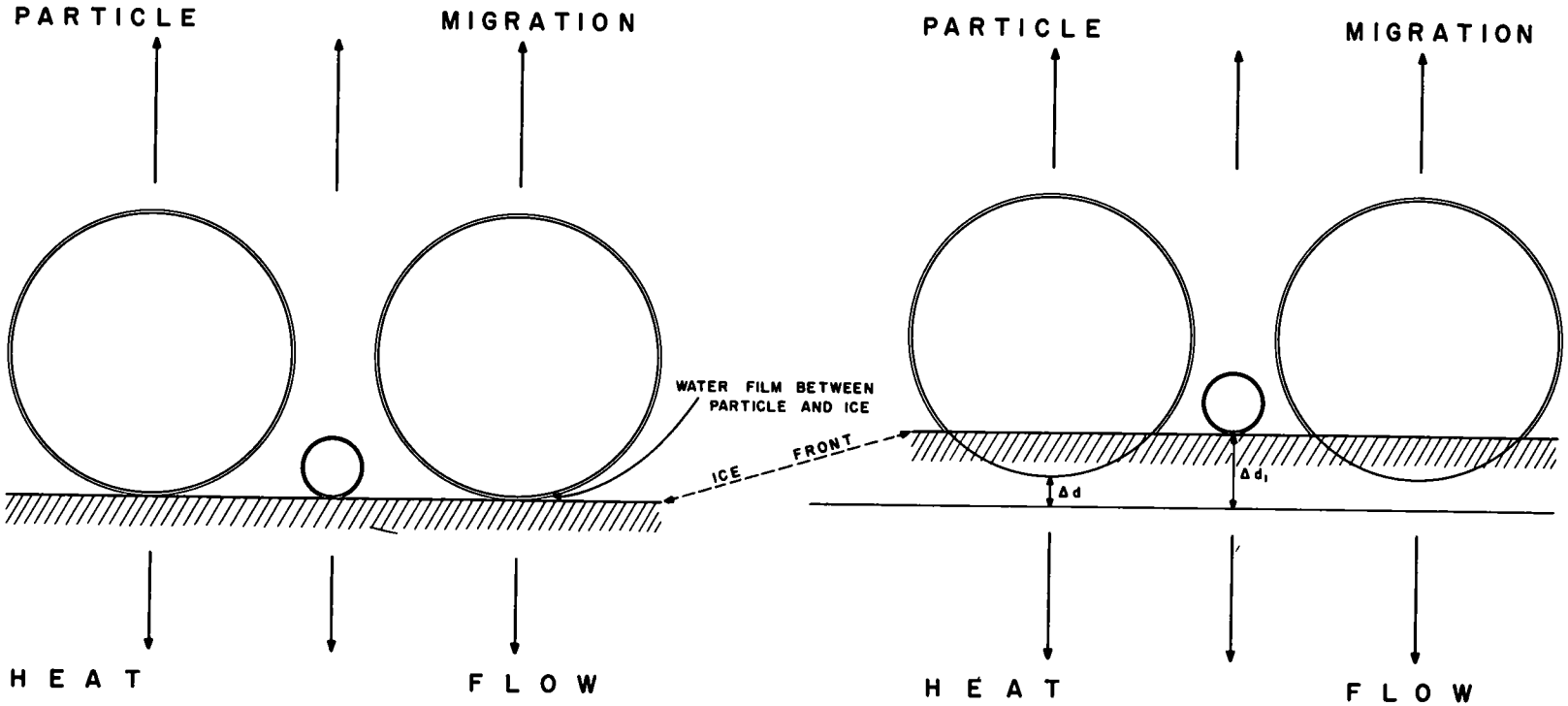

Figure 10. Sorting produced by vertical freezing plane.

$$\Delta v = a + b\ (\log C_u)$$

in which

Δv = volume increase

$$C_u = \frac{D_{60}}{D_{10}}$$

$$\Delta v = 1.000 + 0.19075\ (\log C_u)$$

An increase in the maximum size of the particles in the mixture by a factor of 10 produces an increase in volume of at least 10 percent.

FIELD DATA

Horizontal sorting in the arctic and high mountains is shown by a segregation of like-size particles in soils formed from bedrock, glacial and alluvial deposits. This segregation is manifested at the soil surface by small circles or "islands" of fine material surrounded by coarser particles. The diameter of the islands of fines ranges from 10 cm (Fig. 12) to several meters (Fig. 13), and the surface may be flat, dome-shaped, or depressed. Islands of fines can be isolated or more closely spaced (Fig. 13). When the islands are closely spaced, the coarse part has a polygonal pattern (Fig. 14). Segregation in flat, saturated areas often produces circular patterns; sorted features on a slope tend to become elongated (Fig. 13).

From surface inspection, it appears that these segregated features can be produced in materials with or without fines. Inasmuch as grain-size composition is one of the most important variables in soil frost action, the first step in field work is to determine the range in grain size needed for segregation.

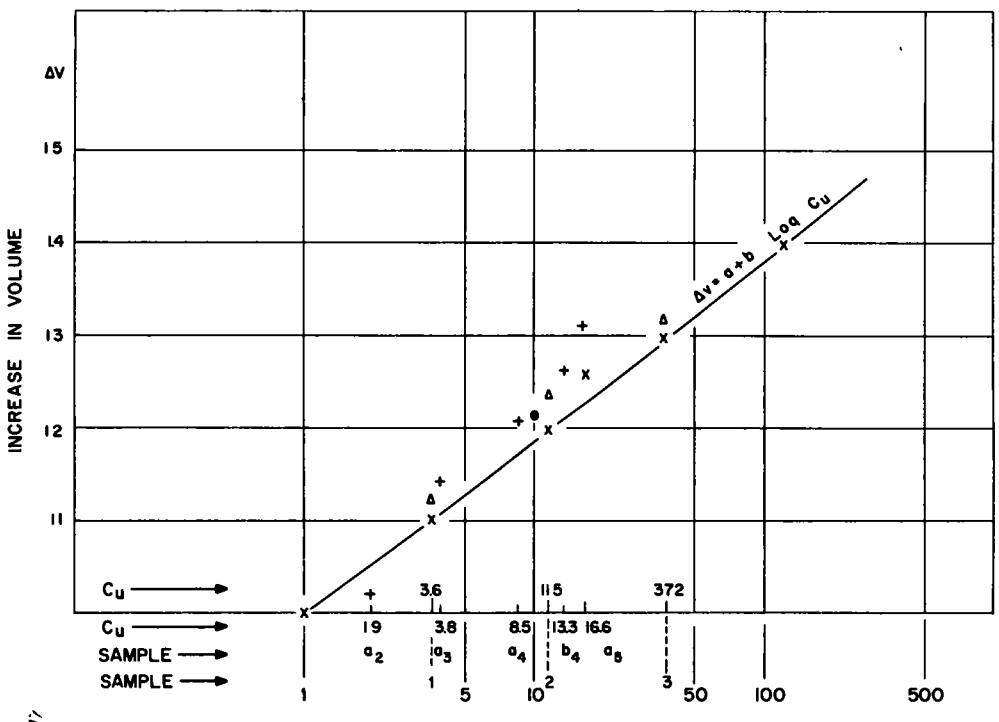

Figure 11. Relationship between volume changes and uniformity coefficient in straight graded samples. Triangles are volume change obtained with sand samples from Lake Michigan shore. Crosses are values obtained with commercial sands. Black dot is sample of glass beads. X on straight line is the 10 percent increase in volume for each 10-mm increase in maximum particle size.

Field data were obtained at the border of the ice cap near Thule, Greenland, where this segregation process has taken place in river-transported materials, moraine deposits, and residual soils. Field data presented here deals especially with transported materials. For clearness and simplicity, it was decided to analyze isolated cells that exhibited variations in their grain-size composition. Eight sorted circles with diameters ranging from 20 to 100 cm were analyzed.

For the analysis of each center of fines, samples were taken from concentric rings with the origin in the center of the circle for the horizontal plane and from equal layers at 20-cm depth intervals for the vertical plane. Alternate layers were taken for vertical sampling and are represented as follows: A, 0-20 cm; C, 40-60 cm; E, 80-100 cm; and F, 100-120 cm. However, for coarser materials, layers were taken at 33.3-cm intervals from 0 to 100 cm.

A grain-size analysis was made on eight sorted circles and all showed horizontal and vertical sorting. Of the eight circles analyzed, three with varying amounts of fines are discussed: Sorted circle No. 3, Figure 15; No. 1, Figure 16a and b; No. 8, Figure 17.

The horizontal and vertical sorting is expressed as the average grain-size value (median value taken from grain-size curves) at different distances from the center of the sorted area (Figs. 18, 19, 20). Because samples were taken at different depths and distances from the center of fines, horizontal and vertical sorting can be determined at any point in the sorted feature. Vertical sorting is expressed as the average grain-size value (median value) for different layers (Figs. 21, 22, 23).

In all three sorted circles analyzed, horizontal sorting shows a maximum at the surface and decreases downward (Figs. 18, 19, 20). Vertical sorting increases with distance from the center of fines (Figs. 21, 22, 23). Computation of the average grain-size value shows that these sorted features are developed in materials which contain 0.1, 1.0, and 2.5 percent by weight particles finer than 0.02 mm (Fig. 24) for sorted circles 8, 1, and 3, respectively, with uniformity coefficients of 10, 428 and 182, respectively. Comparing the grain-size curves with the Beskow frost-susceptibility curves shows that vertical and horizontal sorting occur in the zone of negligible ice segregation or non-frost heaving.

The distribution of the fraction finer than 0.074 mm (No. 200 sieve) in sorted circles 1, 3, and 4 was measured, and the points having equal percentages were connected (Figs. 25, 26, 27). The percentage increases toward the center and downward. The isograms indicate that when horizontal sorting is present, vertical sorting takes place, (Figs. 25, 26, 27). In the case of sorted circle No. 4 (Fig. 27), the finer fraction has risen to the surface and is flowing over it. From this field data, it is possible to make the following conclusions:

1. The horizontal plane of sorted features shows an increase in particle size from the center out, and the vertical plane shows a decrease in particle size downward producing the phenomena called vertical and horizontal sorting. Horizontal sorting is a two-dimensional phenomenon in which sorting is produced along the two directions—horizontal and vertical.
2. The grain-size range where this process has been observed is in the range of "nonfrost-susceptible soils."

CORRELATION BETWEEN LABORATORY AND FIELD DATA

Laboratory experiments show that a soil subjected to a horizontal and vertical freeze-thaw plane will produce vertical and horizontal sorting. Therefore, vertical and horizontal sorting of the active layer has to be produced by a horizontal and vertical freeze-thaw plane. This condition will be present when there are variations in the grain-size distribution in the layer that freezes and thaws. The variations may be produced by original deposition and vertical sorting. Because of the greater heat conductivity, large particles extruded at the surface of soil will freeze before finer ones surrounding them. This will cause a vertical freezing plane around the larger particles. The result will be a migration of fine particles away from the coarser ones. As this migration takes place, the soil under the coarser particles will sink and the soil into which particles migrate will heave.

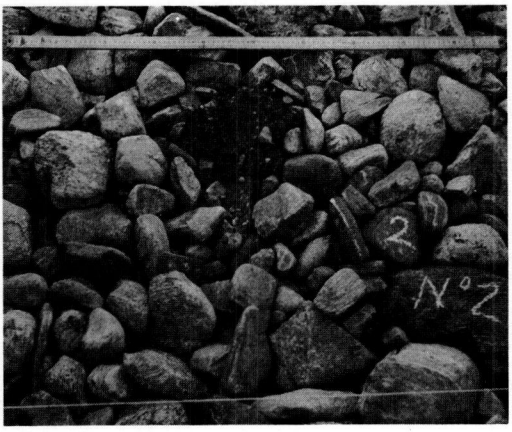

Figure 12. Sorted circle 2.

Figure 13. Air view of sorted circles in Thule area.

Figure 14. Closely spaced sorted circles.

Figure 15. Sorted circle 3.

Figure 16. Sorted circle 1 (a) before excavation for sampling, (b) after removal of outer coarse particles showing layer of finer particles beneath.

Vertical sorting is obtained in the laboratory by freezing from the top, the bottom, or both top and bottom whereas horizontal sorting is produced by side freezing. It is expected that horizontal and vertical sorting may be found in areas of seasonally frozen ground where the ground freezes from the top and from the sides only. Whenever different points in a layer begin to freeze with a horizontal thermal gradient, the finer fraction will tend to accumulate. These centers of fines may be dome-shaped (Fig. 15), flat (Fig. 14), or depressed with respect to the coarser areas.

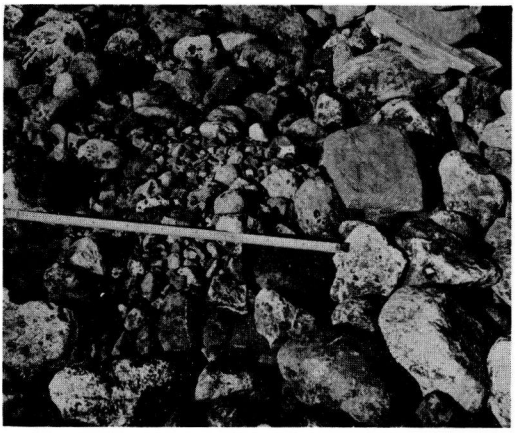

Figure 17. Sorted circle 8 developed in sand and gravel without fines.

Figure 11 shows that sorting of straight samples with a uniformity coefficient between 100 and 400 can produce volume changes between 35 and 45 percent. From this, in circles No. 1, 3, and 8 (Fig. 24) with C_u 428, 182, and 10, respectively, sorting can produce volume changes of 43, 42, and 18 percent, respectively. The volume changes in nature can be more readily compared to the volume changes shown in Figure 11 if sample gradations are straight as in sorted circles No. 1 and 3 (Fig. 24). According to the volume change uniformity coefficient criteria, sorted features 1 and 3 have increased in volume up to 45 percent since the feature started to develop. Volume change can be a phenomenon of vertical and horizontal sorting. Because this sorting occurs in a heterogeneous material about 1 m thick with a C_u between 100 and 400, volume changes of 35 to 45 percent have to be expected.

In the present experimental set-up, a "closed system" cabinet with a limited water supply was employed. The freezing rates used between 30 and 42 mm per hr are too

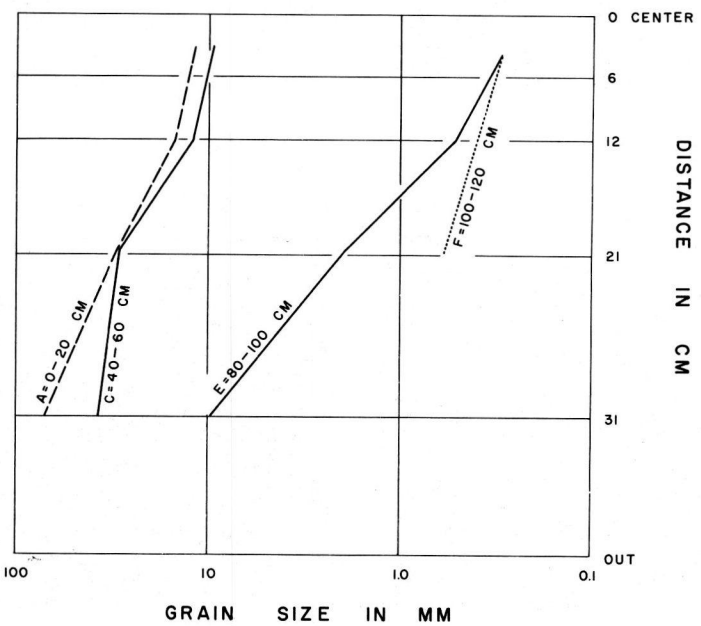

Figure 18. Horizontal sorting in circle 1 expressed as average grain size (median value) for different depths and distances from center of sorting.

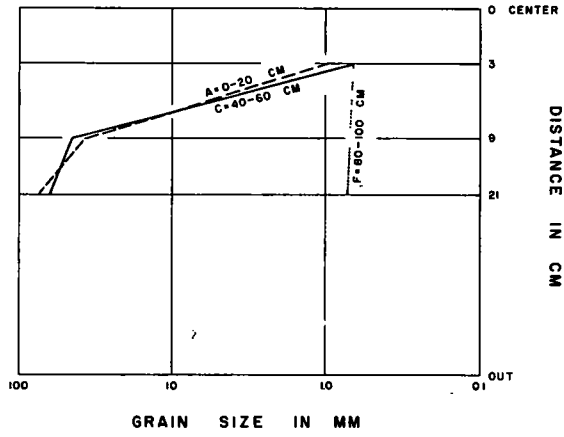

Figure 19. Horizontal sorting in circle 3 expressed as average grain size (median value) for different distances and different depths starting at center of sorting.

high compared to the freezing rates of the active layer. Taylor (8, p. 189) reported freezing rates in the order of 2.4 mm per hr within the active layer in the Thule area. K. A. Linnel (USA CRREL, personal communication) stated maximum rates of freezing in the order of 12 mm per hr for the upper part of the active layer. Part I of this report showed that particles segregation is greater at slow rates of freezing for top down

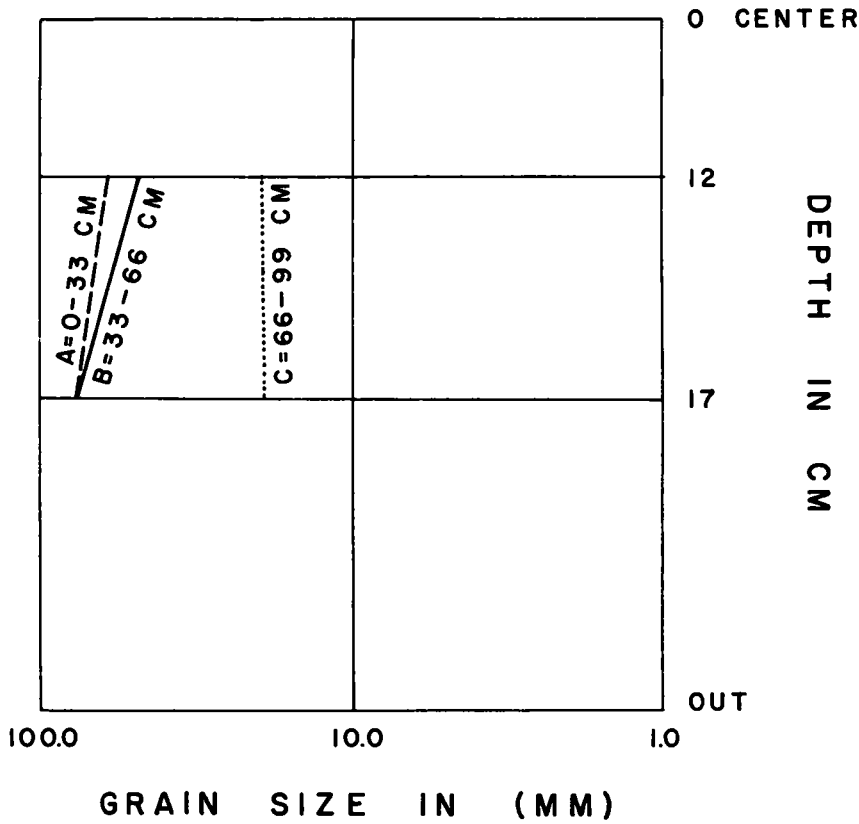

Figure 20. Horizontal sorting in circle 8 expressed as average grain size (median value) for two different distances and different depths starting at center of sorting.

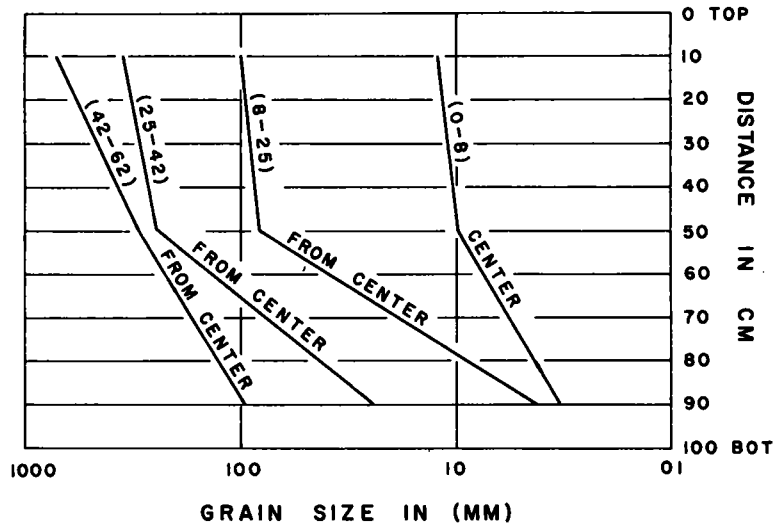

Figure 21. Vertical sorting in circle 1 expressed as average grain size (median value) for different depths and distances from center of sorted circle.

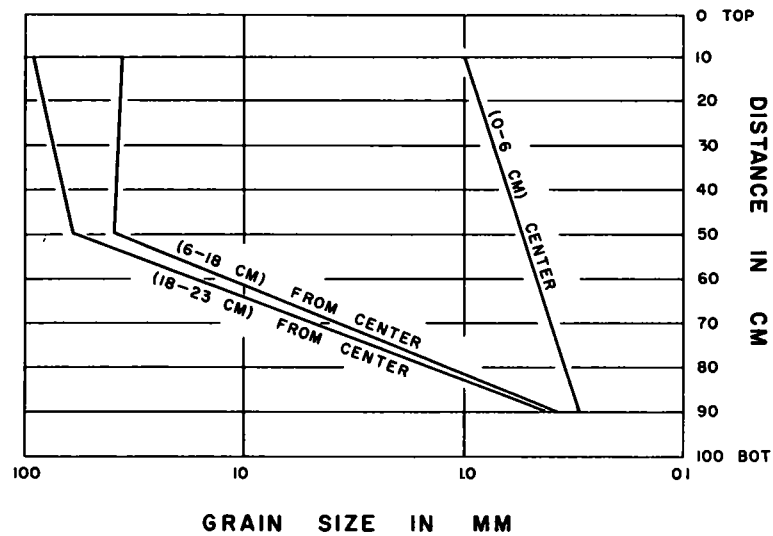

Figure 22. Vertical sorting in circle 3 expressed as average grain size (median value) for different depths and different distances from center of sorted area.

and bottom-up freezing (1, pp. 4, and 13). It is therefore clear that also in the side-freezing cabinet segregation will increase with a decrease of the freezing rate. Inasmuch as segregation of particles must be a direct function of the amount of water available at the freezing plane, it should increase as the moisture supply is increased. Therefore in an "open system" cabinet with an unlimited water supply, segregation of particles should be greater than in a "closed system" cabinet. The present experimental set-up shows segregation of particles regardless of a limited water supply and high rates of freezing. It is predicted that segregation of particles should increase with an increase of the moisture supply and decrease with an increase in the rate of freezing. While this paper was being revised, data became available on the segregation

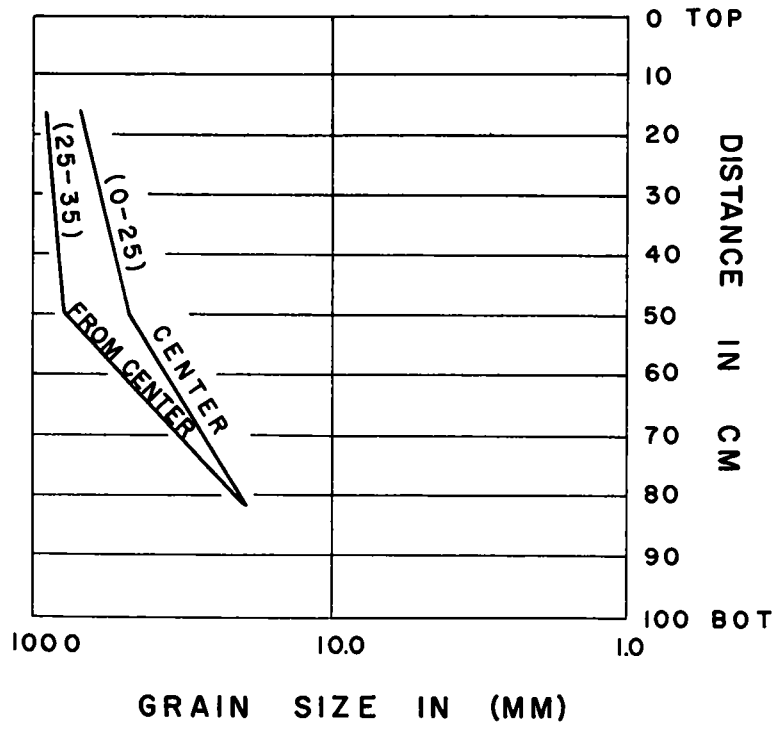

Figure 23. Vertical sorting in circle 8 expressed as average grain size (median value) for different depths and distances from center of sorted area.

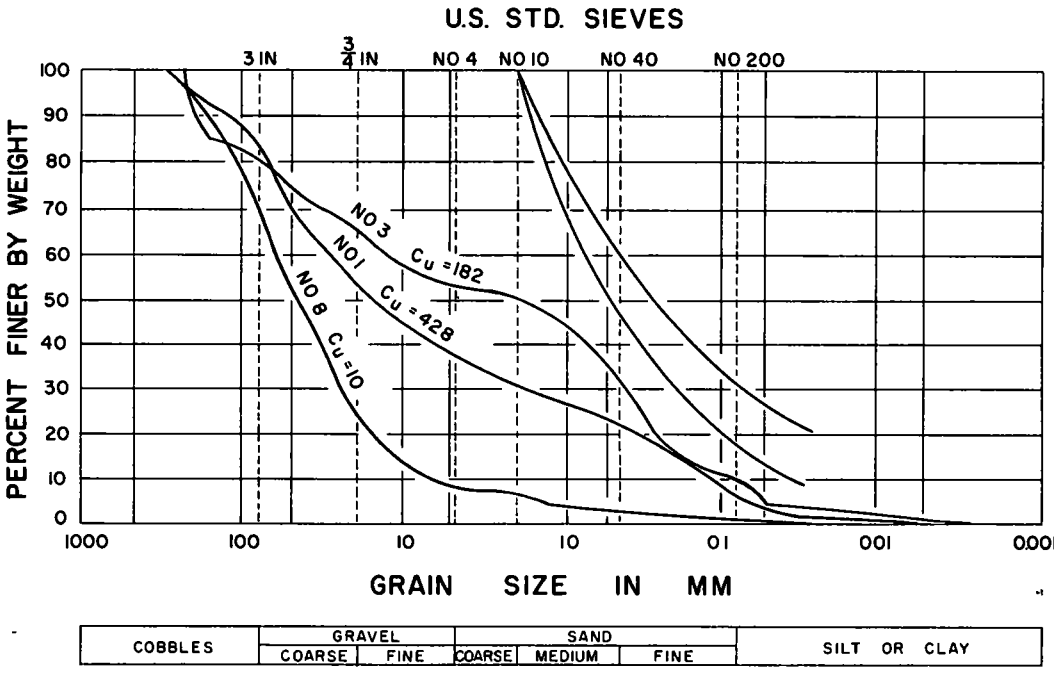

Figure 24. Average gradation curves for sorted circles 1, 3, and 8 for the active layer 0 to 100 cm in depth. Solid line curves are Beskow's frost susceptibility.

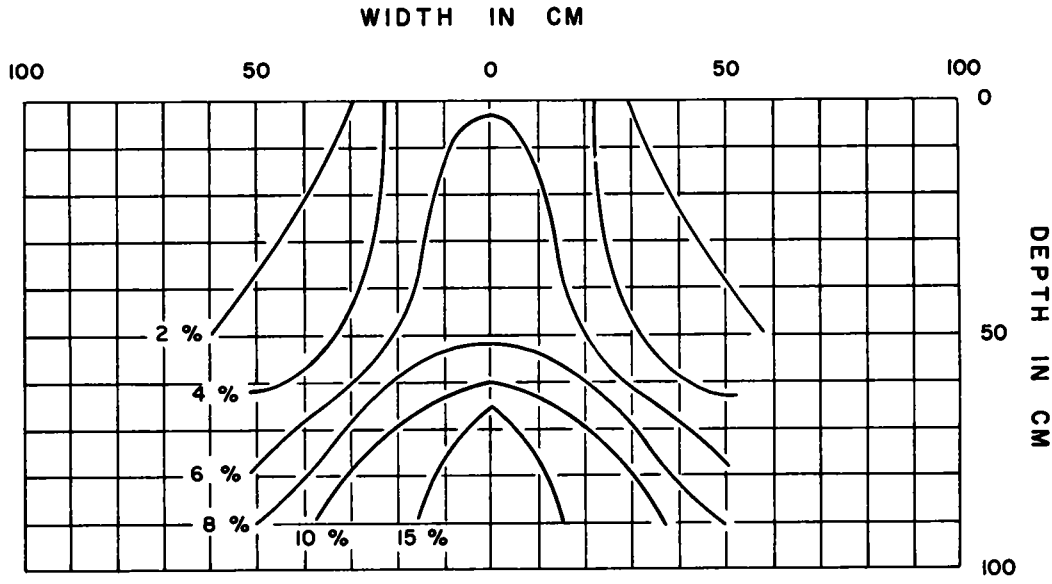

Figure 25. Distribution of equal percent of material finer than No. 200 sieve in sorted circle 1 between 0- and 100-cm depth.

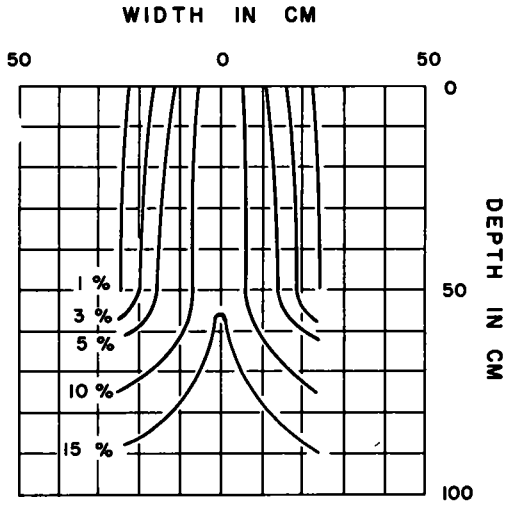

Figure 26. Distribution of equal percent of material finer than No. 200 sieve in sorted circle 3 between 0- and 100-cm depth.

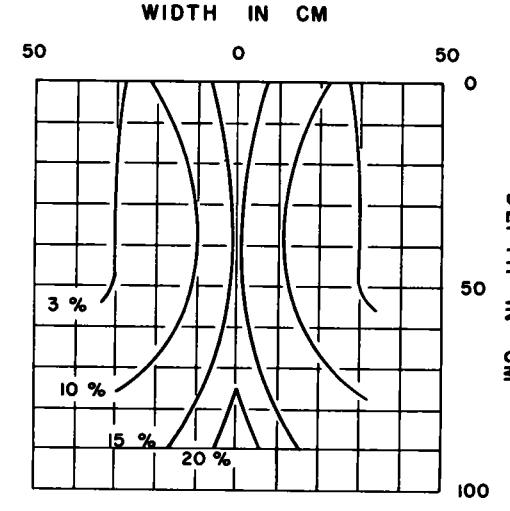

Figure 27. Distribution of equal percent of material finer than No. 200 sieve in sorted circle 4 between 0- and 100-cm depth.

of particles in front of a moving freezing plane (7) confirming the validity of this statement.

CONCLUSIONS AND RECOMMENDATIONS

Laboratory and field studies indicate that a heterogeneous mixture of grains tends to become vertically and/or horizontally sorted when subjected to alternate cycles of freezing and thawing under saturated conditions. Sorting is observed in soils with or

without fractions finer than 0.02 mm. At the present time, engineering standards consider the latter "nonfrost-susceptible." The active layer where such sorting is observed freezes from the top, the sides, and slightly from the bottom up (8, and A. Poulin, oral information). Therefore, the presence of horizontal and vertical sorting in the active layer is attributed to a vertical and horizontal freeze-thaw plane. In natural conditions, horizontal sorting starts around large particles where a vertical freeze-thaw plane is produced. Inasmuch as vertical sorting is obtained by freezing from either the bottom or the top, horizontal sorting is caused by freezing from the sides. It is expected that vertical and horizontal sorting exist outside permafrost regions in areas of seasonal frozen ground where the ground freezes from only the top and sides.

Laboratory experiments performed in a closed system with a vertical freeze-thaw plane demonstrated that particles migrate from the cooling side in a parabolic path. The path is parabolic because of the gravitational forces acting on the particles. As in the case of the inverted open system, the volume changes for the closed system are greater at lower freeze rates. The freezing rates used seem too high for natural conditions. Because it has been demonstrated that segregation is an inverse function of the rate of freezing, it is predicted that lateral segregation should increase if the freezing rate decreases, when a side-freezing "open system" cabinet is used.

On the basis of cyclic experiments in which freezing and thawing proceeds from the top, bottom, and sides, a general principle of sorting which is presented is a function of the rate of freezing and gravitational forces and independent of the direction of freezing. This principle implies that the finer fraction of a mixture tends to move away from the cooling front riding in front of the interface. Therefore, fines move down when freezing is from the top, and move laterally in a parabolic path when freezing is from the side. Upward movement is impeded by gravitational forces when freezing is from the bottom up. When freezing is from the bottom, it has been found that, while the lower layers are being frozen, fine particles move toward the bottom and coarse particles move toward the top of the upper unfrozen layer; therefore, in the light of these experiments, two kinds of sorting are differentiated: (a) sorting by freezing when particles migrate in front of the freezing plane (top and side freezing) and (b) mechanical sorting is produced by disturbance in the upper unfrozen layer while the lower parts are being frozen (bottom-up freezing). Such sorting is inverse of the sorting by migration in front of the freezing plane.

Based on preliminary experiments, the segregation phenomena can be tentatively explained by a tendency for the ice to exclude particles located in the growing front of the ice. It is predicted that the particle size that can migrate depends on the rate of movement of the interface plane where the particles are riding.

Experiments indicate that sorting produces volume changes which are a function of the uniformity coefficient of the soil among other factors. According to this research, vertical and horizontal sorting in soil with a uniformity coefficient C_u between 100 and 400 will produce volume changes between 35 and 45 percent. This research provides the tools for the explanation of areas of fine particles surrounded by coarser ones in the active layer and in seasonal frozen ground. A separate report will treat this problem.

It is recommended that particle migration caused by side freeze-thaw cycles be studied for engineering application in certain types of construction. Research indicated that the soil adjacent to a retaining wall will have a tendency to become less "frost susceptible" as fines migrate away from the cooling surface. A road embankment will tend to become more "frost susceptible" as the fines migrating from the sides towards the middle cause the possibility of a greater differential heaving in the transverse plane.

It is recommended that a new criterion for frost behavior be established that takes account of the effects of freeze-thaw cycles under field conditions with a large range of particle sizes. More research is needed to determine (a) rate of movement for different particle sizes; (b) rate of volume change caused by vertical and horizontal sorting; (c) effect of a fluctuating water table on particle-size migration after thawing; and (d) effect of rate of freezing on sorting different grain-size gradations.

ACKNOWLEDGMENTS

This work has been accomplished under Contract DA-11-190-ENG-118 between the Department of the Army and Arturo E. Corte for "Basic Investigations in Permafrost and Annually Frozen Areas," USA SIPRE Task 022.01.041, Field and Laboratory Study of Patterned Ground, (now 5010.03141. USA SIPRE was redesignated U.S. Army Cold Regions Research and Engineering Laboratory (CRREL), February 1, 1961.)

The author is indebted to the U.S. Army Snow Ice and Permafrost Research Establishment (USA SIPRE) for assistance and cooperation in the research. The research was performed under W.K. Boyd, technical director, and J.A. Bender, chief, Research Division. W. Brule, J. Gallippi, and A. Tice assisted in the work. Jerry Brown assisted in the final editing.

REFERENCES

1. Corte, A.E., "Frost Behavior of Soil—Field and Laboratory Data for a New Concept. Part I: Vertical Sorting." U.S. Army Cold Regions Research and Engineering Laboratory, Corps of Engineers, Research Report 85 (1961).
2. Elton, C.S., "The Nature and Origin of Soil-Polygons in Spitsbergen." Quart. Jour. Geol. Soc. London, 83:163-194 (1927).
3. Corte, A.E., and Higashi, A., "Experimental Research on Desiccation Cracking of Soils. Part II." (Research report in preparation.)
4. Corte, A.E., "Experimental Formation of Sorted Patterns in Gravel Overlying a Melting Ice Surface." U.S. Army Snow Ice and Permafrost Research Establishment, Corps of Engineers, Research Report 55 (1959).
5. Beskow, G., "Tjälbildningen och Tjällyftningen med Särskild Hänsyn till Vägar och Järnvägar (Soil Freezing and Frost Heaving with Special Application of Roads and Railroads)." Sveriges Geol. Undersökn. Arsbok 26., Ser. C. Avhandl. och Uppsat. 375 (1935).
6. Linell, K.A., and Kaplar, C.W., "The Factor of Soil and Material Type in Frost Action." HRB Bull. 225, 81-128 (1959).
7. Corte, A.E., "Vertical Migration of Particles in Front of a Moving Freezing Plane." U.S. Army Cold Regions Research and Engineering Laboratory, Corps of Engineers, Research Report 105 (1961).
8. Taylor, R.S., "A Study of Some High-Latitude Patterned-Ground Features." Ph.D. thesis Univ. of Minnesota (1956).

Pore Size and Field Frost Performance of Soils

THOMAS I. CSATHY and DAVID L. TOWNSEND, Respectively, Project Soils Engineer, Department of Highways, Ontario; Civil Engineering Department, Queen's University, Kingston, Ontario

This paper suggests that the soil property essentially determining frost behavior is pore-size distribution. The existing frost susceptibility criteria are, however, based on grain-size characteristics.

On the basis of the field frost performance of 126 Ontario highway subsoils, the reliability of seven existing frost susceptibility criteria is analyzed. The results indicate the limitations of these criteria. A simple method is developed to determine the pore-size distribution of soils, and a tentative frost susceptibility criterion based on this soil property is established. The reliability of this criterion appears to be more satisfactory than that of the existing criteria. The possibilities for further research work are indicated.

•IT IS a generally observed fact that detrimental frost heaving and thawing on highways is caused by the formation of segregated ice within the subsoil. A soil that serves as a favorable medium for the development of ice segregation under normally encountered temperature and moisture conditions is regarded as "frost susceptible." It is an essential aspect of highway design to recognize and reject frost-susceptible soils. As a practical tool for solving this problem, several frost susceptibility criteria have been proposed (1, 2) with the aim of predicting frost behavior on the basis of certain laboratory test results. The inadequacy of knowledge concerning frost action is apparent in that none of these criteria has proved sufficiently reliable in practice (3, 4).

Almost exlusively, the existing criteria are based on grain-size characteristics. A study of the mechanism of frost action (5) has led the authors to the conclusion that pore size probably has a more significant bearing on frost action than grain size, or any other soil property.

Significance of Pore-Size Distribution

It appears that every essential factor in the mechanism of frost action is intimately related to pore size. It governs freezing point depression inasmuch as it constitutes the size restriction for the growing ice crystal, it reflects pressure effects, and it is a measure of the relative proximity of particle surfaces. The possibility of localized ice formation is determined by the relative distribution of pore sizes. Experiments have shown that the induced suction and the heaving pressures increase with decreasing pore size. The retardation of the ice front is essentially governed by pore restrictions. The ratio of free to bound water during freezing, and the drainage and stability conditions upon thawing depend on the sizes and distribution of the pores. All the potential components induced by freezing (capillary, suction, thermal, vapor-pressure, electrical, and osmotic potentials) appear closely related to pore size. It is the governing factor in the supercooling theory, considering either the nucleation temperature aspect or the relative freezing point depression. In the electro-osmotic theory, pore size indirectly controls the facility with which the double layers are recharged, and thus the electro-osmotic activity of the system. Finally, the basic soil properties apparently influencing the nature of frost action (such as grain size, suction, capillarity, and permeability)

are actually direct functions of pore size, even though these relationships cannot be mathematically expressed with sufficient accuracy.

Although the basic importance of pore size in relation to frost action was originally pointed out by Taber (1) and recently emphasized by Penner (6), no one appears to have attempted to express this soil property quantitatively and to include it in a frost susceptibility criterion. In an early paper Schofield (7) drew attention to the possibility of interpreting suction and, possibly, capillary moisture profile curves in terms of pore-size distribution, and the same idea was later mentioned by Penner (8).

Research Objectives and Approach

The primary objectives of the investigation described in this paper were to relate the field frost behavior of a number of soils to the established frost susceptibility criteria and to consider the possibility of correlating frost susceptibility with pore-size characteristics.

The following specific approach was made:

1. A number of soil samples were taken from highway locations in Ontario where frost damage had been experienced, and the relevant data concerning the field performance of these soils (such as the extent of frost damage, moisture conditions, topography, and design features) were collected.
2. On the basis of these data, the field frost performance was evaluated in the form of a simple "performance index" for each soil.
3. The standard laboratory tests needed to apply the most widely used frost susceptibility criteria were performed. In addition, a method was developed, based on the active capillarity test, to obtain a quantitative assessment of pore-size characteristics.
4. The soils were classified according to the different frost susceptibility criteria, and the relative reliability of these criteria was determined by comparing predicted performance with actual performance.
5. The pore-size characteristics of the soils were related to their frost performance, and a tentative frost susceptibility criterion, based on pore-size characteristics, was developed and compared with the existing criteria.

FIELD WORK

Five highway sites were selected for the investigation. These sites included new and old, flexible and rigid pavement constructions, and also a site where the construction had only reached the grading stage. A brief outline of the conditions is given in Table 1. Pertinent information concerning physiographic data, general soils conditions, construction data and present pavement condition was obtained in each case through a study of the design documents and field observation.

TABLE 1

GENERAL CONDITIONS AT THE SELECTED SITES

Site	Type of Pavement	General Physiography
A	9-in. concrete, about 25 yr old	Imperfectly drained clay, or sandy loam outwash plain
B	Bituminous concrete, 1 to 5 yr old	Till moraine and sand plain
C	Road-mix pavement, 20 to 25 yr old	Pre-Cambrian rock ridges with little overburden
D	Unpaved, under construction	Till plain with sandy loam
E	Bituminous concrete, 25 yr old	Sandy loam outwash soil

At each of these sites, locations of apparent frost damage were selected and the subsoil conditions studied. The general principle was to select places where the problem appeared to be due to soil conditions rather than to construction features such as culverts or transition points between cuts and fills. As is usually the case, most of the damage was observed in cuts and had been caused by in-situ frost susceptible soils that had not been removed to a sufficient depth. On the assumption that fill materials had been selected with at least some regard to frost action, a relatively large number of fill locations were chosen to include as many borderline soils as possible. Care was taken not to include cases where the pavement damage had been due to causes other than frost action. Any location where reasonable doubt arose concerning the origin of the damage was automatically excluded from the study.

At each location, borings were performed with a power auger both inside and just outside the area of frost damage. The holes were drilled along the edge of the pavement to an average depth of 5 ft or to bedrock, the exposed soils were classified by inspection and the log of holes recorded. The average number of boreholes was 4 to 5 per location. Soil samples were normally taken only from those layers that, by inspection, showed the possibility of supporting ice segregation (e.g., a clean gravel base or a coarse sand subbase would not be sampled.) The average weight of the samples was 5 to 6 kg. The type and extent of frost damage, and the moisture and drainage conditions were also recorded to complete the case history records.

The total number of locations and samples was as follows:

Site	No. of Locations	No. of Samples
A	10	56
B	3	8
C	7	23
D	4	17
E	6	22
Total	30	126

Evaluation of Field Frost Performance

At a spot on the highway were frost damage had occurred, at least one of the subsoil layers could be regarded as frost susceptible. The nature of the prevailing moisture conditions (i.e., the position of the ground water table, surface and subsurface drainage, etc.,) obviously affected the degree to which the soil factor was responsible for the damage. The worse these conditions were, the smaller part the soil factor played in causing the frost damage. For example, medium frost damage might have been caused by a combination of very poor drainage and slightly susceptible soil as well as by a combination of good drainage and highly susceptible soil.

It at another spot, sufficiently close to the first one to warrant the assumption that the relevant moisture and temperature conditions were similar, there was no sign of frost damage, all subsoil layers within the depth of frost penetration could be regarded as nonsusceptible.

Thus the two basic factors to be considered for the evaluation of field frost performance were the extent of frost damage and the nature of moisture conditions. An additional factor, the effect of overburden pressure (depth below surface), was also taken into account in a qualitative manner. (Evidently, a highly susceptible soil located 4 ft below the pavement may cause the same degree of frost damage as a slightly susceptible soil located just below the pavement.)

Drawing the necessary information from the case history records and following the general procedure given in Table 2, the soils were divided into four classes denoted by the following performance indexes:

F0 = non-susceptible,
F1 = slightly susceptible,

F2 = moderately susceptible,
F3 = highly susceptible.

Because of the uncertainty of some of the field data, the performance indices were not of equal reliability. At some sections the degree of frost damage would seem obvious, whereas at others settlement independent of frost action might have caused some of the damage. At some sections it was easy to judge the nature of the soil moisture conditions, at others it was difficult. Some combinations of apparent damage and moisture conditions could also render the conclusion less reliable; e.g., in the case of no frost damage and low moisture the soil was probably nonsusceptible, but not necessarily so. Furthermore, it was necessary to estimate at each damaged section

TABLE 2

DETERMINATION OF FIELD PERFORMANCE INDEXES

Relative Scale for Pavement Damage[1]

No frost damage	D0	No sign of damage
Slight frost damage	D1	Surface roughness, hairline cracking
Medium frost damage	D2	Noticeable bump or single crack on new pavements, system of cracking of moderate intensity on old ones
Heavy frost damage	D3	Pronounced bump or cracking on new pavements, complete pavement breakup on old ones

Relative Scale for Moisture Conditions[1]

Low moisture	M1	Good drainage, low ground water table (moisture profile did not indicate the water table to be in the vicinity of the 5- to 6-ft drilling depth)
Moderate moisture	M2	Medium drainage, medium ground water table (moisture profile indicated the water table to be close to the bottom of the borehole)
Excess moisture	M3	Poor drainage, high ground water table (free water table was encountered within the drilling depth)

[1]Double symbols were used to denote borderline cases.

Determination of Performance Index

	M1	M2	M3
D0	F0	F0	F0
D1	F2	F1	F0
D2	F3	F2	F1
D3	F3	F3	F3

which soil layer had possibly caused the damage. This estimation was based on textural considerations and was made with confidence in most of the cases (a typical stratification: pavement, clean gravel, coarse sand, silty loam, bedrock; the silty loam being the critical layer). In some cases, however, the relative responsibility of the different layers for causing the observed damage was more doubtful; consequently, the performance indices arrived at were less reliable, or completely unreliable.

In an attempt to qualify its reliability, a weight factor was assigned to each performance index, using the values 0, 0.5, 1.0, 1.5, 2.0. This weight factor incorporated the various aspects mentioned in the preceeding paragraph, the details of the weighting procedure have been described elsewhere (5).

Following this procedure, a weighted performance index was obtained for each soil, and the subsequent analysis was based on the weighted number of soil samples, neglecting the soil samples with zero weight.

Assessing actual frost susceptibility on the basis of field performance had the advantage that the problem was considered within the framework of the complex field conditions, incorporating both heaving and thawing effects. The method adopted for the evaluation of field performance had certain limitations, because erroneous data may have been included by selecting sections where the damage was due to causes other than frost action, by misjudging the nature of the moisture conditions, or by attributing the damage to the wrong soil within a borehole. It was sought to minimize the effect of such errors by considering the interaction of the various factors and by weighting the field observations. The resulting performance indices were regarded as being sufficiently correct, at least in a statistical sense, to check the reliability of the practical frost susceptibility criteria.

LABORATORY WORK

Standard Tests

To determine those soil properties needed for the application of the present criteria, grain-size analysis (dry and wet sieving as well as hydrometer test) and Atterberg limit tests were performed on all samples according to ASTM Specifications. (In addition, the coefficient of saturated permeability was determined for the soils from sites B, C, D, and E, using a falling head permeameter in case this soil property could be correlated with field frost performance. No immediate correlation was found.)

Capillarity Test

The method adopted for the determination of the pore-size distribution curves was based on the moisture content distribution along a vertical capillarity tube after equilibrium had been reached. The soils were compacted and tested at one density only, using a uniform compactive effort throughout the tests. Samples from sites B, C, and D were tested.

The capillarity tubes consisted of 15-cm long segments of plexiglass tubing. The segments were sealed together with hot wax and tape to obtain a watertight and rigid connection, and the bottom of the lowest segment was closed with a perforated foil stopper (Fig. 1). The diameter of the tubes was chosen according to the maximum grain size of the soil, and the number of segments according to the expected capillary rise. The position of the wetted front was observed daily, and the test was normally discontinued when the difference between two consecutive readings was less than 1 mm. Even if this condition had not been achieved, however, the test was terminated at 35 days, or when the capillary rise reached a value of 160 cm. Even though complete equilibrium had not been established with some of the very fine soils, it was accepted as a permissible assumption, inasmuch as even in these cases the test gave sufficient indication of the value of the final capillary rise, and of the character of the moisture distribution. At the end of the test, the tube segments were disassembled and the moisture content determined for each portion of the sample. These data were used to determine the pore-size distribution curves.

Determination of Pore-Size Distribution Curves

The standard formula, based on the surface tension concept, for the capillary rise in a vertical tube is

$$h_c = \frac{4\,\sigma_w \cos\alpha}{d\,\gamma_w}$$

in which

h_c = maximum capillary rise;
σ_w = surface tension of water;
α = contact angle between water and wall;
d = diameter of the tube; and
γ_w = the unit weight of water.

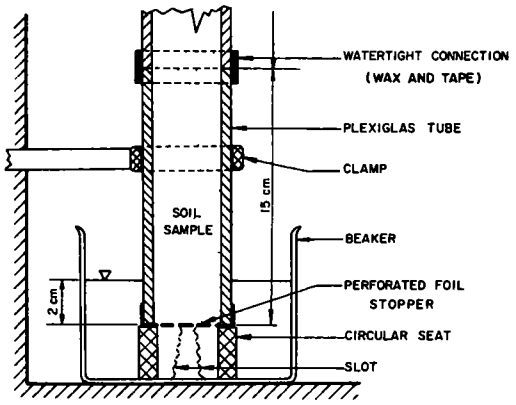

Figure 1. Equipment for capillarity test.

At equilibrium, the contact angle is very close to 0^0, and it is a good approximation to take $\cos\alpha = 1$. The value of the surface tension varies slightly with temperature, but little error is involved in using an average figure of 0.075 g per cm (9). Finally, taking 1.0 g per cu cm for the unit weight of water, the formula reduces to

$$h_c\,(\text{cm}) = 0.30/d\,(\text{cm})$$

If a bundle of tubes of different diameters is considered, the diameter of the largest tube that is still filled with capillary water at a height h above the free water level can be expressed as

$$d\,(\text{mm}) = 3.0/h(\text{cm})$$

Considering the highly irregular pore space within a soil sample as a similar bundle of capillary tubes (9), the maximum pore diameter still filled with capillary water can be estimated in a similar manner at any height above the water table.

An example of the method adopted to determine the pore-size distribution curves is shown in Figure 2. At the end of the capillarity test, the capillary moisture content was determined along the height of the tube at 15-cm intervals. Such a moisture profile curve is shown in Figure 2a. Assuming that the void ratio was constant along the height of the sample, the degree of saturation can be calculated from each moisture content value, yielding the "saturation vs height above water table" curve plotted in Figure 2b. Using the expression given in the preceeding paragraph, the maximum pore diameter that was still filled with water at any particular height can then be determined, obtaining the curve shown in Figure 2c. The abscissa of any point on this curve is an "effective" pore diameter, p (= the diameter of the largest pore filled with water at a height h), and the corresponding ordinate gives the percentage of pore space that is composed of pores smaller than p; i.e., the percentage of pore space filled with water. By merely changing the nomenclature in Figure 2c, the pore-size distribution curve shown in Figure 2d is obtained in a form similar to a standard grain-size distribution curve. It is actually sufficient to plot only the second curve (Fig. 2b), which can then be interpreted as the pore-size distribution curve by a suitable superposition of scales. The curves for the 45 soils tested are given in the Appendix.

The method described was of an approximate nature. The approximation used in taking average values for surface tension, contact angle, and unit weight of water was of minor importance, inasmuch as these quantities vary only in a very limited range. The fact that complete equilibrium was not achieved with some of the very fine soils did not affect the major part of the pore-size distribution curve but only a narrow range of the finest pores. A more appreciable error was introduced by the assumption that the void ratio was constant along the height of the tube. Although check calculations indicated

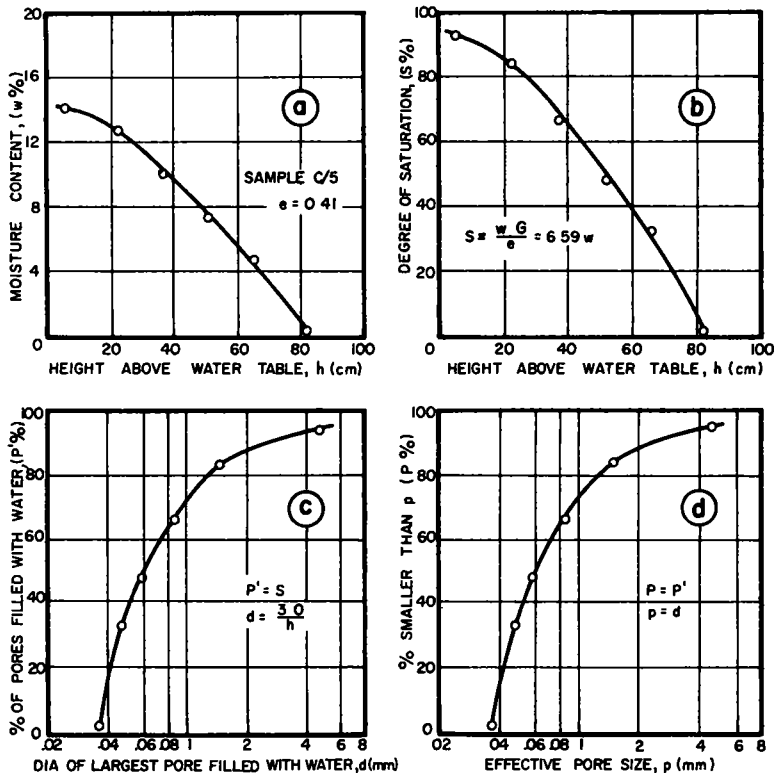

Figure 2. Determination of pore-size distribution curve.

that a sufficiently uniform initial compaction was achieved, nonuniform void ratio changes occurred during the test due to swelling. The finer the soil, the more pronounced this effect was. Finally, a serious limitation was imposed by using the capillary bundle concept, which could be regarded only as a drastically simplified illustration of the actual pore system.

The pore-size distribution curves obtained by this method did not, therefore, indicate the "true" pore conditions. On the other hand, they did give a realistic picture of the effective pore conditions as reflected by an unsaturated upward moisture flow. The curves incorporate the effect of void ratio changes due to swelling, but this effect is also present during the upward moisture flow to the freezing front. The capillary bundle concept has serious limitations, but it does describe how the pores "seem to behave" during an unsaturated upward flow. Thus it seems to be logical to conclude that the "effective" pore characteristics determined by this approximate method are closely related to pore conditions relevant to frost action.

ANALYSIS OF RESULTS

The essential function of a frost susceptibility criterion is to predict before construction whether a soil is likely to prove frost susceptible if included in the highway structure. The "bad" soils can then be rejected, and the "good" ones accepted, at the design stage. An ideal criterion would reject all soils that are apt to cause frost damage on the road under normal temperature and moisture conditions and would accept all those that are not. In addition, it would be based on relatively simple laboratory tests and would thus be simple to apply in practice.

It follows that the usefulness of a criterion can be assessed by comparing predicted frost behavior to field frost performance for a number of soils. The degree of agreement between prediction and performance is a measure of the reliability of the criterion.

This comparison should be made on the basis of the two parallel aspects of reliability, rejection of bad soils and acceptance of good ones. To conduct such an analysis, it is necessary to (a) evaluate in some numerical manner the field performance of the soils, (b) evaluate in a similar manner the predictions implied by the criterion, and (c) develop a method for comparing the two sets of values.

Phase (a) was described in the section dealing with field work, while the remaining two phases are discussed in the following paragraphs.

Frost Susceptibility Criteria Based on Grain Size and on Pore Size

Essentially all the currently applied frost susceptibility criteria are based on grain-size limits. Some of them also utilize such soil properties as Atterberg limits, capillarity, and hygroscopicity. Seven of the most widely used systems (2, 5) were selected for the present investigation (Casagrande 1931, Beskow 1935, Beskow 1938, U.S. Civil Aeronautics Administration 1948, Croney 1949, U.S. Corps of Engineers 1951, Schaible 1954). Using the laboratory test data, the soils were classified accoriding to each of these criterion systems. A number of different terms are used in these criteria to describe "degree of frost susceptibility." To conform with the notation adopted for the evaluation of field performance, these terms were interpreted to fit three basic categories:

F0 = non-frost susceptible,
F1 = borderline, slightly frost susceptible,
F2+ = frost susceptible.

By a procedure of trial and error, correlation was sought between performance indices and pore-size characteristics. It was found that the slope of the upper branch of the pore-size distribution (PSD) curve could possibly be related to frost susceptibility. The slope between the 90 percent and 70 percent limits showed a tendency to become steeper with increasing susceptibility. Using the notation p_{90} and p_{70} for the pore diameters larger than 90 and 70 percent of the pores, respectively, the $P_u = p_{90}/p_{70}$ value was calculated for each soil.

Establishing a tentative criterion, soils with $P_u < 6$ were classified as frost susceptible (F2+), and soils with $P_u > 6$ as nonsusceptible (F0).

The "predicted indices," together with the performance indices, were given in detail elsewhere (5).

Performance Indexes vs Predicted Indexes

The reliability of a criterion depends on how closely the predicted indexes agree with the performance indexes. To assess the extent of agreement, an "agreement factor" (A) was determined for each soil, in the following manner:

1. In case of complete agreement (i.e., F0 (performance index) predicted as F0 (predicted index)) F1 as F1, and F2+ and F2+, the agreement factor was taken as twice the weight of the performance index, A = 2W.
2. In case of partial agreement (i.e., F0 or F2+ soil predicted as F1 and vice versa), A = W.
3. In case of complete disagreement (i.e., F0 soil predicted as F2+ and vice versa), A = 0.

The sum of the individual agreement factors was regarded as a measure of the reliability of the criterion. The two aspects of reliability were separately investigated.

In the first step only the frost susceptible soils (performance indexes F1 or F2+) were considered. The sum of the agreement factors for these soils, expressed as the percentage of the sum for an ideal criterion, was termed the

$$\text{rejection factor} = \frac{\sum A_f}{2 \sum W_f} \cdot 100$$

It indicated what percentage of the actually frost-susceptible soils were predicted as such by the particular criterion. For example, if the rejection factor for a criterion is 80 percent, then, had this criterion been applied at the time of construction, 80 percent of those soils that later caused frost damage would have been eliminated.

In the second step only the nonsusceptible soils (performance index F0) were considered. The sum of the agreement factors for these soils, expressed as the percentage of the sum for an ideal criterion, was termed the

$$\text{acceptance factor} = \frac{\sum A_{F0} \cdot 100}{2 \sum W_{F0}}$$

It indicated what percentage of the actually nonsusceptible soils were classified as such by the particular criterion. For example, if the acceptance factor for a criterion is 80 percent, then, had this criterion been applied at the time of construction, 80 percent of those soils that later proved frost-safe would have been regarded acceptable.

The following reliability figures were obtained for the different criteria:

Criterion	Rejection Factor (%)	Acceptance Factor (%)
Casagrande, 1931	84	20
Beskow, 1935	77	32
Beskow, 1938	75	24
Civil Aeronautics Admin., 1948	87	6
Croney, 1949	58	52
Corps of Engineers, 1951	86	19
Schaible, 1954	85	13
PSD criterion	75	79

These results are based on 118 soil samples, with the exception of the figures for the PSD criterion. Because of time limitations, only 39 samples were used for analyzing the PSD criterion.

Reliability Figures

In regard to the rejection and acceptance factors, the field performance indexes on which the analysis was based were certainly not 100 percent accurate. The range and relative magnitude of the factors obtained nevertheless indicate that such an error probably was not serious. Also, due to the nature of the sampling procedure, the obviously nonsusceptible soils were excluded from the analysis. At an undamaged section of the highway usually only one of the subsoils was sampled, the one that appeared to be the least frost safe on the basis of textural classification. Consequently, although the rejection factors were based on both obviously susceptible and doubtful soils, the acceptance factors reflect the reliability of the criteria almost exclusively in the doubtful zone. This gives a partial explanation of why the acceptance factors are so low compared to the rejection factors. The relative magnitude, rather than the exact value, of the reliability figures should therefore be considered when comparing the different criteria.

Among the grain-size criteria, the Casagrande criterion proved reassuringly safe in rejecting bad soils (84 percent), but too conservative in accepting good ones (20 percent). Actually, both these trends had already been indicated by practical experience (e.g., 10). An unquestioned advantage of the method is its simplicity. The other criteria are more complicated without apparent gain in reliability. As already noted, the Civil Aeronautics Administration criterion, although the frost aspect is also taken into account. It is primarily based on strength considerations for subbases, thus all the finer soils investigated (and the great majority of the samples were finer than coarse sand) were necessarily rejected regardless of their expected frost behavior. This explains the high rejection factor and low acceptance factor for this criterion.

An improvement of the rejection and acceptance factors for the different criteria was attempted by slightly altering the specified grain-size limits. For example, in the case of the Casagrande criterion, both the susceptible and nonsusceptible soils (field performance), and also the dividing line suggested by Casagrande, were plotted on a graph that had the percent finer than 0.02 mm on one axis and the uniformity coefficient on the other. It was then attempted to shift the dividing line so as to include more susceptible soils into the "danger zone" and more nonsusceptible soils into the "safe zone." For each grain-size criterion it was found that any gain in one factor was to be paid for by a comparable loss in the other. This suggested a rather irregular distribution of data, which in turn was taken to indicate that the grain-size characteristics on which these criteria were based did not constitute the soil property basically influencing frost behavior.

Considering the PSD criterion, it gave a rejection factor as good as, and an acceptance factor considerably better than, the average values for the established grain-size criteria:

Criterion	Rejection (%)	Acceptance (%)
PSD	75	79
Avg. for grain-size	78	24

Thus the PSD criterion appears to be both safe in rejecting the bad soils and economical in accepting the good ones. Also significant, the rejection and acceptance factors for this criterion are of the same magnitude, even if not ideally high. This suggests that a definite relationship exists between pore-size characteristics and frost susceptibility, although this tentative criterion is not necessarily the best form to express the relationship. It seems reasonable to expect that the reliability of this criterion, as opposed to the others based on grain-size limits, could be further improved by refining the criterion and by eliminating the possible experimental errors.

The preceding analysis appears to indicate that pore-size distribution is the soil property that has the fundamental and primary influence on frost susceptibility. The influence of grain-size distribution is of secondary nature, exerted probably through its effect on the primary factor of pore size. Frost susceptibility criteria should therefore be based on pore-size characteristics.

Some Theoretical Aspects

The PSD criterion, as presented here, is based on the slope of the pore-size distribution curve between the 70 and 90 percent limits. It appears that this slope is considerably steeper for frost susceptible soils than for nonsusceptible soils. In other words, the presence of relatively large pores, in an amount of approximately 20 percent of the total pore space, tends to make the soil frost-safe. One possible explanation is that the large pores break the continuity of the capillary water column, thereby hindering the upward moisture movement to the freezing zone. Another aspect is that ice propagation is relatively easy through these large pores, and the resulting ice projections act as anchors, resisting the heaving pressure. It seems to be logical that, in addition to this criterion referring to the large pores, there should be another valid criterion bringing into consideration the size of the relatively small pores, which probably govern the induced suction; e.g., p_{20}, the pore size that is larger than 20 percent of the pores. This second criterion was not indicated by the present work, probably because only a very limited number of coarse soils were considered.

The soil property having the fundamental influence on frost susceptibility is pore size according to the thermodynamic theory of frost heaving (11) and grain size according to the electro-osmotic theory (12). The results of the present work would favor the former hypothesis. No evidence against the validity of this hypothesis has yet been reported.

The present work also gives an indirect indication that capillarity is a factor of considerable importance in frost action. This soil property has been neglected by recent investigators, mainly on the basis that surface tension forces cannot be effective once

the water column reaches the ice front and the meniscus disappears. At this stage the suction forces induced by freezing replace the effect of surface tension. However, the significant point is that the pore water must somehow reach the vicinity of the freezing front before the suction forces become effective. For such a "presaturation," the most plausible mechanism is still capillarity. Therefore, it seems probable that even if capillarity does not play a direct role in frost heaving, it is an essential prerequisite for the upward moisture movement to the freezing front.

The method developed in this work for the determination of pore-size characteristics is based on the active capillarity test. Although this test does not involve much work, it requires much time (several weeks). Hence, if pore-size criteria are to be used in practice, it would be desirable to develop a more rapid and at least as reliable a laboratory procedure. The obvious possibility is to use the suction curve instead of the capillary moisture profile. Such a method would be fast and would yield the "effective" pore-size distribution curve in a manner quite similar to the one described here. A further advantage of the suction method would be that the effect of void ratio could also be considered by testing disturbed samples under more closely controlled density conditions and by carrying out the test at different densities. The possibility of testing undisturbed samples could also be considered. It would probably be advantageous to determine both the drying and the wetting curves, which would yield the limits for the possible behavior of the soil in the field (the point representing the field moisture conditions may lie anywhere within the hysteresis loop, depending on the earlier moisture history of the soil). Also, the hysteresis loop could possibly give some much needed information regarding the "shape factor" for both the particles and the pores.

Finally, there is a further possible practical use of the pore-size distribution curve. It appears logical that the overburden pressure-suction relationship, when heaving is stopped—found to be linear by Penner (6)—should be closely related to pore-size characteristics. Similarly, the maximum suction at which an appreciable flow can still be maintained should also depend on pore-size distribution. Further research is needed to establish these correlations, but positive results would have great practical significance because simple data derived from the pore-size distribution curve would immediately indicate the depth at which the particular soil ceases to be frost susceptible. This would be a definite improvement on the present concept of frost susceptibility classification.

CONCLUSIONS

Subject to the limitations previously mentioned for the experimental work, the following conclusions can be stated.

1. Among the present frost susceptibility criteria the Casagrande criterion is the simplest and is as reliable as any other, though definitely conservative.
2. The experimental results indicated serious limitations of the criteria based on grain-size limits. Grain-size distribution is thus probably not the most important soil property influencing frost behavior.
3. The pore-size distribution curves determined from capillarity moisture profiles at equilibrium reflect the pore conditions relevant to frost action.
4. A tentative frost susceptibility criterion based on pore-size characteristics was introduced and was found to be considerably more reliable than the grain-size criteria.
5. The results of this study, together with certain theoretical considerations, indicate that pore-size distribution would provide a more rational basis for frost susceptibility criteria.

ACKNOWLEDGMENT

The investigation described in this paper was carried out at Queen's University, Kingston, Ontario, under the auspices of the Ontario Joint Highway Research Programme.

REFERENCES

1. Johnson, A.W., "Frost-Action in Roads and Airfields. A Review of the Literature 1765-1951." HRB Special Report 1 (1952).

2. Townsend, D. L., and Csathy, T. I., "A Compilation of Frost Susceptibility Criteria." Queen's University, Ontario (1961).
3. Linell, K. A., and Kaplar, G. W., "The Factor of Soil and Material Type in Frost Action." HRB Bull. 225, 81-125 (1959).
4. Ruckli, R., "Discussion of Proceedings Sep. 445." Proc., ASCE, Sep. 656, 5-6 (1955).
5. Townsend, D. L., and Csathy, T. I., "Soil Type in Relation to Frost Action." Queen's University, Ontario (1961).
6. Penner, E., "The Mechanism of Frost Heaving in Soils." Discussion by R. T. Martin, A. R. Jumikis and R. D. Miller. HRB Bull. 225, 1-22 (1959).
7. Schofield, R. K., "Pore-Size Distribution as Revealed by the Dependence of Suction (pF) on Moisture Content." Trans. 1st Commission of Internat. Soc. of Soil Science, A:38-45 (1938).
8. Penner, E., "The Nature of Frost Action." Canadian Good Roads Assoc. Proc., 38th Convention, pp. 234-243 (1957).
9. Terzaghi, K., "Theoretical Soil Mechanics." Wiley (1956).
10. Schaible, L., "On the Increasing Danger of Frost Damage to Our Highways." Die Bautechnik, 9:31 (1954). (Translated by D. Sinclair, TT 568, National Research Council of Canada, 1955.)
11. Jackson, K. A., and Chalmers, B., "Freezing of Liquids in Porous Media with Special Reference to Frost Heave in Soils." Jour. Appl. Physics, 29:8 (Aug. 1958).
12. Cass, L. A., and Miller, R. D., "Role of Electric Double Layer in the Mechanism of Frost Heaving." U. S. Army SIPRE Research Report 49 (1959).

Appendix

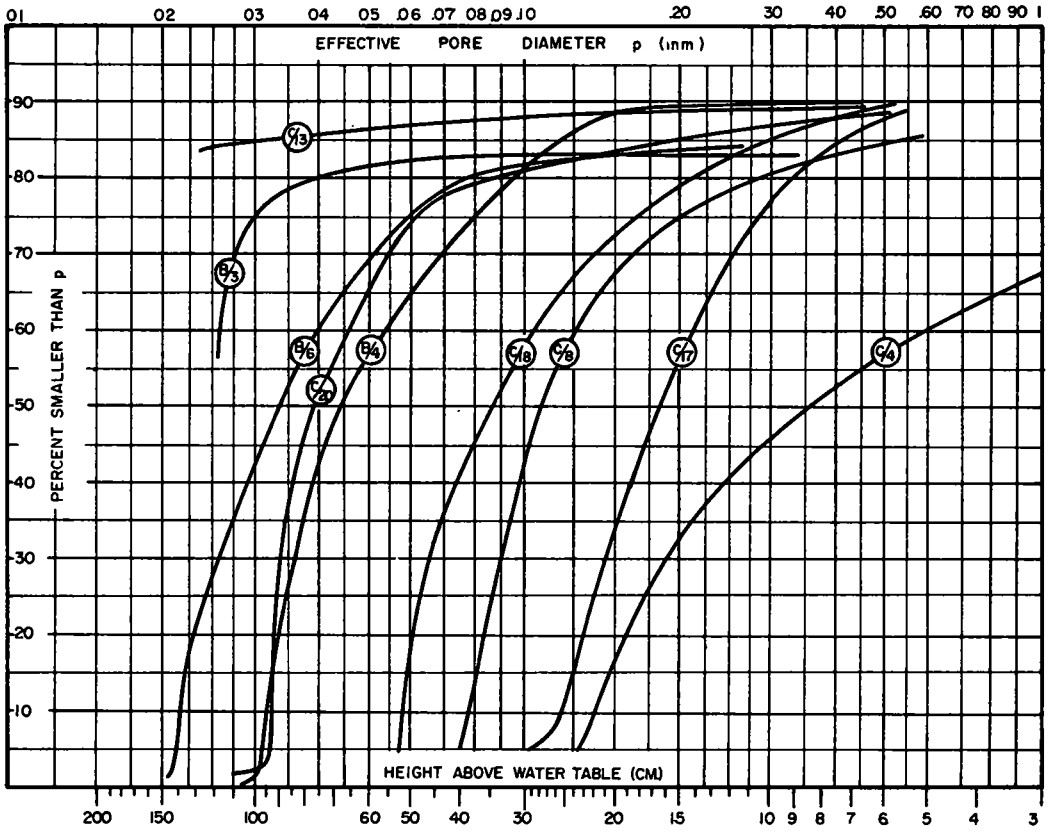

Figure 3. Pore-size distribution curves, FO soils, Sites B and C.

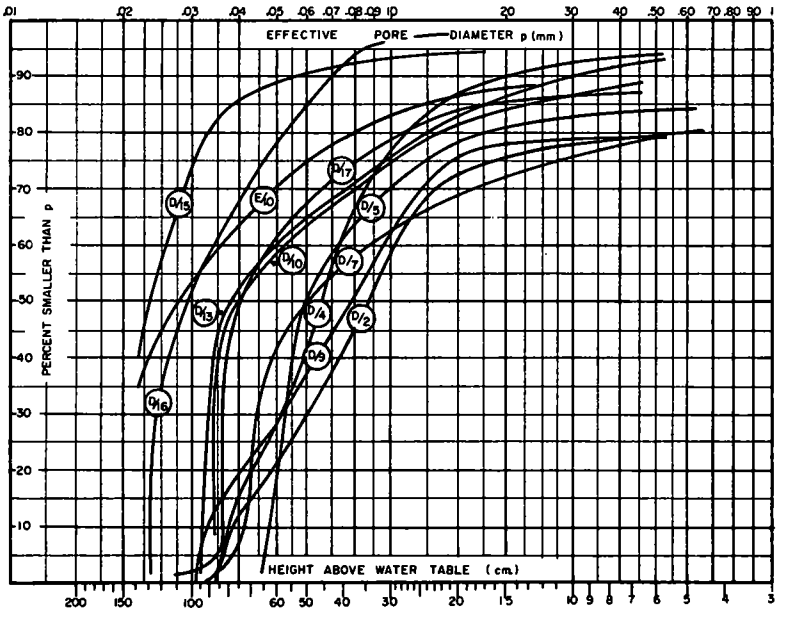

Figure 4. Pore-size distribution curves, FO soils, Sites D and E.

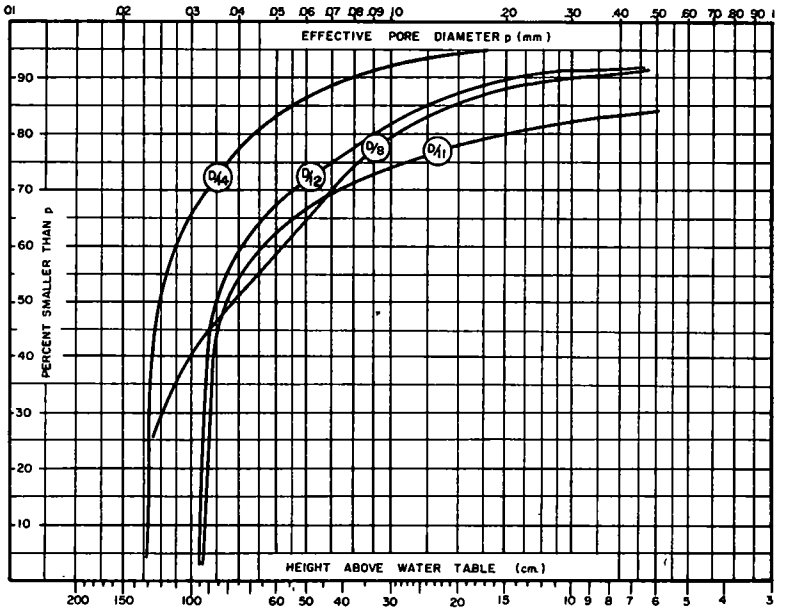

Figure 5. Pore-size distribution curves, F1 soils.

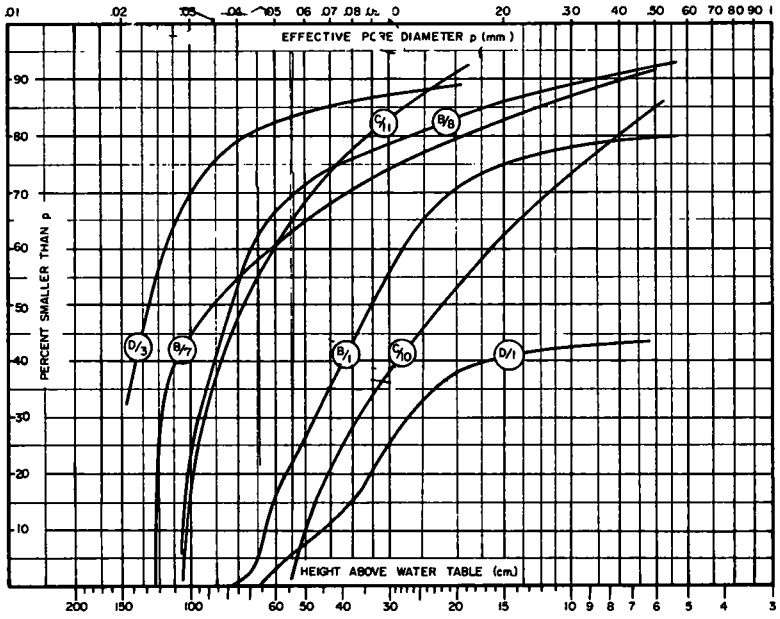

Figure 6. Pore-size distribution curves, F2 soils.

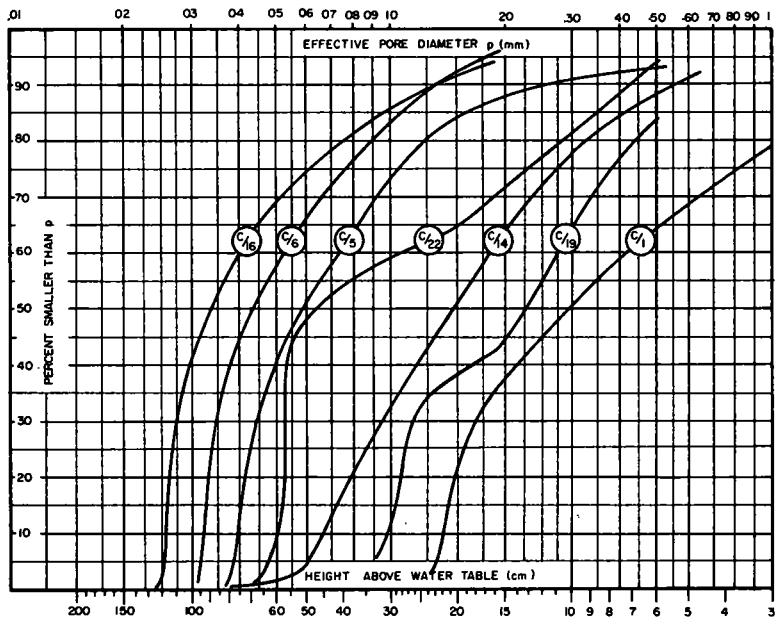

Figure 7. Pore-size distribution curves, F3 soils.

Frost Action Theories Compared with Field Observations

WILBUR M. HAAS, Civil Engineering Department, Michigan College of Mining and Technology, Houghton, Michigan

Recent investigations of the mechanism of frost action in soils have increased the understanding of the basic nature of this mechanism. Two recent studies have related the heat flow through the soil system to the moisture migration and the resulting frost heave. Both investigators obtained good correlation between theory and laboratory experimental results, but arrived at somewhat different conclusions.

This paper reports some results of field observations on suitably prepared field observation plots. Although these observations were made with a view toward exploring several aspects of frost action, only the relationship of the heat balance to heaving and penetration is discussed. Measured heave rates were compared with estimated heat flow rates for the condition of zero penetration rate. Although there are variations in the behavior of the four soils evaluated and variations between seasons, field observations agree well with theoretical predictions. For the case of a penetrating frost line, neither of the conflicting concepts can be verified completely. On the basis of the limited data available, it appears that the validity of either concept depends on the soil type.

•RECENT INVESTIGATIONS of the mechanism of frost action in soils have increased understanding of the basic nature of this mechanism. Certain of these studies have related the heat flow through the soil system to the moisture migration and the resulting frost heave. Two of these researchers, Higashi (1) and Penner (2), in particular have produced excellent results. Both studies were conducted in the laboratory, and the investigators obtained rather good correlation between experimental results and theory. These investigators reached somewhat different conclusions, however, with respect to the relationship between the rate of penetration of the frost line and the rate of heaving.

It is of considerable interest that these investigators reached differing conclusions in view of the fact that they used similar concepts. Both concerned themselves with the difference in heat conduction between the frozen and unfrozen zones. Higashi concluded that for the case of a nonadvancing frost line, the heave rate is proportional to this heat conduction difference up to some critical cooling rate. Beyond this critical cooling rate, the heaving rate decreases as the rate of frost line penetration increases.

Penner conducted laboratory experiments in which the heat flow through both the unfrozen and frozen zones was directly measured. He did not specifically consider the case of a nonadvancing frost line, and concluded that the rate of frost heaving increased as the rate of frost penetration increased.

Due to the difference in the conclusions reached, it is pertinent to determine how well these concepts apply to natural conditions of freezing in the field. It is the purpose of this paper to report on some results of field observations that will aid in the evaluation of these concepts and lead to their effective extension to field conditions. These observations were made on suitably prepared observation plots at the Keweenaw Field Station (KFS) of the U. S. Army Cold Regions Research and Engineering Laboratory (CRREL) located at Houghton, Mich.

Heaving rates were compared with estimated heat flow rates for the condition of zero frost penetration rate. The field observations agree fairly well with the theoretical predictions. The agreement is better for certain soils than for others, and the agreement is better for a season of moderate temperature fluctuations than for a season of sharp temperature fluctuations. Although the field data do not fit the theoretical relationship as well as the results of laboratory investigations, due in large measure to the comparative difficulties of field studies, it is believed that they are significant.

The relationship between heave rate and penetration rate for the condition of rapid frost penetration was also studied. The field data do not form a well-defined general relationship for this case, so neither of the theories applying to this condition can be verified with certainty from the field observations. Some tentative relationships for specific conditions are indicated from the limited data available. However, it should be pointed out that the field freezing took place with the distance to water table progressively decreasing from about 3 to 0 ft, with the thickness of overburden progressively increasing from 0 to about 3 ft. These conditions were different from those of either of the laboratory investigations mentioned above.

DESCRIPTION OF STUDY

Field Observation Plots

Four soils were used in the field observation plots, ranging from a fat clay to a sand with fines. A water-resistant basin was constructed in such a manner than a nearby reservoir would control the water level in the basin. A graded filter was placed in the bottom of the basin, and the selected soils placed over the filter. These soils were placed on lifts about 6 in. high and compacted by field methods. The depth of test soil over the filter is about 46 in. (see Fig. 1).

The test plots were instrumented with thermocouples for measuring temperatures at suitable depth increments, heave plates for determining the heaving at various levels, and frost tubes for a direct indication of the frost penetration during the freezing-down period. In the late autumn of 1959 this instrumentation was supplemented by the addition of moisture tensiometers.

To obtain the maximum freezing effect and permit ready sampling of the soils, no pavement was placed over the soils. Snow was cleared from the site to eliminate the insulating effect of a snow cover.

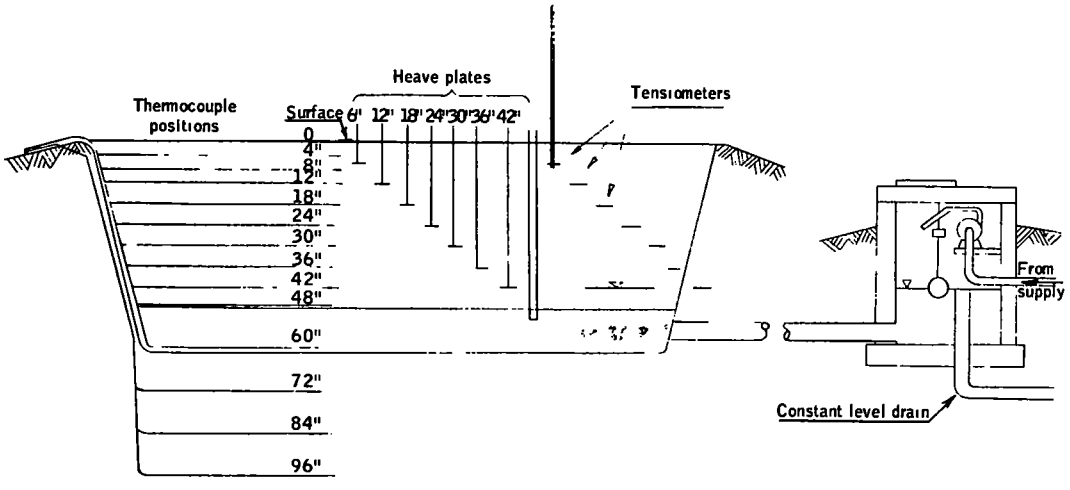

Figure 1. Cross-section of field observation plot (not to scale).

Data Obtained

With the advent of freezing conditions, the thermocouples were read to determine the temperature gradients, and the heave plates were read periodically with an engineer's level and rod to determine the heave at the various levels. The slurry frost tubes also were read at periodic intervals, thus obtaining a direct indication of the frost line. These observations were continued throughout the freezing season.

The depth of frost penetration was determined by a comparison of three kinds of data or indications. The primary method was to determine the break in the temperature gradient which occurs at the frost line. This break is caused by the difference in thermal conductivity between frozen and unfrozen soil.

The position of the frost line as determined by this method was then checked by comparing it with the location of heaving as indicated by the several heave plates at their respective depths (see Fig. 2). The time when a given heave plate first showed vertical movement was taken as the time the frost line reached that given level. Finally, the data from the slurry frost tubes were considered. All three indicators agreed quite closely.

RESULTS OF OBSERVATIONS

Surface heave and the penetration of the frost line were plotted against time for each of the four soils studied, for the three seasons of record. The surface heave for all soils was considerably smaller for the first season following construction than for the two succeeding seasons. This first season was quite severe (2,200 degree-days) compared to the two following seasons, 1,780 and 1,650 degree-days, respectively.

The surface heave rate was not constant at all times, but varied somewhat, including some periods when the rate was essentially zero. The changes in heaving rate, or breaks in the plot of accumulated heave against time, were quite definite.

Likewise, the rate of frost penetration was not constant with time but showed considerable variation For certain soils and specific temperature conditions, the frost line remained constant at a given level for several days before further penetration occurred. The results of these observations of heave and penetration are summarized in Figures 3 to 6.

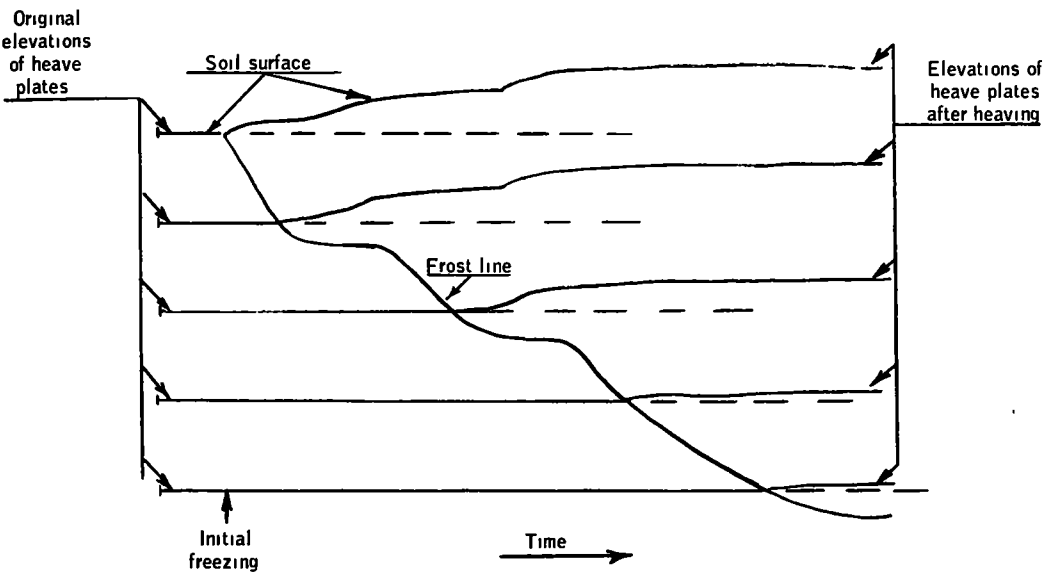

Figure 2. General relationship of frost penetration and frost heaving at various levels with time.

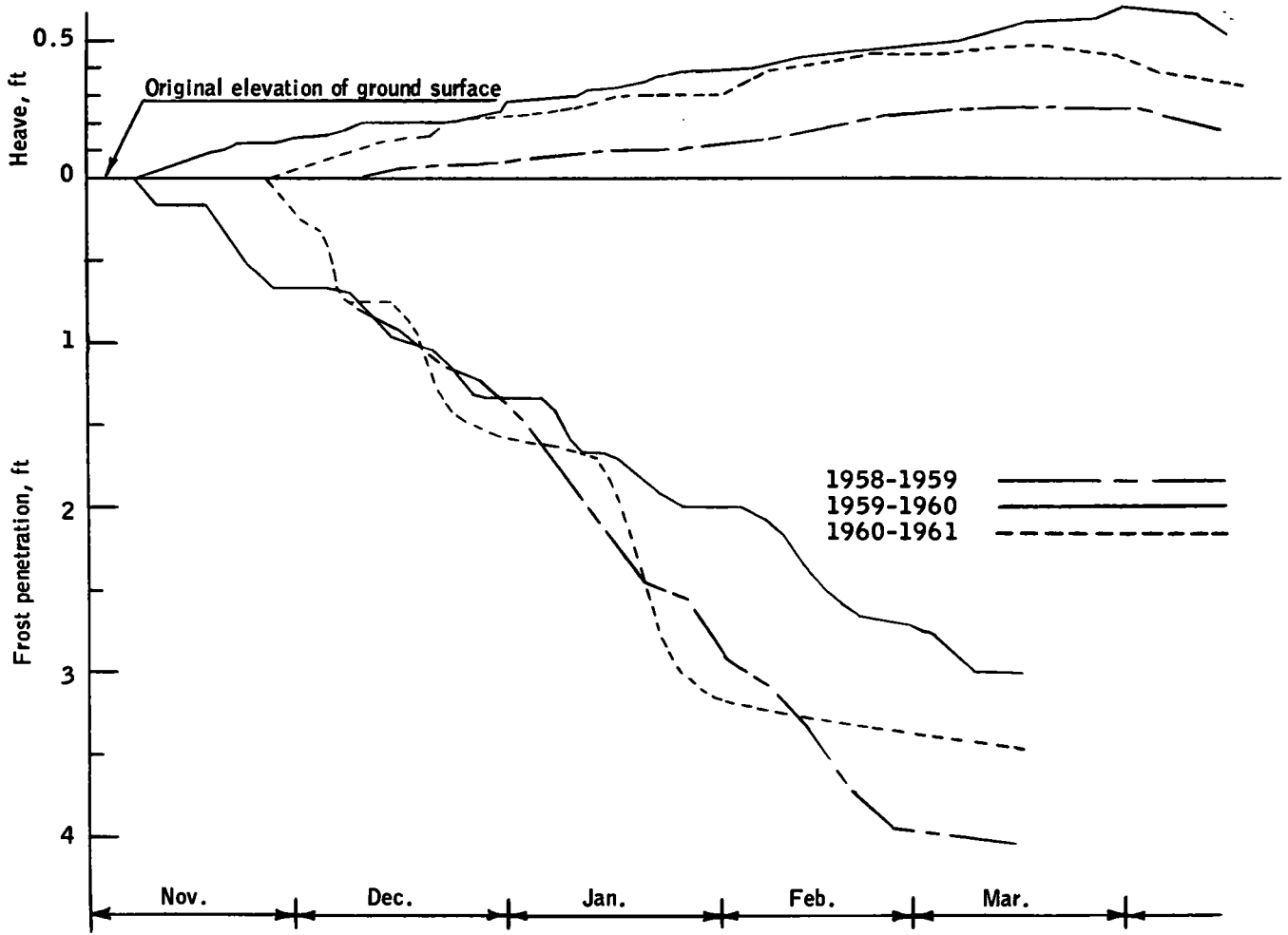

Figure 3. Surface heave and frost penetration for three seasons. Laminga silt (ML).

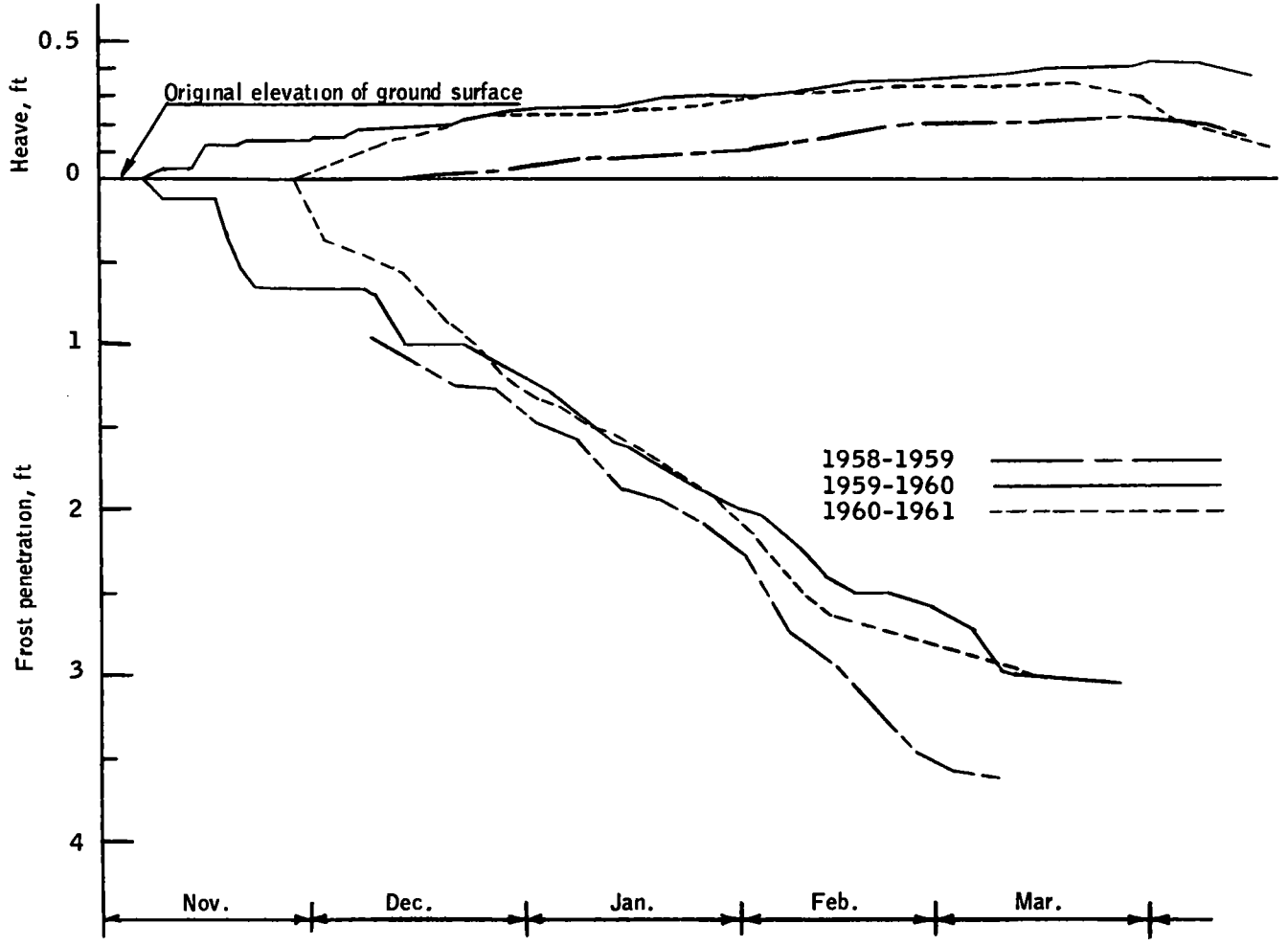

Figure 4. Surface heave and frost penetration for three seasons. Oneco sand (SP).

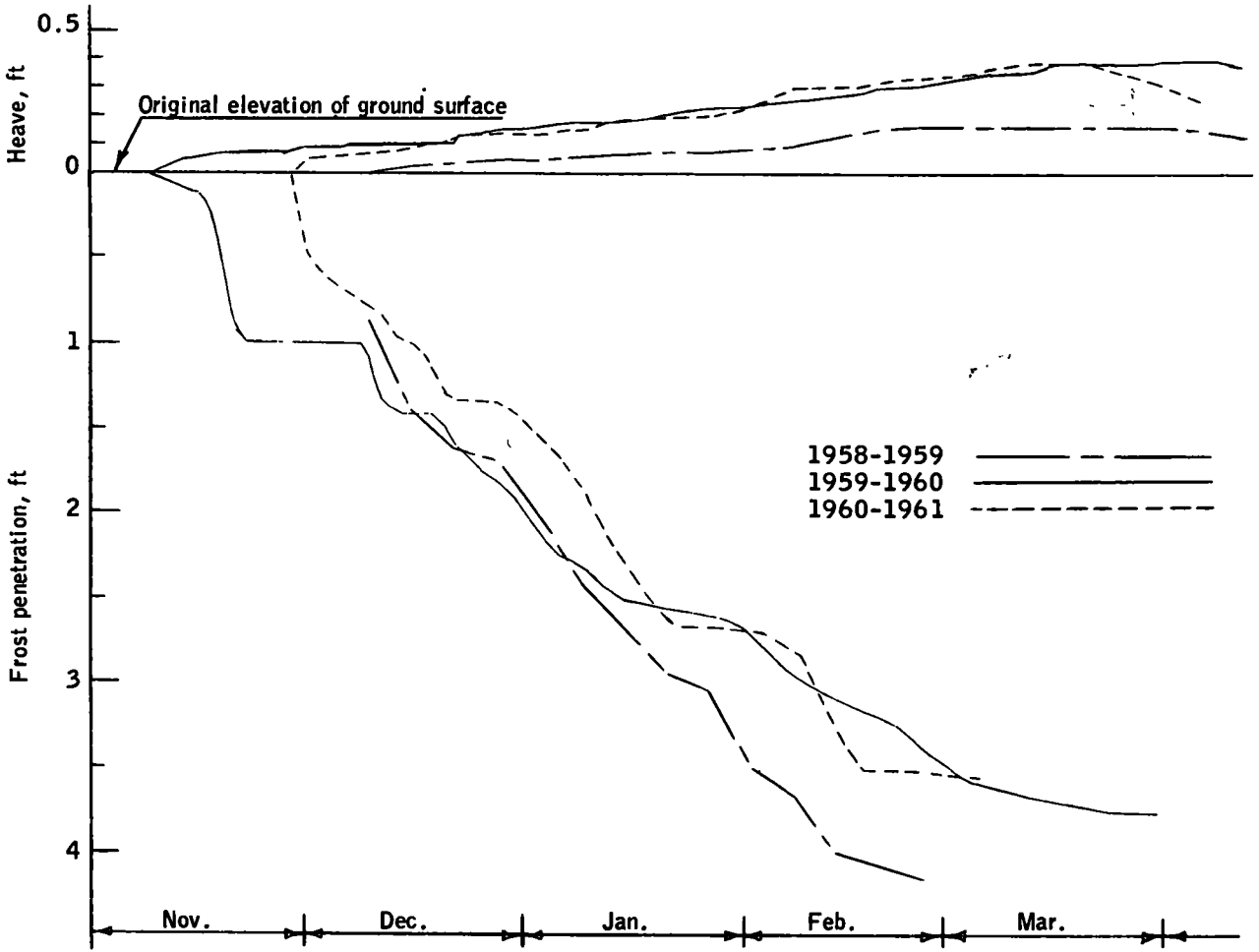

Figure 5. Surface heave and frost penetration for three seasons. Pike Bay (SC).

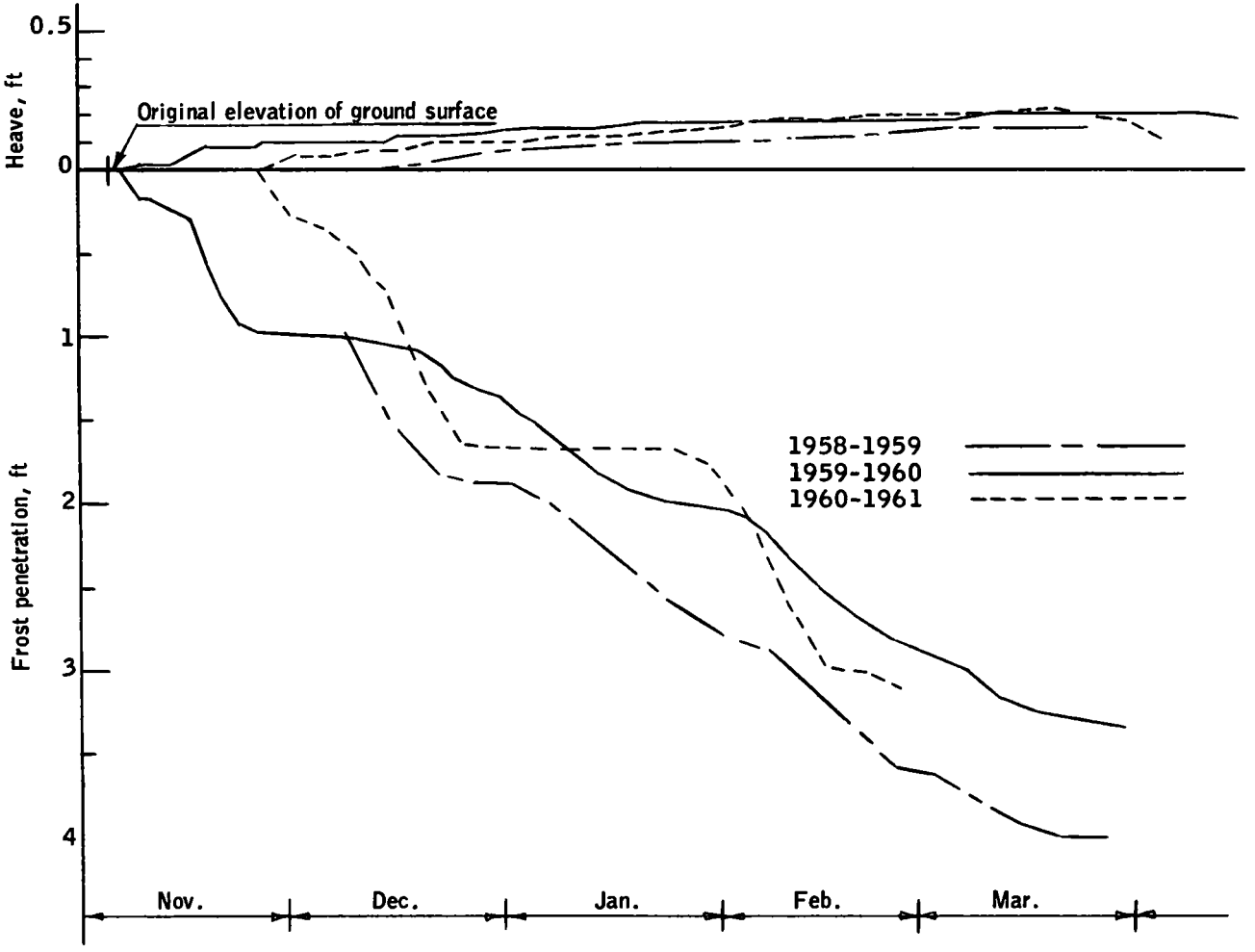

Figure 6. Surface heave and frost penetration for three seasons. Canal clay (CH).

ANALYSIS

In considering the energy balance that applies to frost action in soils, a number of terms or quantities must be considered. The most important of them may be summed up as follows: the heat flow by conduction through the frozen zone must be supplied by (a) the heat flow by conduction through the unfrozen zone, (b) the latent heat of fusion of migrating moisture when it reaches the freezing front, (c) the over-all cooling of the unfrozen soil and its included water when the frost front advances or proceeds deeper into the soil, and (d) the latent heat of fusion of the included water as it is frozen out by an advancing frost front (see Fig. 7). Other terms that might be considered include the mechanical work of raising the water of migration from the free water table to the frost line, and the mechanical work of lifting the frozen overburden. These terms do not appear to be very important when compared with the several heat terms itemized, however, and are not considered further.

The listing is for the most general case, in which both heaving and frost penetration are taking place. If the frost line penetration rate is zero or the freezing is taking place at a fixed level, the heat flow through the frozen zone is balanced by only the heat flow by conduction through the unfrozen zone and the latent heat of fusion of the migrating moisture as it is brought up to the frost front and converted into ice. This is an important case and is of interest because it permits some simplification of the problem.

To establish the background for the analysis of the field observations, the theory advanced by Higashi is reviewed here, followed by some comments of the present author. Because of their pertinence to the problem, some of Penner's data will also be presented.

Higashi's Concepts and Studies

Higashi suggested that frost action falls into two cases when considered on the basis of the heat balance. Which of these cases applies at a given time depends on the thermal regime at that time. The first case is that in which there is no penetration of the frost line. For this case, the heave rate is proportional to the excess of the heat flow through the frozen zone over that by conduction through the unfrozen zone. This quantity will be

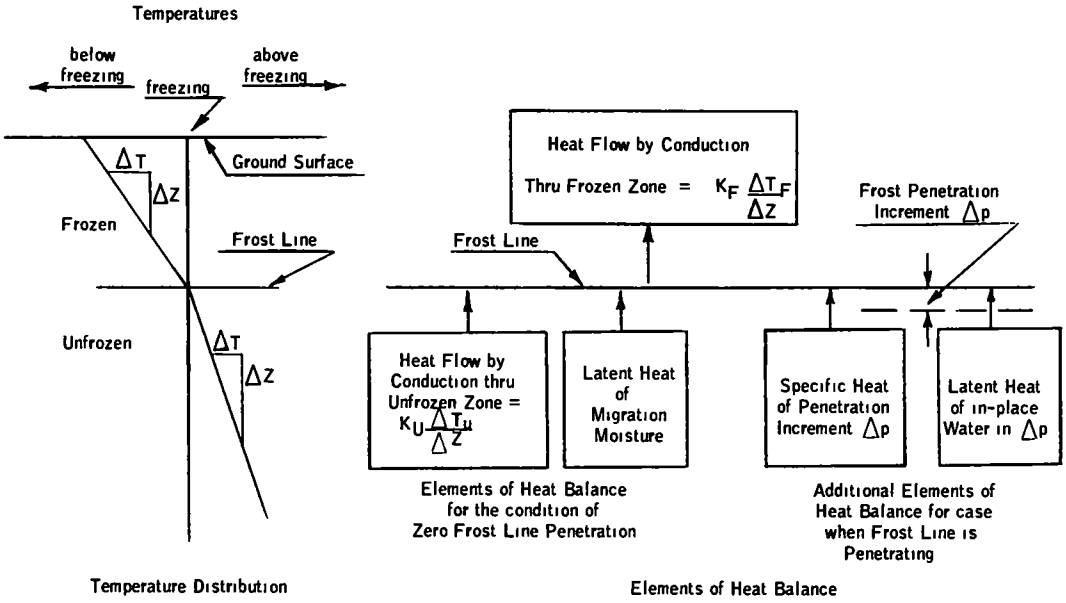

Figure 7. Schematic heat balance in soil freezing.

called the heat conduction difference in this paper. The heat conduction difference must be made up by the latent heat of fusion of the migrating water as it freezes out at the frost line. As the migrating water causes an increase of the over-all volume of the soil system the heave is proportional to the heat supplied by the latent heat of fusion. As this heat quantity relates only to the migration moisture, the proportionality can be determined from the latent heat and the specific volume of ice, and is therefore independent of soil characteristics or properties. This, of course, assumes that all of the migration moisture is changed to ice.

Although the theoretical proportionality factor is independent of soil properties, the limits of this case are not. For the condition when the heave rate is zero and the penetration rate is zero, the latent heat quantity is zero and the heat flow by conduction through the frozen zone is exactly balanced by the heat flow by conduction through the unfrozen zone. This condition then depends on the existence of a suitable thermal regime and on the thermal conductivities of the frozen and unfrozen soils.

The other limit of this case would represent the maximum heave rate. The proportionality between heave rate and the heat conduction difference is valid only up to the point that the necessary flow rate of moisture through the soil can actually occur. As the flow is the product of the unsaturated permeability and the moisture tension gradient, this flow will be limited by the unsaturated permeability of the soil, the moisture tension regime that occurs at a given time, and the overburden effect of the frozen layer. If the heat flow through the frozen zone cannot be supplied by the conduction through the unfrozen soil plus the migration moisture, then an additional heat source is required. This would probably be supplied by the heat given up the over-all cooling of the unfrozen zone which would accompany further penetration of the frost line. When this situation occurs, the first case no longer applies, and a second case must be considered.

On the basis of certain assumptions made in his analysis of this second case, Higashi suggests that penetration of the frost line will be accompanied by a reduction in the heaving rate. Thus as the cooling rate increases beyond the limit for the first case (that of zero penetration rate), the heaving rate would decrease from the maximum as the penetration rate increases. In theory, at least, such a large penetration rate might be reached that there would be no heaving at all.

Higashi presented data from laboratory freezing tests on a glacial clay (CL in the unified classification system) compacted to two density ranges. His data showed good agreement with theory for the first case (zero frost penetration rate) and indicated an empirical agreement with his theory for the second case Examples of his results for the two cases are shown in Figures 8 and 9. Higashi's samples were frozen in an open system with wicks simulating a depth to ground water of several feet.

A Generalized Concept

The basic considerations involved in the energy balance, when considered in conjunction with Higashi's results, suggest a unified concept of the relationship between the heaving rate, the penetration rate, and the thermal regime of the freezing soil system. This is shown schematically by Figure 10. At some low cooling rate, the heat flow by conduction through the frozen zone is just balanced by the conduction heat flow through the unfrozen zone. No migration moisture is required to maintain the heat balance, thus neither heaving nor penetration occurs. With an increase in the cooling rate, the heat flow through the frozen zone increases, with the increase being balanced by the latent heat of the migration water and therefore requiring no additional conduction of heat in the unfrozen zone nor any penetration. This type of balance would continue to exist with increasing cooling rate until the further increase in the flow of migration water would be limited by the unsaturated permeability, the moisture tension regime, and the overburden effect. That this limit would be a function of the distance to the water table is somewhat implicit in the consideration of the moisture tension regime.

As the cooling rate increases beyond the critical value associated with the critical heave rate, penetration of the frost line occurs, probably increasing with an increase in the cooling rate. The effect of this behavior on the heaving could depend on various factors. Certainly the relationship is made more complex by the fact that the temperature regime is less stable when penetration is occurring than when it is not. It would

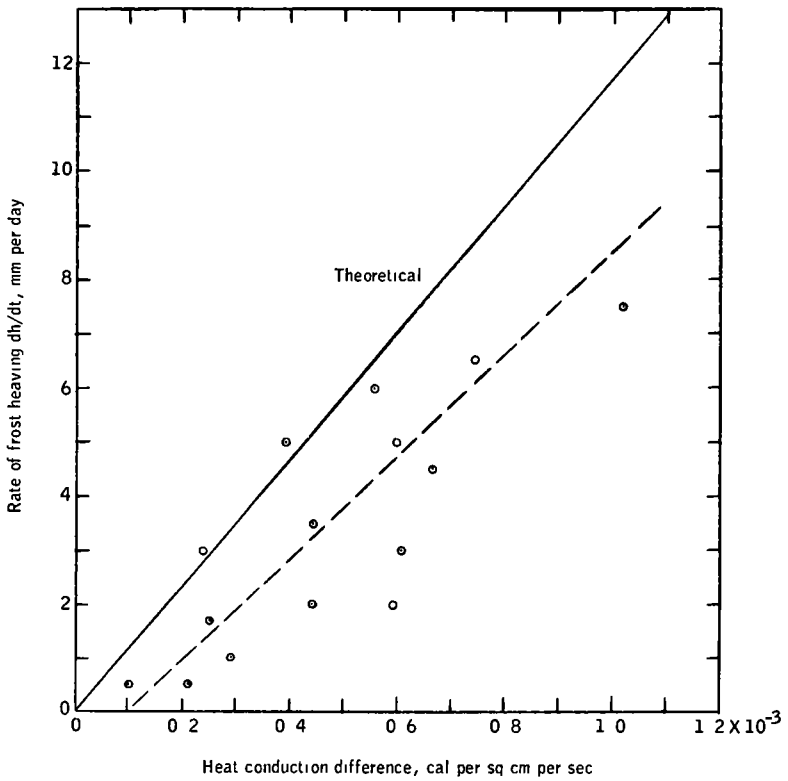

Figure 8. Relation between rate of heaving and heat conduction difference when frost penetration rate is zero.

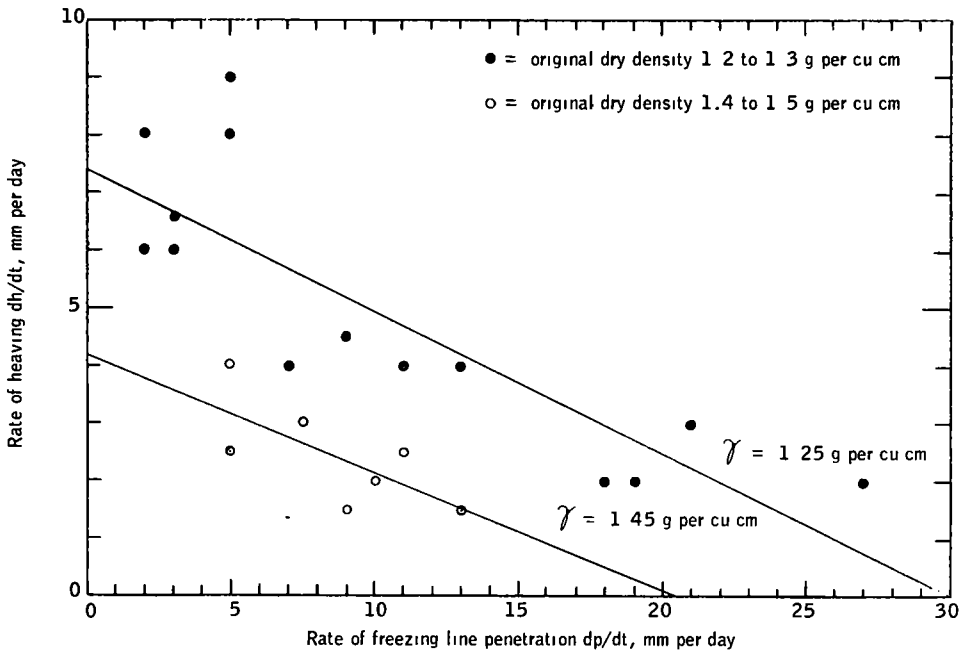

Figure 9. Rate of heaving vs rate of freezing line penetration.

seem that there are two possibilities. The first is that indicated by Higashi, in which the heaving rate decreases as the penetration rate increases. Keeping in mind that his experiments simulated the condition of a distance of several feet to the free water table, this possibility seems reasonable for the case of a relatively deep water table.

The second possibility is that the heave rate could continue at or near the critical or maximum value in spite of penetration of the frost line. This might be the case if the cooling rate were to increase rather slowly beyond the critical value, or the distance from the frost line to the free water table were moderate.

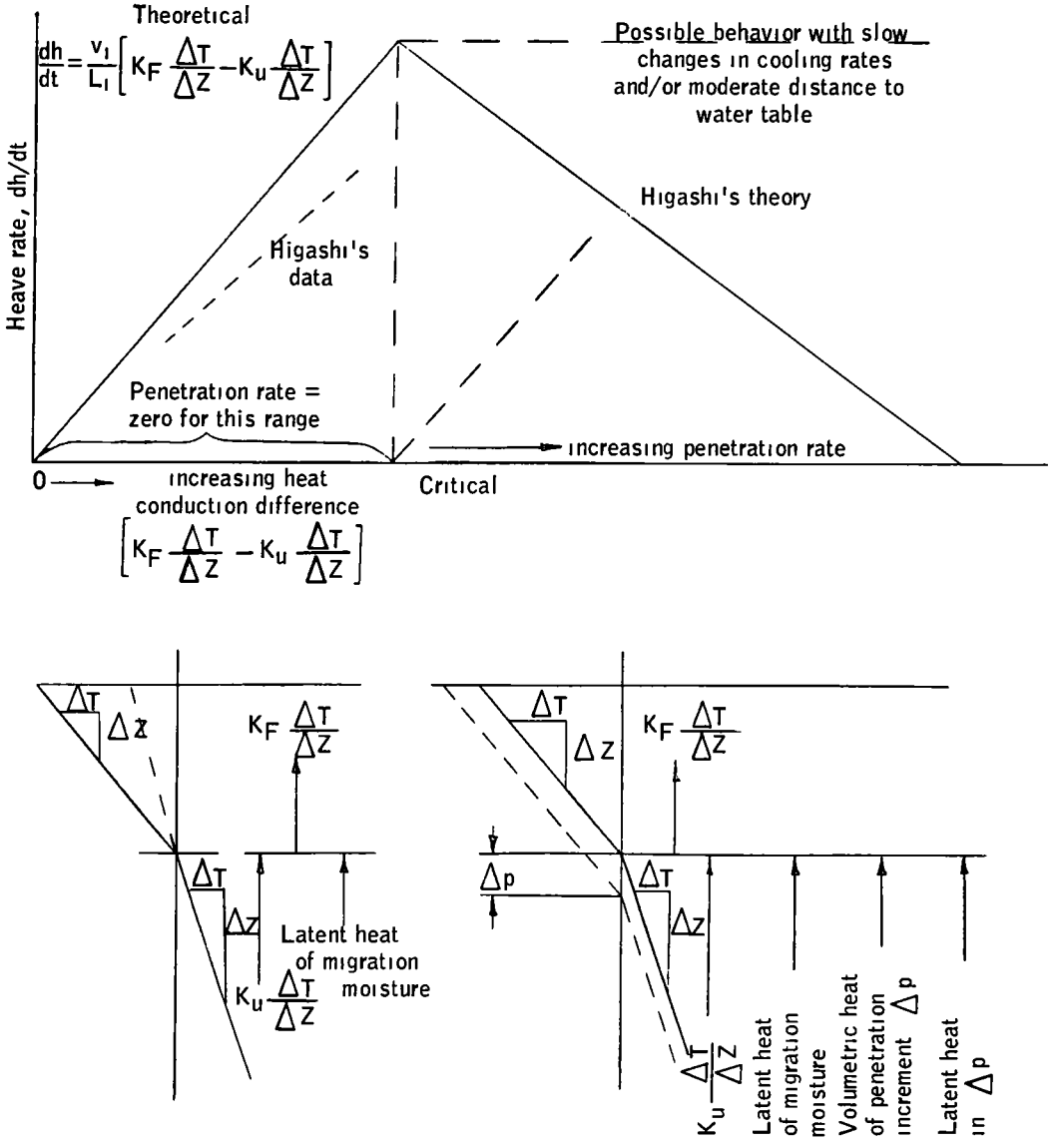

Figure 10. Generalized concept of frost heave and penetration with heat balance considered.

It is recognized that other factors may enter into these relationships, such as the amount of water remaining unfrozen in what has been termed the frozen zone. Although factors such as this may prove to be important, is it believed that this generalized concept provides a good starting point for further discussion and research.

Penner's Investigations

Penner's experiments involving the direct measurement of heat flows are of interest, as he found that the heave rate increased with the penetration rate. He measured the heat flow into the warm end (bottom) of a sample 3 in. high and also measured the heat flow out of the cold end. In this way he was able to determine the difference between the conduction in the two zones. His technique did not distinguish between zero frost penetration rates and fairly large penetration rates. Apparently his samples had some definite penetration during most of the duration of the test. One series of tests was run with the free water table at the base of the 3-in. high samples, and another series was run with the free water table 12 in. below the base of the samples. There was little difference between the results of these two series. Some of Penner's results are shown in Figure 11. The author has taken the liberty to place the theoretical line relating heave and heat conduction difference on these plots. In general, his points lie to the right of this theoretical line, as was also the case with Higashi's experiments.

Analysis of Data from Field Observation Plots

Analysis of the heave and penetration plots indicated that there were distinct intervals or periods of time when both the heave rate and the penetration rate were constant. Thus, a given interval ended and the next one started with a change in the heave rate, the penetration rate, or both. For the intervals of zero or very small penetration rate, the temperature gradients were determined for both the frozen and unfrozen zones. The gradients used in the subsequent calculations were the average gradients for all the days of the given interval.

Thermal conductivities were selected from Kersten's curves (3) for similar materials and also from limited thermal conductivity determinations made in conjunction with these field studies. Thus the heat flow values for conduction in the frozen and unfrozen zones could be calculated, and the excess of the conduction in the frozen zone over that of the unfrozen zone was determined. These values of heat conduction difference were then plotted against the corresponding heave rates. The results for the four soils are shown in Figure 12.

Although there is some scatter in the points, probably due to errors in determining the temperature gradients or to variations of the actual thermal conductivities from

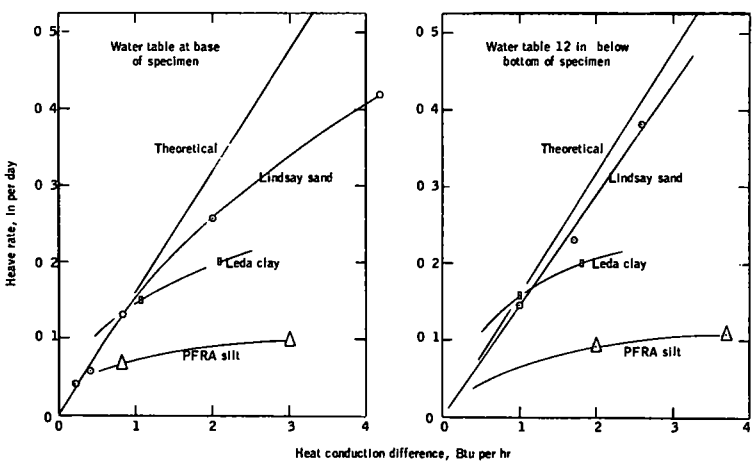

Figure 11. Heave rate vs heat conduction difference.

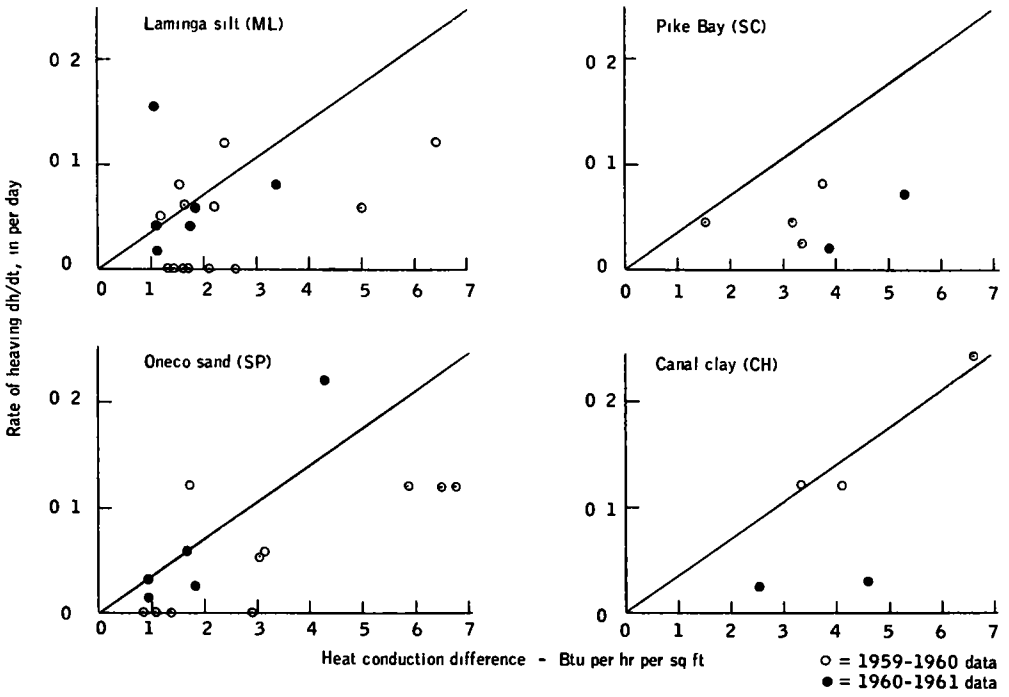

Figure 12. Heave rate vs heat conduction difference (based on field observations): symbols in parentheses indicate unified soil classification.

the selected values, the general trend of the data corresponds to the theoretical curve reasonably well. Most of the points lie to the right of (or below) the theoretical curve, just as in Higashi's and Penner's data. Also, in general the data are closer to the theoretical curve for the season of moderate temperature fluctuations (1959-1960) than are the data for the season of rather sharp temperature fluctuations (1960-1961). This suggests that the relationship is affected by a stronger cooling rate or that some other factor not presently understood is acting.

Data are also shown for the condition of significant penetration of the frost line. In this case, the penetration rate is plotted against the heaving rate. The scatter of the data is such that it is difficult to establish any over-all trend with certainty. However, some fairly definite trends can be noted for specific soils (see Fig. 13).

In the case of the silt, several of the points very nearly fit a straight line through the origin of these plots. This is true for both seasons, and furthermore, the slopes of these lines are nearly identical. Heave rate equals 0.14 times the penetration rate for 1959-1960, and heave rate equals 0.13 times the penetration rate for 1960-1961. If this is in fact the most valid interpretation of these data, it would agree in general with Penner's observations.

On the other hand, if the data for the sand are considered for the season 1959-1960 a a line with a negative slope would envelop nearly all the data points. This would agree more nearly with Higashi's concepts. Although several of the points for the 1960-1961 season do fit this envelope quite well, the scatter is noticeably greater for this season.

The data for the Pike Bay soil (sand with plastic fines) also suggest that the penetration rate will increase at the expense of the heave rate. This trend seems to be better established for this soil than for the sand, especially if the two seasons are considered separately. Two lines are drawn on the plot of heave rate vs penetration rate for this soil to correspond to the data for the two seasons considered. The trend is somewhat better defined for the 1959-1960 season, when the temperature changes were comparatively moderate.

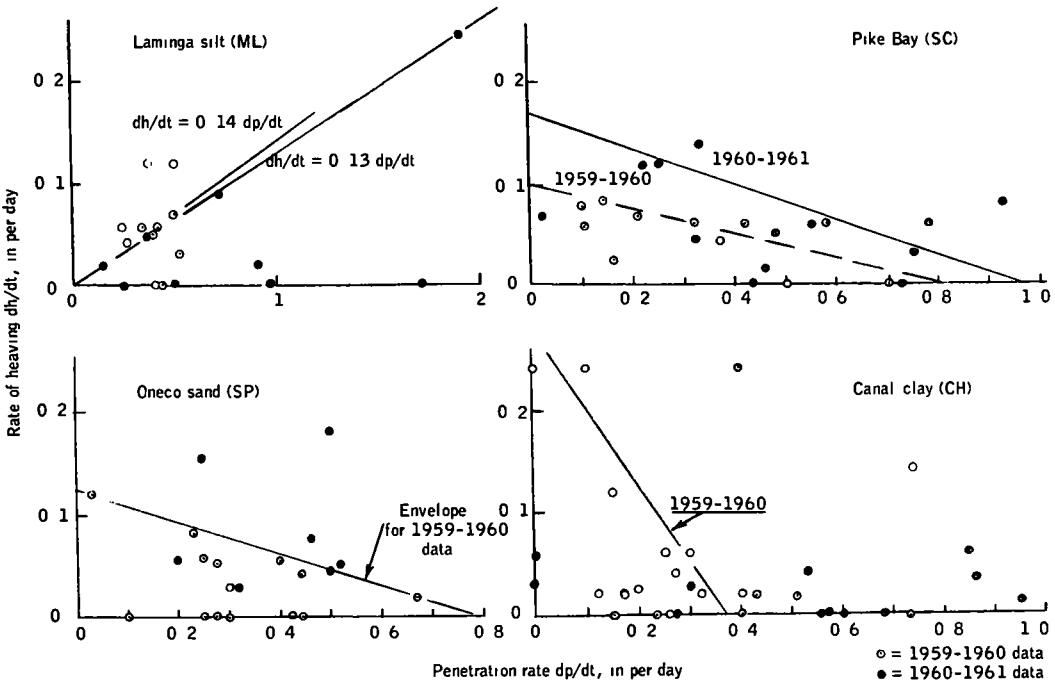

Figure 13. Heave rate vs penetration rate for rapid penetration case: symbols in parentheses indicate unified soil classification.

The data for the clay are not as conclusive. Considering the 1960-1961 data, there appears to be no relationship between heave rate and frost penetration rate. However, the heaving rate for this season is generally low for all penetration rates as well as for the case of zero penetration rate.

The data on the clay for the 1959-1960 season include some higher heave rates than for 1960-1961. This is true for the zero frost penetration case as well as for the rapid penetrating case. One possible interpretation of these data is sketched on the figure, showing an increase in the frost penetration rate with a decrease in the heave rate. Although it probably should not be considered as conclusive because of the scatter of data, it can be seen that this interpretation is compatible with Higashi's concepts.

SUMMARY AND CONCLUSIONS

A theoretical analysis of the mechanism of frost action in soils has been presented, with particular emphasis on the heat balance and its relationship to the heaving rate and rate of penetration of the frost line. The results of two previous laboratory investigations have been presented and discussed. A generalized concept of frost action mechansim has been suggested, based on theoretical considerations and on the results of previous investigations. The results of observations of soil freezing under natural conditions have been presented and analyzed for the purpose of attempting to verify the validity of the general concept and to test its applicability to freezing under natural conditions.

The following conclusions are drawn from this investigation: (a) when the frost line is not penetrating, the heaving rate is essentially proportional to the heat conduction difference between the frozen zone and the unfrozen zone, the conduction through the frozen zone being the larger quantity; (b) the observed relationship of the previous conclusion agrees quite closely with theoretical predictions in the case of laboratory studies were relatively accurate measurements are possible; (c) observed field behavior agrees reasonably well with the theoretical, considering the somewhat less favorable

conditions for obtaining good measurements; (d) the relationship between the rate of frost line penetration and the heaving rate needs further study, but limited data indicate some specific trends for specific cases; (e) the reported apparent conflict of opinion of previous investigations, based on somewhat contradictory laboratory results, may in fact be due to significantly different moisture conditions in the respective test procedures; and (f) the agreement of observed behavior with theoretically predicted behavior seems to depend on the magnitude and rate of natural air temperature fluctuations, although the data are somewhat limited.

ACKNOWLEDGMENTS

The investigations reported were sponsored by the U.S. Army Cold Regions Research and Engineering Laboratory, Hanover, N. H. The site of the study was the Keweenaw Field Station of that organization, located at Houghton, Mich. The analytical portion of the study was performed by personnel of the Michigan College of Mining and Technology, Houghton, as part of a research contract.

The author would like to express his appreciation to W.K. Boyd, James Bender, and Kenneth Linell of the Cold Regions Research and Engineering Laboratory for their encouragement and helpful suggestions. William Parrott, Director of the Keweenaw Field Station, and his staff supported the investigation in a very substantial manner. Alan Isola and Larry Watson, formerly of the Keweenaw Field Station, planned and supervised the construction of the observation plots and their instrumentation and obtained the data for the first frost season. Martin Britz of the Keweenaw Field Station obtained field data and helped in various other ways. The author is also indebted to the several student research assistants who have participated in this investigation, especially to Marvin Oosterbaan, Maurice Bowers, and Allan Green, who contributed in particular to this portion of the over-all project.

The author wishes to thank the American Society for Testing and Materials and the National Research Council of Canada for permission to reproduce the figures showing the results of Penner's investigation.

REFERENCES

1. Higashi, A., "Experimental Study of Frost Heaving." Snow Ice and Permafrost Research Establishment, Corps of Engineers, U.S. Army, SIPRE Research Report 45, (1958).
2. Penner, E., "The Importance of Freezing Rate in Frost Action in Soils." Proc., ASTM, Vol. 60 (1960). (Also published by the National Research Council of Canada as Division of Building Research Paper 126.)
3. Kersten, M., "The Thermal Conductivity of Soils." HRB Proc., 28:391-409 (1948).

Discussion

E. PENNER, Soil Mechanics Section, Division of Building Research, National Research Council of Canada—The writer was interested in the theories presented in this paper but wishes to comment on the interpretation of the information given in Figure 13. The usually accepted procedure to evaluate the usefulness of the information contained in such scatter diagrams is by analyzing the results statistically. In addition, the best fitting line is normally determined by the method of least squares. In the opinion of the writer the majority of the experimental results in Figure 13 cannot be used as a sound basis to judge the validity of the various proposed relationships between the frost penetration rate and rate of frost heaving.

To support this statement, the writer has carried out these statistical computations on the author's results and the information is presented in this discussion.

Assuming the frost penetration rate to be the independent variable, the frost heaving rate the dependent variable and that the relation between the variables is linear, regression equations have been determined for most of the results in Figure 13 by the method of least squares. These regression lines are shown in Figure 1 on the author's scatter diagrams and differ markedly from his interpretation.

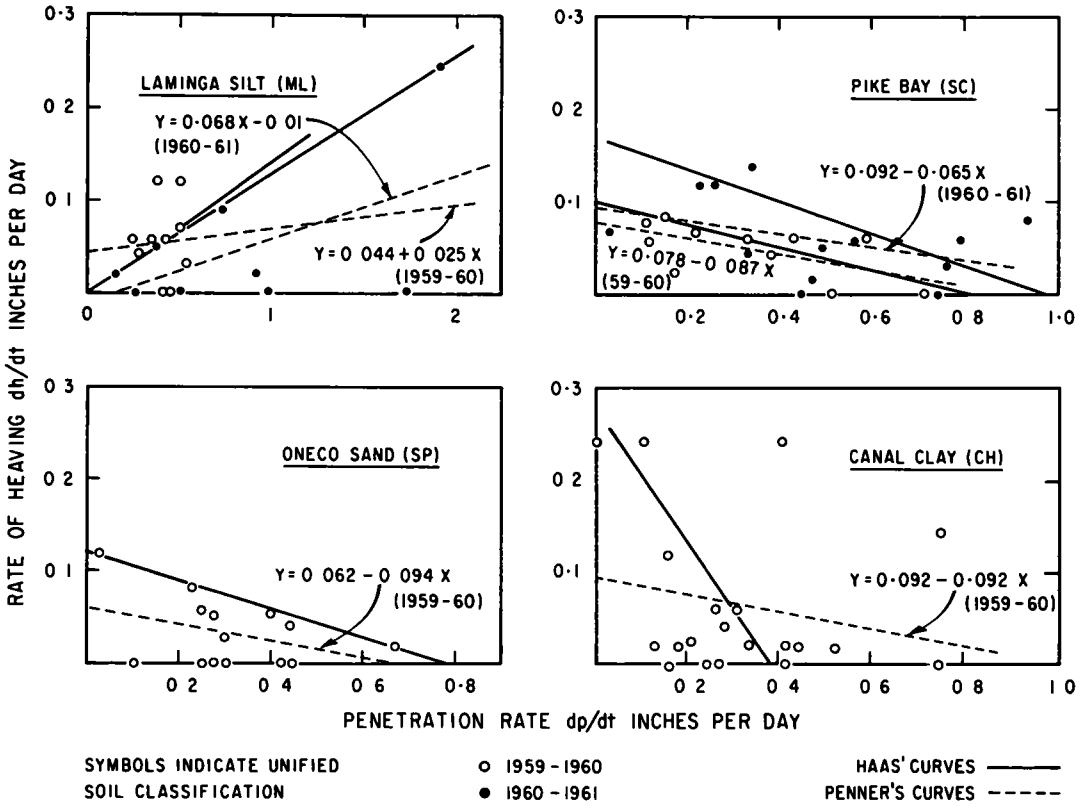

Figure 1. Regression lines calculated by least squares method from results in Figure 13 of author's paper.

TABLE 1

RESULTS OF THE STATISTICAL ANALYSES OF FIGURE 13

Soil	Year	Number of Paired Comparisons, n	Correlation Coefficient, r	Dependence of Frost Heaving on Frost Penetration, $r^2 \times 100$ (%)	Error Variance, $100-(r^2 \times 100)$ (%)	Slope of Regression Line	Statistical Significance	
							5 Percent	1 Percent
(1a)	(1b)	(2)	(3)	(4)	(5)	(6)	(7)	
Laminga silt	1959-60	11	0 059	0 31	99 7	0 025	Not sig	Not sig
	1960-61	9	0 543	29 5	70 5	0 068	Not sig	Not sig
Oneco sand	1959-60	14	0 389	15 1	84 9	-0 094	Not sig	Not sig
Pike Bay	1959-60	11	0 624	39 0	61 0	-0 087	Sig	Not sig
	1960-61	13	0 381	14 5	85 5	-0 065	Not sig	Not sig.
Canal clay	1959-60	20	0 210	4 4	95 6	-0 092	Not sig	Not sig

To test the significance of the correlation between the rate of frost heaving and rate of frost penetration, the correlation coefficient was determined and its statistical significance was tested by the widely accepted t-test. The results of the t-test show that no statistically significant correlation exists between these variables, except in one case, and thus the validity of the other regression lines must be rejected on statistical grounds.

Table 1 gives the results of the statistical analyses. The first column identifies the soil and the year of the experiment. Column 2 gives n, the number of paired determinations shown on the author's Figure 13. Column 3 gives the calculated correlation coefficient r and column 4 gives $r^2 \times 100$ which is the percentage variation in y (frost heaving rate) directly attributable to x (frost penetration rate). By subtracting this percentage from 100, the percentage variance of the errors of estimation (error variance) is obtained and is given in column 5. Column 6 gives the slopes of the regression lines, which are in fact statistically inadmissible, except in one case, because the t-test results show that at the levels of significance (5 or 1 percent) usually acceptable, the correlation coefficient r is statistically not significant.

Frost Penetration Beneath Concrete Slabs Maintained Free of Snow and Ice, With and Without Insulation

WILLIAM F. QUINN and EDWARD F. LOBACZ, U. S. Army Cold Regions Research and Engineering Laboratory, Corps of Engineers, Hanover, New Hampshire

This paper presents the results of an investigation relative to the prediction of frost penetration in soils beneath concrete slabs, both insulated and uninsulated. A one-dimensional periodic heat-flow solution of the Fourier conduction equation was used to determine the effect of concrete and/or insulation in reducing frost penetration. For simplicity, the solution assumed an annual sinusiodal temperature distribution at the surface boundary. The freezing index at the concrete-soil interface (and insulation-soil interface) was found by calculating the amplitude of the sinusoidal temperature wave at this depth and then converting it to a freezing index. This freezing index was then used in the modified Berggren equation to calculate the depth of frost penetration into the underlying soil.

During the 1960-61 winter season, subsurface temperatures were recorded at three small-scale concrete-slab test sections at Waltham, Mass. The slabs were 8, 12, and 24 in. in thickness. A 2-in. layer of insulation was placed under the 8-in. slab. Slab surfaces were exposed to the natural climatic influences and were generally kept free of snow and ice.

Results indicated reasonable agreement between actual and predicted depths of frost penetration for the uninsulated slabs and suggested a solution for frost penetration problems in a multilayer profile of portland cement concrete, insulation, and soil.

•THIS STUDY was conducted to substantiate design criteria in use by the Corps of Engineers for estimating the amount of non-frost-susceptible soil required beneath uninsulated concrete pavements greater than 12 in. in thickness and to determine a suitable heat-flow computational technique for predicting the total depth of frost penetration under conditions in which an insulating layer is placed directly beneath a PCC pavement.

Corps of Engineer design criteria for estimating the amount of non-frost-susceptible soil required beneath uninsulated pavements kept free of snow or ice make use of the relationship between air freezing index, soil properties, and frost penetration shown in Figures 1 and 2. As indicated in note 2 of Figure 1, the frost penetration depths are measured from the pavement surface and are computed for 12-in. PCC pavements by means of the modified Berggren equation (1). An adjustment is made in this equation to convert the air-freezing index to a surface-freezing index in order to establish the upper boundary conditions for heat flow.

Many present-day runways are more than 12 in. thick and the effect of thicker pavements on the total frost penetration must be considered in design. This is done by assuming that 10 degree-days of air-freezing index are required for each inch of frost penetration in concrete pavement below the top 12 in. as shown in the following example.

If a PCC pavement thickness of 18 in., a design air-freezing index of 3,000 degree-days, F, and a base-course material having an average dry unit weight of 135 pcf and

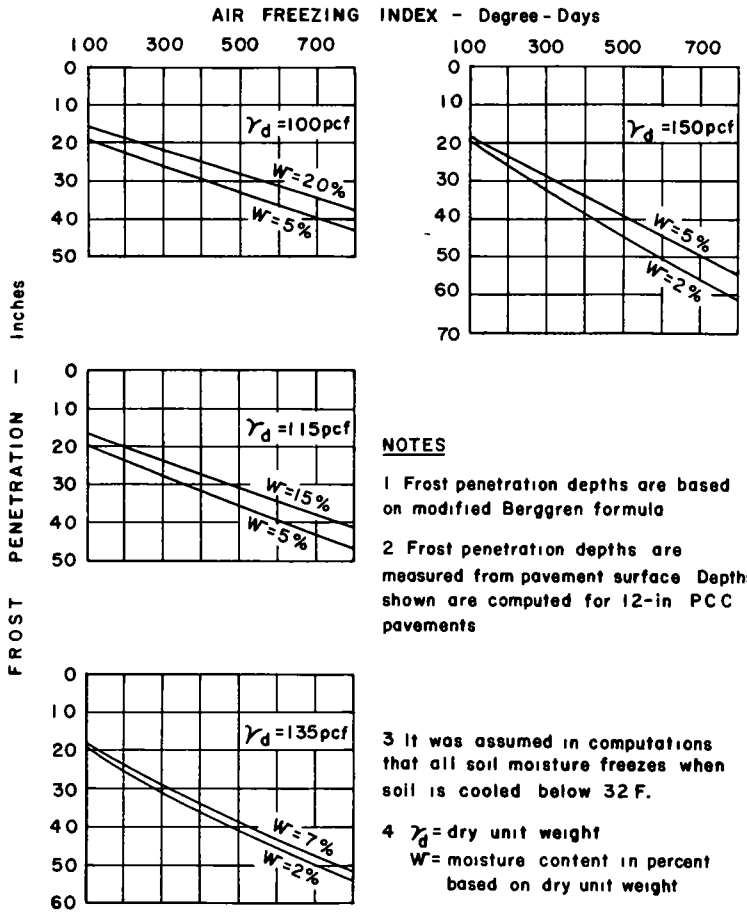

Figure 1. Relationships between air-freezing index and frost penetration into granular, non-frost-susceptible soil beneath pavements kept free of snow and ice for freezing indexes below 800.

an average water content after drainage of 5 percent is assumed, each inch of concrete pavement in excess of 12 in. is considered to reduce the air-freezing index by 10 degree-days. Thus, the modified freezing index is 3,000-10x(18-12) = 2,940 degree-days, F. From Figure 2, the combined thickness of 12-in. pavement and base required to prevent freezing of the subgrade is 138 in.; adding the originally deducted 6 in. of pavement results in a combined thickness of pavement and base of 144 in.

Inasmuch as the empirical 10 degree-day factor is based on field experience and the judgment of design engineers, it was thought advisable to check the validity of this factor by an appropriately instrumented field test in which the number of degree-days associated with the frost penetration for a 12-in. PCC slab could be compared with that for a 24-in. PCC slab.

For the case of the insulated concrete slab, the periodic heat flow method developed by A. H. Lachenbruch (2) was used to analyze frost penetration. This method was also found applicable to predict frost penetration for the case of uninsulated slabs. An insulating layer under a concrete slab might be used when site conditions or economic considerations make it an advantageous alternative to hauling non-frost-susceptible material over great distances or to establishing an aggregate washing operation. The possibility also exists that an insulating layer might be used together with a non-frost-susceptible fill to reduce the required thickness of the fill and still prevent frost penetration into an underlying frost-susceptible subsoil.

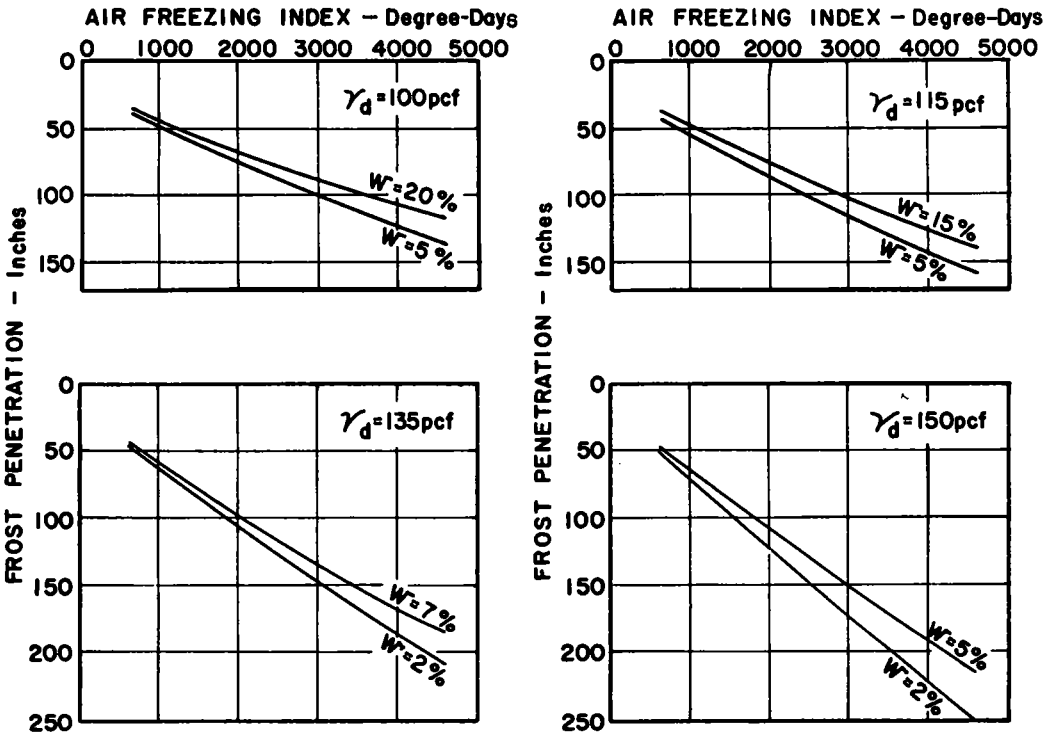

Figure 2. Relationships between air-freezing index and frost penetration into granular non-frost-susceptible pavements kept free of snow and ice (see notes on Fig. 1).

DEFINITIONS

The following specialized frost terms (3) are used in this report:

Non-Frost-Susceptible Materials. —Cohesionless materials such as crushed rock, gravel, sand, slag and cinders in which significant detrimental ice segregation does not occur under normal freezing conditions.

Average Daily Temperature. —The average of the maximum and minimum temperatures for one day or the average of several temperature readings taken at equal time intervals during one day, generally hourly.

Average Annual Temperature. —The average of the average daily temperatures for one year.

Mean Annual Temperature. —The average of the average annual temperatures for several years. In this report it is abbreviated MAT.

Degree-Days. —The degree-days for any one day equals the difference between the average daily air temperature and 32 F.

Freezing Index. —The number of degree-days between the highest and lowest points on a curve of cumulative degree-days vs time for one freezing season. The index determined for air temperatures at 4.5 ft above the ground is commonly designated as the air-freezing index, and that determined for temperatures immediately below a surface is known as the surface-freezing index.

Design-Freezing Index. —The average air-freezing index of the three coldest winters in the latest 30 yr of record. If 30 yr of record are not available, the air-freezing index for the coldest winter in the latest 10-yr period may be used.

Mean Freezing Index. —The freezing index determined on the basis of mean temper-

atures. The period of record over which temperatures are averaged is usually a minimum of 10 yr, and preferably 30, and should be the latest available.

n-Factor. —The ratio of surface freezing index to air freezing index.

FIELD INSTALLATION AND TEMPERATURE OBSERVATIONS

Three small-scale concrete test slabs were constructed on the property of the U. S. Army Engineer Division, New England, in Waltham, Mass. The slabs measured 5 by 5 ft in plan with thicknesses of 8, 12, and 24 in. A 2-in. layer of cellular-glass insulation was placed under the 8-in. slab. At the midpoint of each slab a string of 18-gage copper-constantan thermocouples was installed and connected to an automatic strip-chart recorder timed to print temperatures at approximately 75-min. intervals. The slabs were placed on the south side of the property to expose them to the warming effects of the sun. Photographs of the test area are shown in Figure 3, and plan and section in Figure 4. The slabs were inspected daily during the work week and any new-fallen or drifted snow and ice was removed from the surfaces. On two cold January weekends, however, a thin layer of snow drifted on the 24-in. slab.

The 12-in. and 24-in. slabs were built in the fall of 1959 on an 8-in. base course of silty gravelly sand (SW-SM) having a dry density of 109 pcf and a moisture content of 5.5 percent. The 8-in. slab, with a 2-in. insulating layer, was built in the fall of 1960 and was placed on top of a 4-in. base course of silty gravelly sand (SW-SM) having a dry density of 137 pcf and a moisture content of 2.6 percent. The natural soil at the site is a silty gravelly, coarse to fine sand (SM) having a dry density of about 130 pcf and a moisture content of 4 percent. No subsurface water table was found within the drilling depth of 11.5 ft for installation of the thermocouple assemblies.

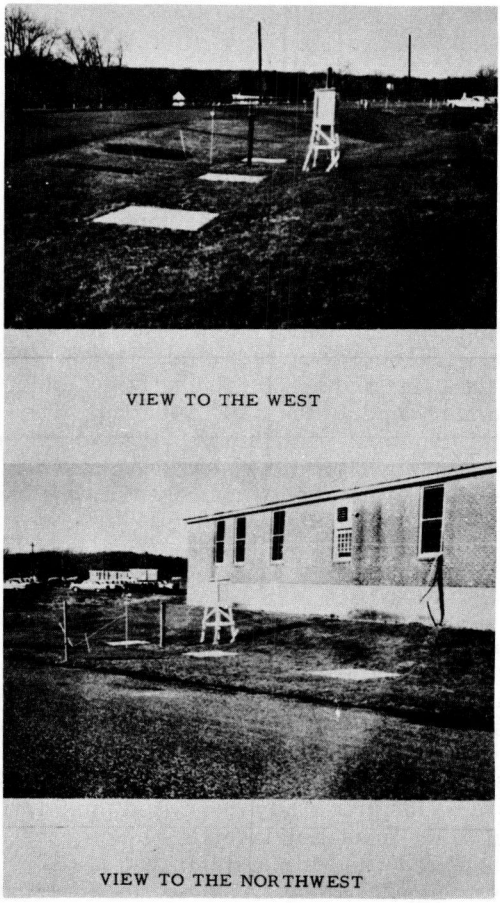

Figure 3. Test installation.

Air temperatures were continuously recorded with a thermograph placed in a standard U. S. Weather Bureau shelter at the site. The 1960-1961 air-freezing index at the site was 663 degree-days, F, and the mean annual temperature, 49 F (estimated). Because long-term weather records are not available for Waltham, Boston records were used to determine the relative intensity of the freezing season. The 1960-61 air-freezing index at the official U. S. Weather Bureau station in Boston (approximately 10 mi east of Waltham) was 428 degree-days, F. The mean freezing index for Boston is 166 degree-days, F, and the design freezing index (based on the coldest year in 10) is 620 degree-days, F. Although the 1960-61 index of 428 is not unusually high for Boston, a severe siege of cold befell the area on January 16 when temperatures remained below 32 F for 16 consecutive days. This was the longest such period in 43 years and the second longest of record.

A plot of the seasonal accumulation of degree-days for air temperature and surface temperatures for each slab is shown in Figure 5. Surface temperatures were obtained from thermocouples located $\frac{1}{8}$ in. below each slab surface. The test slabs underwent num-

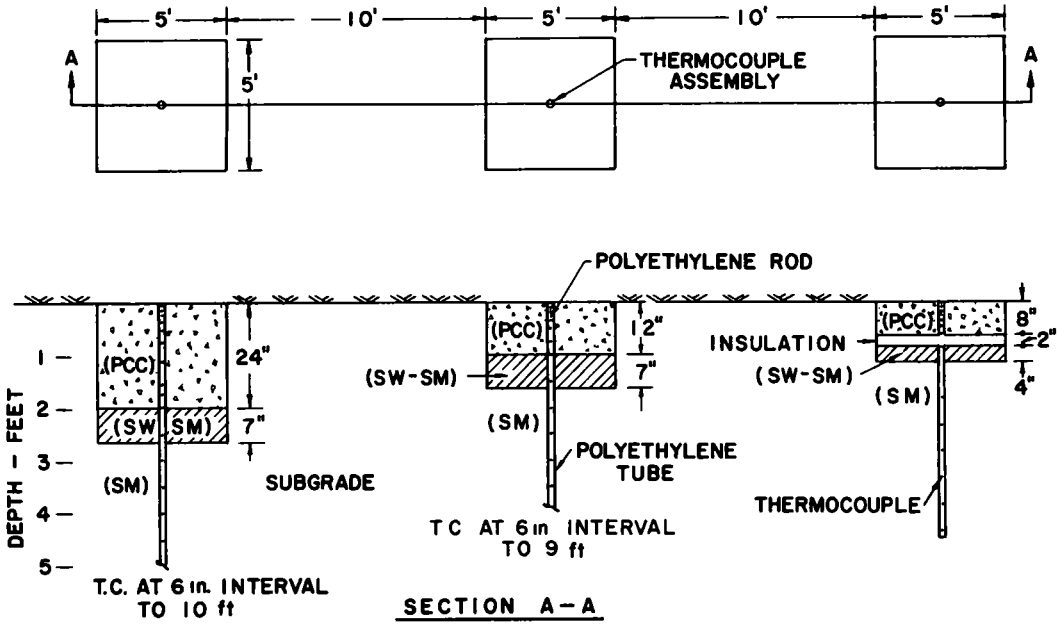

Figure 4. Plan and section of test slabs.

erous freeze-thaw cycles as shown in Figure 6. Although freezing penetrated the soil beneath the 12-in. uninsulated slab early in December and also reached the bottom of the 24-in. slab, freezing did not take place below the insulation layer of the 8-in. slab until after mid-January. The large number of freeze-thaw cycles in the uninsulated concrete slabs throughout the winter season, and the similarity between the air and the insulated slab surface cumulative degree-day measurements. The fact that the base course under the 12-in. slab froze during the early part of the season made it less susceptible to change under diurnal temperature variations (owing to latent heat effects) than the 24-in. slab, under which no base-course freezing occurred in this period. The total measured frost penetration was 24 in. at the 8-in. slab; 34 in. at the 12-in. slab; and 36 in. at the 24-in. slab, based on the maximum depth of the 32 F isotherm. The loss of heat (edge effect) around the periphery of the small-scale slabs may have tended to reduce the depth of frost penetration from what it would have been had one-dimensional (vertical) heat flow taken place. Temperature gradients for representative times during the freezing season appear in Figure 7.

VARIATION OF FREEZING INDEX WITH DEPTH

Cumulative degree-days were tabulated for the surface and for the 1-ft and 2-ft depth under the 12-in. and 24-in. slabs and for the 8-in. and 10-in. depths under the 8-in. sla (Fig. 8). Degree-days were determined by averaging the maximum and minimum daily recorded temperatures at the designated depth and accumulating the differences between the average daily temperature and 32 F. The surface-freezing indexes were 439 degree-days, F, for the 12-in. slab, 471 for the 24-in. slab, and 646 for the 8-in. insulated slab. The greater surface-freezing index of the 24-in. slab may be attributed in part to the higher reflectivity of the slab surface caused by the previously mentioned thin layer of drifted snow. Figure 8 also shows the effect of the insulating layer in reducing the accumulation of degree-days at the top of the subgrade; there is a difference of 617 degree-days, F, between the top and bottom of the insulation layer. Also, the freezing indexes at the top and bottom of the 8-in. slab were very similar, the bottom index being 23 degree-days, F, greater than at the top. (It would be logical to expect the sur-

face index to exceed the 8-in. depth index.) This observed anomaly may have been caused by minor errors in temperature measurement.

The computed n-factors for the three slabs (8-, 12-, and 24-in.) are 0.98, 0.66, and 0.71 respectively. The surface reflectivity of the insulated slab was found to be slightly higher than that of the uninsulated slabs, but this does not entirely explain the large difference in n-factors. The surface reflectivity measured with a light meter held vertically at a height of about 2 ft above the slab surface. The reading obtained with the meter facing downward was divided by the reading obtained with the meter facing upward. The discontinuity in the temperature gradient for the insulated slab (see Fig. 7) may offer some explanation; i.e., the relatively warm temperature of the soil underlying the insulation (lower boundary condition) does not have the same opportunity to affect the slab temperatures as it would if the insulation were not present. No discontinuity appears in the temperature gradients for the uninsulated slabs.

Figure 8 shows that from January 18 to February 18 the cumulative number of degree-days at the 1-ft depth in each of the uninsulated slabs was 170 degree-days, F. However, for that portion of the freezing season before January 18, the cumulative number of degree-days at the 1-ft depth in the 12-in. slab was 40 degree-days, F, greater than in the 24-in slab. Temperature records indicate that during this period the 1-ft depth temperatures in the 24-in. slab were more responsive to surface diurnal temperature fluctuations than in the case of the 12-in. slab. This effect may have been partly due to the temperature dwell at 32 F resulting from the freezing of soil pore water beneath the 12-in. slab.

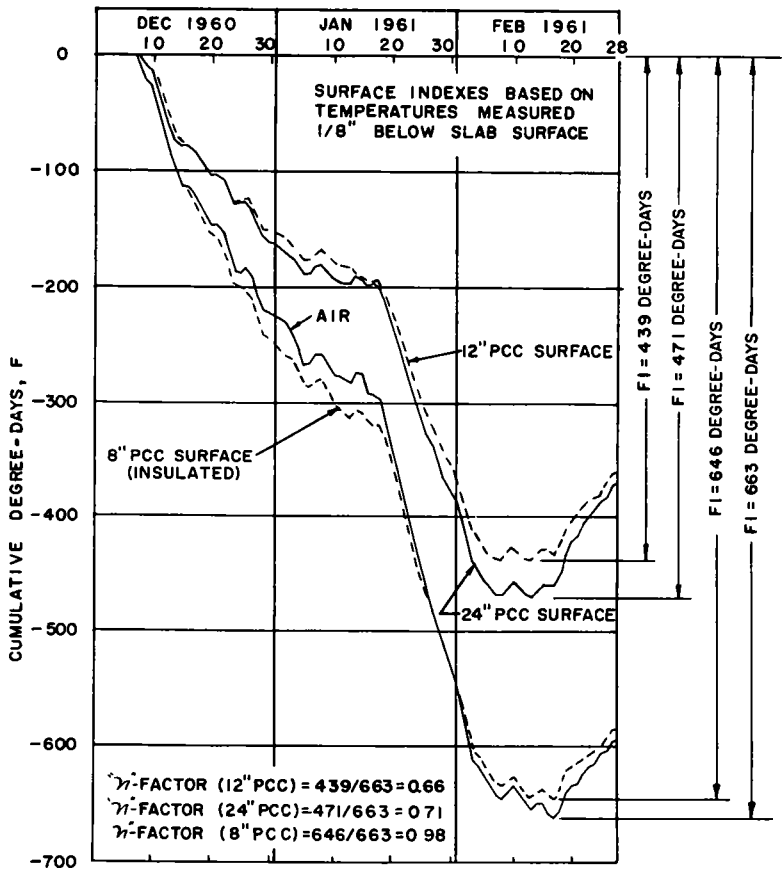

Figure 5. Air and surface cumulative degree-days.

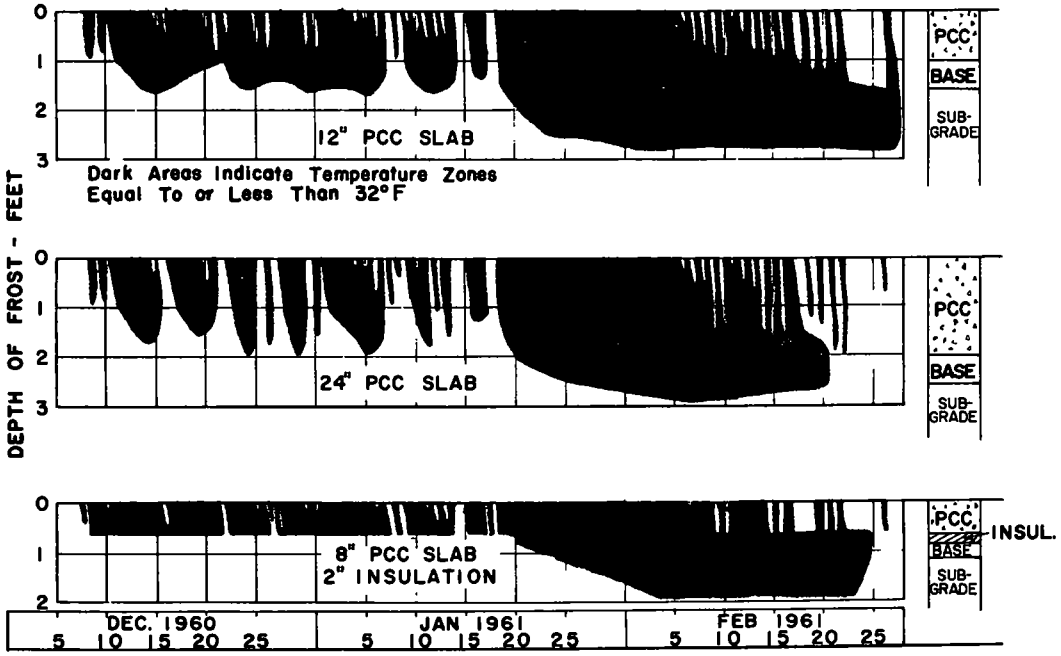

Figure 6. Frost penetration vs time.

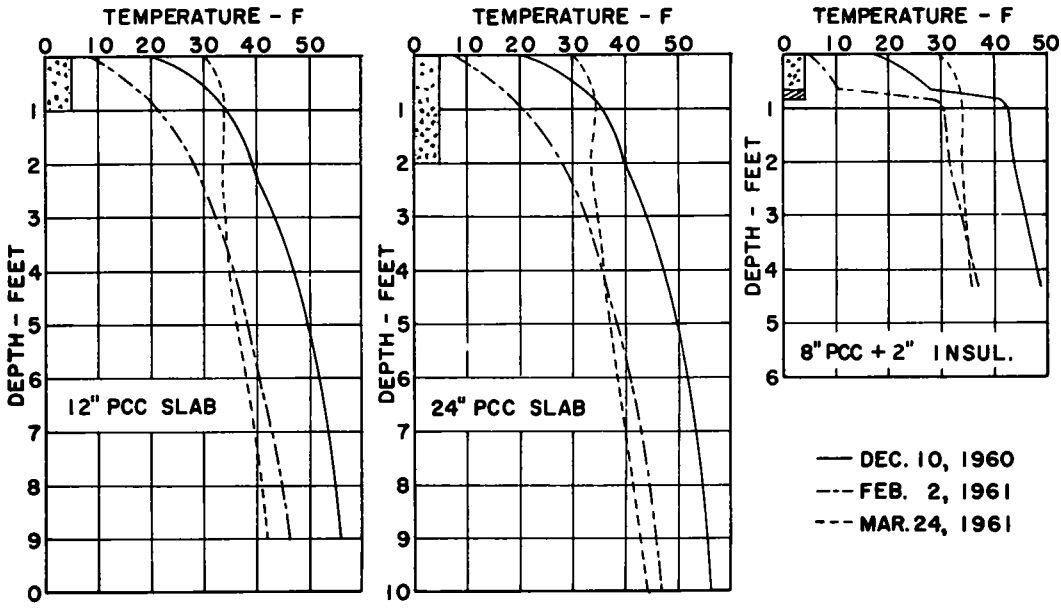

Figure 7. Temperature gradients.

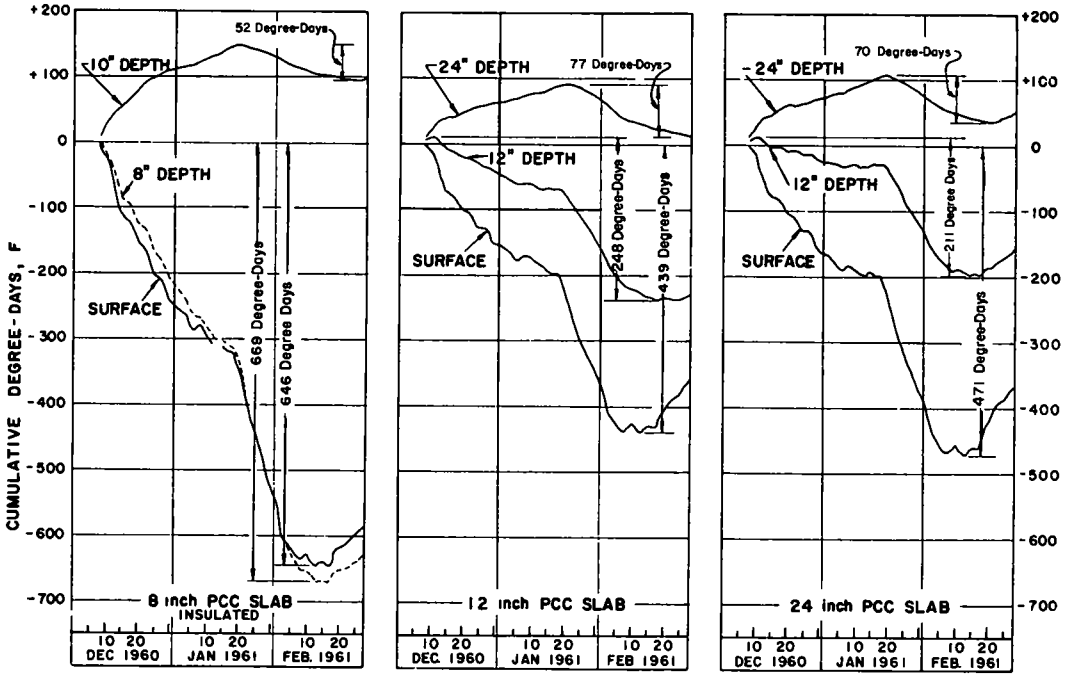

Figure 8. Variation in cumulative degree-days with depth.

The average decrease in freezing index per inch of concrete was $\frac{(439-248)}{12} = 15.9$ degree-days, F, per in. for the 12-in. slab and $\frac{(471-70)}{24} = 16.7$ degree-days, F, per in. for the 24-in. slab. In the 24-in. slab, the average decrease in freezing index was 21.7 degree-days, F, per in. in the upper foot and 11.75 degree-days, F, per in. in the lower foot. As stated previously, the present design method recommends deducting 10 degree-days, F, per in. from the air-freezing index for each inch of concrete over 12 in. To convert the 11.75 degree-days, F, per in. to an air-freezing index datum, it should be divided by the applicable n-factor, which in this case is 0.71. Thus $\frac{(11.75)}{0.71} = 16.5$ degree-days, F, per in. represents the average reduction in air freezing index per inch of concrete over 12 in. for this particular test. On the basis of this single, small-scale experiment in an area of relatively low air-freezing index, consideration might be given to raising the recommended design criteria from 10 degree-days, F, per in. to 12 degree-days, F, per in., which should more nearly predict frost penetration.

ANALYSIS OF INSULATED SLAB BY PERIODIC HEAT FLOW

The depth of frost penetration under the combined layer of portland cement concrete and insulation was analyzed using the one-dimensional periodic heat-flow solution of the Fourier conduction equation (4). This equation takes into consideration the thermal contact coefficients, β (defined later), of the heterogeneous materials comprising the cross-sectional profile of the insulated section. The mathematical development of this solution, presented by Lachenbruch (2), assumes a simple annual sinusoidal temperature distribution as the surface boundary condition and constant termal properties of each stratum. The freezing index at the insulation-soil or concrete-soil interface was determined by calculating the amplitude of the sinusoidal temperature wave at this interface and then converting this amplitude to a freezing index. This freezing index was

then applied in the modified Berggren equation to calculate the depth of frost penetration into the underlying soil. The modified Berggren equation takes into consideration the concurrent thermal effects of temperature changes and soil water phase transformations and may be applied to either homogeneous (5) or stratified (6) soil conditions.

If the effect of the thermal contact coefficient, β, is ignored, however, the amplitude of the sinusoidal temperature wave is damped logarithmically as its depth increases and the mathematical expression for this condition becomes

$$A_x = A_0 \exp(-y) \tag{1}$$

in which

$$y = x_1\sqrt{\frac{\pi}{a_1 P}}$$

x_1 = depth from surface within upper layer, feet;
a_1 = thermal diffusivity of upper layer, ft^2/day;
P = period of sine wave, 365 days;
A_0 = amplitude of surface sine wave, F; and
A_x = amplitude of sine wave at depth x, F.

When the effect of contact coefficients are taken into consideration, Eq. 1 may be modified as follows:

$$A_x = A_0\left[\frac{1+M}{\sqrt{S}}\right]\exp(-y) \tag{2}$$

in which

$$(1+M) = \frac{2\beta_1}{\beta_1+\beta_2} \quad \text{(dimensionless)}$$

$$\text{(upper layer)}\quad \beta_1 = \sqrt{k_1 \cdot C_1}, \quad \text{Btu/ft}^2, \text{F}\sqrt{\text{hr}}$$

$$\text{(lower layer)}\quad \beta_2 = \sqrt{k_2 \cdot C_2}, \quad \text{Btu/ft}^2, \text{F}\sqrt{\text{hr}}$$

k_1 = thermal conductivity of upper layer, Btu/ft-hr-F;
k_2 = thermal conductivity of lower layer, Btu/ft-hr-F;
C_1 = volumetric specific heat of upper layer, Btu/ft^3-F;
C_2 = volumetric specific heat of lower layer, Btu/ft^3-F; and

$$S = 1 + 2M_1 \cos 2x_1\sqrt{\frac{\pi}{a_1 P}} \exp\left[-2x_1\sqrt{\frac{\pi}{a_1 P}}\right] +$$

$$M_1^2 \exp\left[-4x_1\sqrt{\frac{\pi}{a_1 P}}\right].$$

If β_1 is greater than β_2, the A_x of Eq. 2 is larger than that of Eq. 1 and conversely, if β_1 is less than β_2, the A_x of Eq. 2 is smaller. The effect of thermal contact resistance is most pronounced when analyzing heat flow through materials having considerably different β values, such as concrete, insulation, and soil.

The freezing index represented by a sinusoidal temperature wave at any depth may be determined from the relationship between the amplitude of an equivalent sinusoidal wave and the mean annual temperature, as

$$F_x = \frac{365}{\pi}\left[\sqrt{A_x^2 - \nu_0^2} - \nu_0 \cos^{-1}\frac{\nu_0}{A_x}\right] \quad (3)$$

in which

F_x = freezing index at depth x, degree-days, F;
A_x = amplitude of sine wave at depth x, F; and
ν_0 = (average annual temperature −32F), F.

Eq. 1 and 3 are shown graphically in Figure 9.

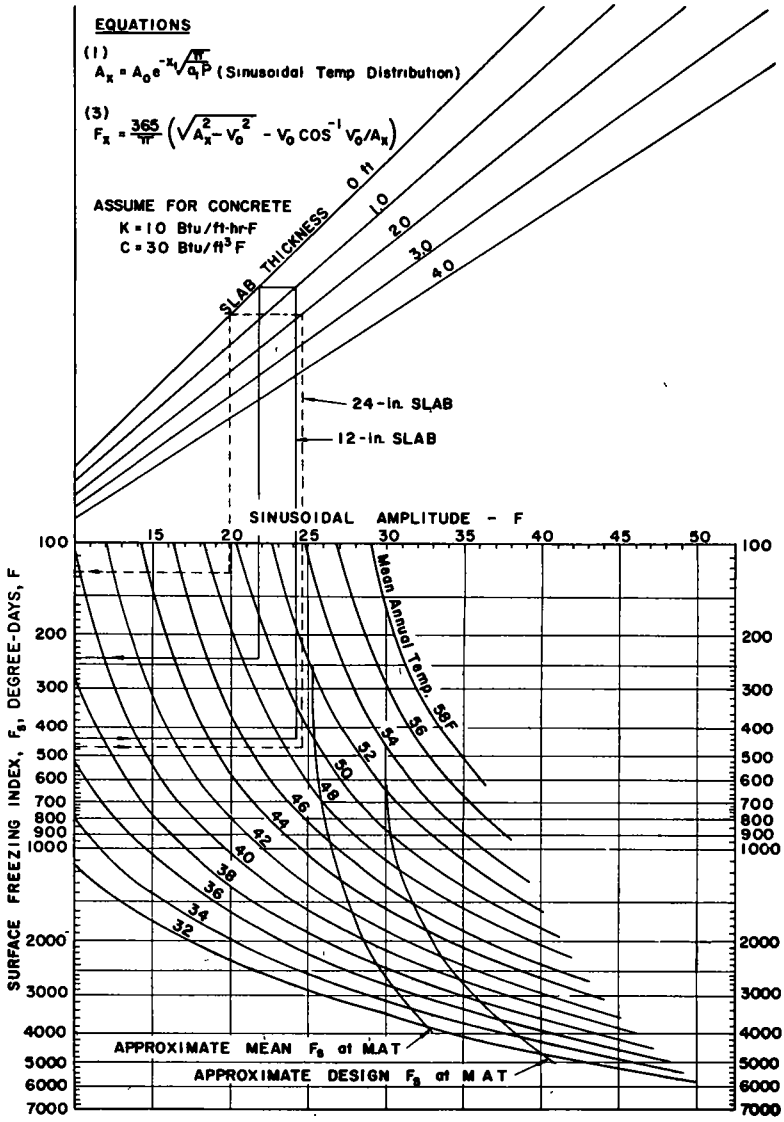

Figure 9. Freezing index at bottom of concrete slabs.

EVALUATION OF FROST PENETRATION UNDER TEST SLABS

A discussion of frost penetration, measured vs predicted, follows. The thermal properties of the materials used in the analysis are given in Table 1. The mean annual temperature used in the calculations was 49 F.

TABLE 1

THERMAL PROPERTIES

Material	Thermal Conductivity, k (Btu/ft-hr-F)	Volumetric Specific Heat, C (Btu/ft^3-F)	Thermal Diffusivity, α (ft^2/day)	Thermal Contact Coef., β (Btu/ft^2-F-$\sqrt{hr}$)
Concrete	1.00	30.0	0.800	5.48
Insulation	0.0317	1.8	0.423	0.239
Soil:				
8-in. slab	1.20[a]	26.0	1.109	5.60
12- and 24-in. slabs	0.80[a]	23.0	0.835	4.30

[a]After Kersten (7).

Uninsulated Slabs

12-In. Slab.—Entering Figure 9 with a surface freezing index of 439 and a mean annual temperature of 49 F, the surface sinusoidal amplitude is found to be 24.25 F and the freezing index at the bottom of the slab, 240 degree-days, F, with a corresponding sinusoidal amplitude of 21.7 F. This predicted freezing index of 240 degree-days, F, is in close agreement with the measured index of 248.

The predicted frost penetration using the modified Berggren equation for a multilayer condition is 36 in. (Appendix A) in comparison to the measured depth of 34 in.

As the thermal contact coefficients of the concrete and base course are of similar magnitude, Eq. 1 was used for this solution. In general, the β-values of concrete and granular base courses will be reasonably equivalent, which permits a much simpler solution of the problem. The magnitude of the $(1 + M) / \sqrt{S}$ modifier is 1.022 for this case; this was determined (Table 1) as

$$\beta = 5.48 \text{ for concrete}$$
$$\beta = 4.30 \text{ for soil}$$
$$(1 + M) = 1.12$$
$$\sqrt{S} = 1.096$$

thus,

$$\frac{1 + M}{\sqrt{S}} = 1.022.$$

Because of the many simplifying assumptions made in applying the periodic heat flow solution to the frost penetration problem, the effect of slightly differing thermal contact coefficients may be ignored when dealing with portland cement concrete and a high-quality base-course material. However, this effect must be considered when dealing with a stratified profile involving an insulation layer.

24-In. Slab.—The surface freezing index of the 24-in. slab was 471 degree-days, F. From Figure 9, the surface sinusoidal amplitude is 24.5 F and the freezing index at the base of the 24-in. slab is 125 degree-days, F, compared to the measured 70 degree-days, F. The difference between the predicted and measured freezing indexes at the base of the slab may be due to the influence of three-dimensional heat-flow and

to the inaccuracy of representing low freezing indexes by means of a simple sinusoidal wave form.

The frost penetration calculations (Appendix B) predict a total frost penetration of 39 in. The measured frost penetration was 36 in. based on the maximum depth of the 32 F isotherm.

Insulated Slab

The surface-freezing index of the 8-in. slab was 646 degree-days, F, which in Figure 9 corresponds to a surface sinusoidal amplitude of 26.5 F for a mean annual temperature of 49 F. The calculated freezing index at the bottom of the 8-in. slab is 638 degree-days, F, compared to the measured index of 669 degree-days, F. If the effect of the different thermal contact coefficients had not been considered the predicted freezing index would have been 480 degree-days, F, at the 8-in. depth.

The calculated freezing index at the bottom of the 2-in. insulation layer was 2 degree-days, F, compared to the measured index of 55 degree-days, F; however, if the effect of contact resistances had been neglected, the predicted index would have been 580 degree-days, F. Although the predicted index was smaller than that which actually occurred, it was of the correct order of magnitude compared to what it would have been if the effect of contact resistances had been neglected. The calculation technique is presented in Appendix C.

The fact that the measured index at the bottom of insulation was greater than predicted is largely attributed to the flow of heat around, rather than through, the insulating layer, creating an other than one-dimensional problem. If one-dimensional conditions had been maintained, it is expected that the predicted index would have been more nearly correct and the depth of frost penetration in the soil would have been negligible.

CONCLUSIONS

The assumption that 10 degree-days, F, of air-freezing index are required for each inch of frost penetration in concrete pavements below the top 12 in. was found conservative in this study. The use of 12 degree-days, F, per in. is suggested as more suitable and would still permit an element of conservatism in the design. Mathematical analysis by means of the periodic heat-flow method indicates that the number of degree-days required to penetrate concrete slabs more than 12 in. thick will vary, depending on the magnitude of the surface-freezing index and mean annual temperature. In zones of relatively high freezing indexes, a greater reduction in freezing index might be allowed than in zones of low freezing index.

The periodic heat flow solution for the insulated case (Eq. 2) gave results in the proper order of magnitude, although the quantitative results were slightly untenable. This is partly attributed to the lateral heat flow around the insulation due to the small-scale slabs employed in the field experiment. However, the test did indicate that the effect of the markedly different thermal contact coefficients should be taken into consideration when dealing with periodic heat flow through a concrete, insulation, and soil profile.

The use of the periodic heat flow equation for the uninsulated case (Eq. 1) appears to be a valid solution when dealing with portland cement concrete slabs placed on sound granular base courses. Such a procedure eliminates the need for evaluating the relatively complex (1 + M)//S term used when termal contact coefficients are considered. The assumption of an annual sinusoidal temperature distribution at the surface boundary appears to give sufficiently accurate results even though the temperature distribution is more complicated than assumed.

REFERENCES

1. Aldrich, H. P., Jr., "Frost Penetration Below Highway and Airfield Pavements." HRB Bull. 135, 145-149 (1956).

2. Lachenbruch, A. H., "Periodic Heat Flow in a Stratified Medium with Application to Permafrost Problems." Geological Survey Bull. 1083-A, U. S. Govt. Printing Office, (1959).
3. Hennion, F., "Frost and Permafrost Definitions." HRB Bull. 111, 107-110 (1955).
4. Ingersoll, L. R., Zobel, O. J., and Ingersoll, A. C., "Heat Conduction—with Engineering and Geological Application." McGraw-Hill (1948).
5. Aldrich, H. P., Jr., and Paynter, H. M., "First Interim Report—Analytical Studies of Freezing and Thawing of Soils." Arctic Construction and Frost Effects Laboratory, New England Division, Boston (1953).
6. Department of Civil and Sanitary Engineering, M. I. T., "Frost Penetration in Multilayer Soil Profiles." Arctic Construction and Frost Effects Laboratory, New England Division, Boston (1957).
7. Engineering Experiment Station, University of Minnesota, "Laboratory Research for the Determination of the Thermal Properties of Soils." Permafrost Division, St. Paul District, St. Paul, Minn. (1949).

Appendix A

Problem

To predict the frost penetration in the multilayer soil profile under the uninsulated 12-in. concrete slab using the modified Berggren method.

Solution

The following physical and thermal properties are used in this solution:

Layer	Depth, x (ft)	Dry Unit Wt., γ_d (pcf)	Moist. Cont., w (%)	Latent Heat, L (Btu/ft^3)	Avg Volumetric Specific Heat, C (Btu/ft^3 F)	Avg. Thermal Conduc., k (Btu/ft hr F)	Unified Soil Class
A	0-0 67	109	5.5	865	23.0	0 8	SW-SM
B	0.67-2.00	130	4 0	750	26.0	1 3	SM

in which

$L = 1.44\ w\ \gamma_d$;

$C_{avg} = \gamma_d\ (0.17 + 0.75\ x\ \frac{w}{100})$;

$k_{avg} = \frac{1}{2}\ (k_{frozen} + k_{unfrozen})$ after Kersten (7); and

x = depth below bottom of concrete slab.

The freezing index required to penetrate each layer is given by

$$F_n = \frac{L_n\ x_n}{24}\ (\Sigma R + \tfrac{1}{2}\ R_n)\ \frac{1}{\lambda_n^2}$$

in which

L_n = volumetric latent heat of layer, Btu/ft^3;

x_n = thickness of frozen layer, feet;

$R_n = x_n/k_n$ = thermal resistance of layer, ft^2 hr F/Btu;

ΣR = sum of resistances above layer considered:

λ_n = correction factor - function of μ and α (Fig. 10).

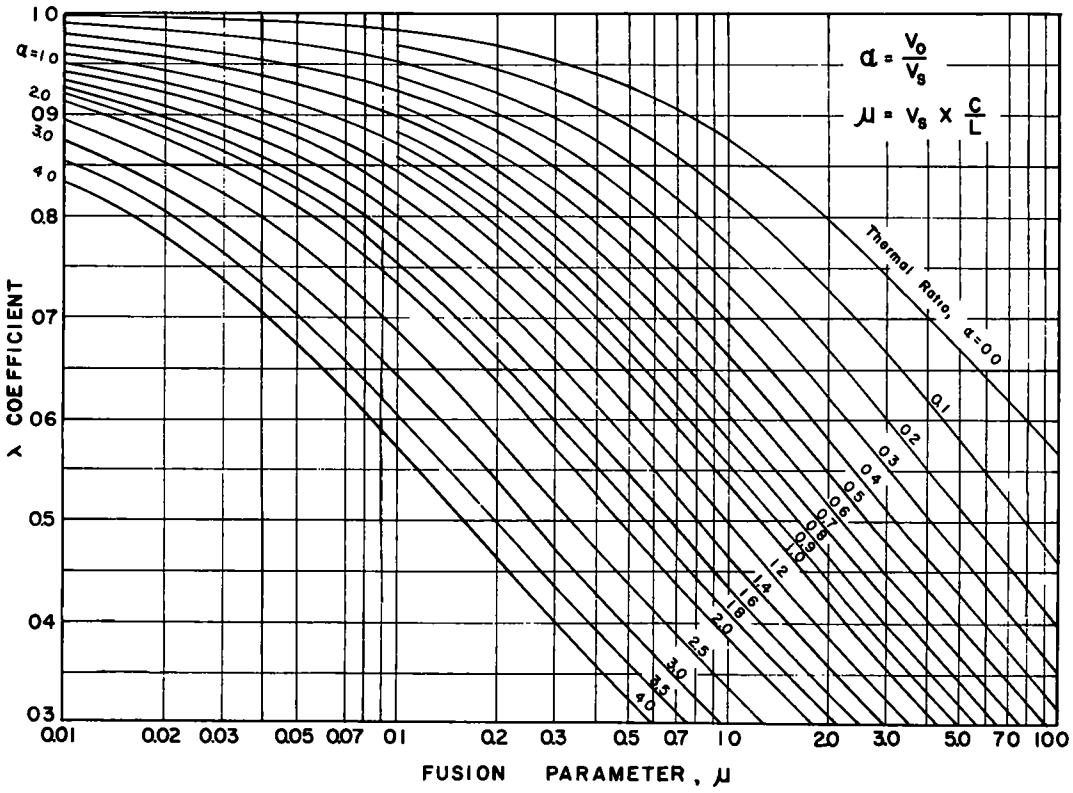

Figure 10. λ coefficient in the modified Berggren formula.

$$\mu = \frac{\overline{C}_n}{\overline{L}_n} \times \nu_s; \text{ where } \nu_s = \Sigma F/t;$$

ΣF = total freezing index at bottom of concrete, degree-days, F;
t = duration of freezing index, days (Fig. 11); and

$$\alpha = \frac{\nu_o}{\nu_s} \text{ where } \nu_o = \text{mean annual temperature - 32 F.}$$

Frost penetration in a multilayer soil profile is solved by trial and error, so that the total of the F_n values for each layer is equal to ΣF. The solution is given in Table 2 and predicts a frost penetration into the soil of 24 in. The total predicted frost penetration, which includes the concrete slab and soil, is (24 + 12) = 36 in.

The duration of the freezing season, t, at the surface of the slab was 68 days (Fig. 5). If a pure sinusoidal temperature waveform existed, the duration of the surface freezing index would have been 93 days. This is determined from the relationship between the $\frac{\nu_o}{A} = \frac{17}{24.25}$ term and the length of the freezing season, t (see Fig. 11). The length of freezing season required for a sinusoidal temperature variation at a 12-in. depth with an amplitude of 21.7 F is 77 days. Assuming proportional relationships, the predicted length of the freezing index at the 12-in. depth is 77/98 x 68 = 57 days. Thus, the duration of ΣF is taken as 57 days.

TABLE 2

FROST PENETRATION—12-IN. SLAB

Layer	x	Σx	C	k	L	Lx	ΣLx	$\overline{L}$	Cs	ΣCx	$\overline{C}$	μ	λ^2	R	ΣR	$\Sigma R + \frac{R}{2}$	F_n	ΣF_n
A	0 67	0 67	23.0	0 8	865	580	580	865	15.4	15.4	23 0	0 112	0.304	0 84	0	0.42	34	-
B	1 33	2 00	26 0	1 3	750	997	1,577	788	34.6	50 0	25 0	0 133	0 277	1 02	0.84	1 34	201	235

ΣF_n = 235 degree-days, F, compared to the total available index (ΣF) of 240 degree-days, F This is considered to be sufficiently close agreement, and the total predicted frost penetration in the soil (Σx) is 2 00 ft

ΣF = 240 degree-days, F

t = 57 days

ΣF/t = 4.21

$\alpha = \frac{49 - 32}{4\ 21} = 4\ 04$

λ is taken from Figure 10

$\overline{L} = \frac{\Sigma Lx}{\Sigma x} = \frac{1,577}{2\ 00} = 788$

$\overline{C} = \frac{\Sigma Cx}{\Sigma x} = \frac{50.0}{2\ 00} = 25$

$\mu = \frac{\overline{C}}{\overline{L}} \times \frac{\Sigma F}{t} = \frac{25}{788} \times 4\ 21 = 0\ 133$

$R = \frac{x}{k} = \frac{1\ 33}{1\ 3} = 1\ 02$

$F_B = \frac{Lx}{24} (\Sigma R + \frac{R}{2}) \frac{1}{\lambda^2} =$

$\frac{997}{24} (1.34) \times \frac{1}{0\ 277} =$

201 degree-days, F

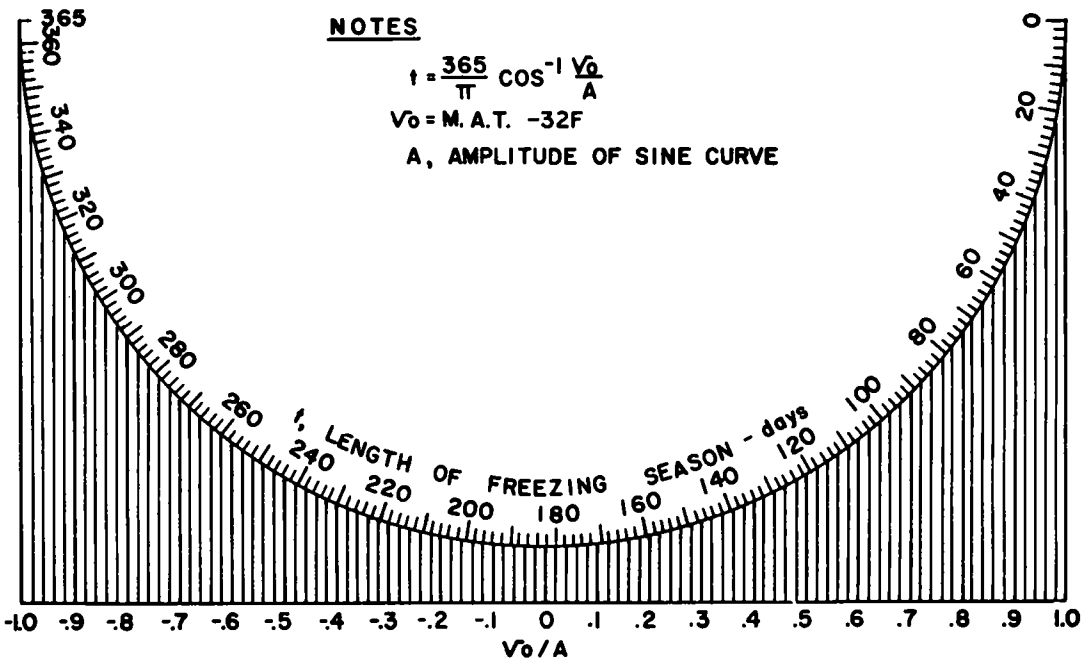

Figure 11. Length of freezing season for sinusoidal temperature variation.

Appendix B

Problem

To predict the frost penetration in the multilayer soil profile under the uninsulated 24-in. concrete slab.

Solution

The physical and thermal properties used in this solution are the same as those indicated in Appendix A. The solution is compiled in Table 3 and predicts a frost penetration into the soil of 15 in. The total frost penetration is (15 + 24) = 39 in.

The duration of the freezing season at the surface of the slab was 68 days (Fig. 5). If a sinusoidal temperature wave form had existed, the duration of the surface freezing index would have been 93 days ($\nu_o/A = 17/24.5$). The length of freezing season required for a temperature variation at a 24-in. depth with an amplitude of 19.9 F is 63 days. The predicted length of the freezing season at the 24-in. depth is

$$\frac{63}{93} \times 68 = 46 \text{ days}$$

TABLE 3
FROST PENETRATION–24-IN SLAB

Layer	x	Σx	C	k	L	Lx	ΣLx	$\bar{L}$	Cx	$\bar{C}$Cx	$\bar{C}$	μ	λ^2	R	ΣR	$\Sigma R + \frac{R}{2}$	F_n	ΣF_n
A	0 67	0 67	23.0	0 8	865	580	580	865	15 4	15 4	23.0	0 072	0 250	0.84	0	0 42	40	40
B	0 60	1.27	26 0	1 3	750	450	1,030	810	15 6	31 0	24.4	0 082	0.230	0.46	0 84	1 07	87	127

As shown in Table 3, ΣF_n = 127 degree-days, F, which is in agreement with the total available index of 125 degree-days, F. The total predicted frost penetration in the soil (Σx) is 15 in.

ΣF = 125 degree-days, F

t = 46 days

$\frac{\Sigma F}{t}$ = 2.72

$\alpha = \frac{49 - 32}{2.72} = 6.25$

λ (is taken from Fig. 10).

$\mu = \frac{\bar{C}}{\bar{L}} \times \nu_s$

Appendix C

Problem

To predict the freezing index at the bottom of the insulated 8-in. slab and at the bottom of the 2-in. insulation layer. The subscript 1 refers to the concrete, 2 refers to the insulation, and 3 refers to the base course.

Solution

Heat Flow Through Concrete Slab. —Eq. 2 is used for establishing the sinusoidal temperature amplitude at the bottom of the 8-in. concrete slab. The surface freezing index was 646 degree-days, F, and the mean annual temperature is 49 F.

$$A_1 = A_0 e^{-x_1\sqrt{\frac{\pi}{a_1 P}}} \left[\frac{1 + M_1}{\sqrt{S_1}}\right]$$

in which

$$A_0 = 26.5 \text{ F (Fig. 9)};$$

$$e^{-x_1\sqrt{\frac{\pi}{a_1 P}}} = e^{-\frac{8}{12}\sqrt{\frac{\pi}{(0.80)\ (365)}}} = 0.933;$$

$$(1 + M_1) = \frac{2\beta_1}{\beta_1 + \beta_2}; \quad = \frac{2(5.48)}{5.48 + 0.239} = 1.915;$$

$$M_1 = 0.915;$$

$$S_1 = 1 + 2M_1 e^{-2x_1\sqrt{\frac{\pi}{a_1 P}}} \cos 2x_1\sqrt{\frac{\pi}{a_1 P}} + M_1^2 e^{-4x_1\sqrt{\frac{\pi}{a_1 P}}}$$

$$= 1 + 1.580 + 0.635$$

$$= 3.215; \text{ and}$$

$$\sqrt{S_1} = 1.791.$$

Thus,

$$\frac{1 + M_1}{\sqrt{S_1}} = 1.069 \text{ and}$$

$$A_1 = (26.5)\ (0.933)\ (1.069) = 26.4 \text{ F}$$

(from Fig. 9) the freezing index, F_1 = 638 degree-days, F.

This compares favorably with the measured index of 669 degree-days, F. If the effect of thermal contact coefficients had been neglected, the sinusoidal amplitude would be (26.5 x 0.933) = 24.7 F. This would correspond to a freezing index of 480 degree-days, F, thus the damping effect is less than it would have been if Eq. 1 were used. This is attributed to the fact that β_1 (5.48) is greater than β_2 (0.239).

Heat Flow Through Insulation Layer.—The sinusoidal temperature amplitude, A_1, at the bottom of the concrete slab (top of insulation layer) is utilized in determining the temperature amplitude at the bottom of the insulation layer. The amplitude, A_2, at the bottom of the insulation is given by Eq. 2.

$$A_2 = A_1 e^{-x_2\sqrt{\frac{\pi}{a_2 P}}} \left[\frac{1 + M_2}{\sqrt{S_2}}\right]$$

in which

$$A_1 = 26.4\ F;$$

$$e^{-x_2\sqrt{\frac{\pi}{a_2 P}}} = e^{-\frac{2}{12}\sqrt{\frac{\pi}{(0.423)\ (365)}}} = 0.9766;$$

$$(1 + M_2) = \frac{2\beta_2}{\beta_2 + \beta_3} = \frac{2\ (0.239)}{0.239 + 5.60} = 0.08186;$$

$$M_2 = -0.9181;$$

$$S_2 = 1 + 2M_2 e^{-2x_2\sqrt{\frac{\pi}{a_2 P}}} \cos 2x_2\sqrt{\frac{\pi}{a_2 P}} + M_2^2 e^{-4x_2\sqrt{\frac{\pi}{a_2 P}}}$$

$$= 1 - 1.7511 + 0.7622$$

$$= 0.0151;\ \text{and}$$

$$\sqrt{S_2} = 0.1229.$$

Thus,

$$\frac{1 + M_2}{\sqrt{S_2}} = 0.666\ \text{and}$$

$$A_2 = (26.4)\ (0.9766)\ (0.666) = 17.17F$$

(from Eq. 3) the predicted freezing index, F_2 = 2 degree-days, F.

The measured freezing index was 52 degree-days, F; a probable explanation for the disparity between this value and the predicted value is given in the main text. If the effect of thermal contact coefficients had been ignored, the predicted sinusoidal amplitude would have been (26.4 x 0.9766) = 24.8 F. This represents a freezing index of 580 degree-days, F; therefore, the damping effect is greater than it would have been if Eq. 1 were used. In this case β_2 (0.239) is less than β_3 (5.60).

In analyzing the three-layer problem, a slight departure has been made from the Lachenbruch method, which for this case is more conservative and is also a simplification of the more rigorous Lachenbruch technique.

THE NATIONAL ACADEMY OF SCIENCES—NATIONAL RESEARCH COUNCIL is a private, nonprofit organization of scientists, dedicated to the furtherance of science and to its use for the general welfare. The ACADEMY itself was established in 1863 under a congressional charter signed by President Lincoln. Empowered to provide for all activities appropriate to academies of science, it was also required by its charter to act as an adviser to the federal government in scientific matters. This provision accounts for the close ties that have always existed between the ACADEMY and the government, although the ACADEMY is not a governmental agency.

The NATIONAL RESEARCH COUNCIL was established by the ACADEMY in 1916, at the request of President Wilson, to enable scientists generally to associate their efforts with those of the limited membership of the ACADEMY in service to the nation, to society, and to science at home and abroad. Members of the NATIONAL RESEARCH COUNCIL receive their appointments from the president of the ACADEMY. They include representatives nominated by the major scientific and technical societies, representatives of the federal government, and a number of members at large. In addition, several thousand scientists and engineers take part in the activities of the research council through membership on its various boards and committees.

Receiving funds from both public and private sources, by contribution, grant, or contract, the ACADEMY and its RESEARCH COUNCIL thus work to stimulate research and its applications, to survey the broad possibilities of science, to promote effective utilization of the scientific and technical resources of the country, to serve the government, and to further the general interests of science.

The HIGHWAY RESEARCH BOARD was organized November 11, 1920, as an agency of the Division of Engineering and Industrial Research, one of the eight functional divisions of the NATIONAL RESEARCH COUNCIL. The BOARD is a cooperative organization of the highway technologists of America operating under the auspices of the ACADEMY–COUNCIL and with the support of the several highway departments, the Bureau of Public Roads, and many other organizations interested in the development of highway transportation. The purposes of the BOARD are to encourage research and to provide a national clearinghouse and correlation service for research activities and information on highway administration and technology.